

TECHNISCHE UNIVERSITÄT MÜNCHEN

Lehrstuhl für Brau- und Getränketechnologie

Numerical investigations of thermo-physical and material property interactions in cereal foam microstructures

Simone Chriemhilde Mack

Vollständiger Abdruck der von der Fakultät Wissenschaftszentrum Weihenstephan für Ernährung, Landnutzung und Umwelt der Technischen Universität zur Erlangung des akademischen Grades eines

Doktor-Ingenieurs

genehmigten Dissertation.

Vorsitzender: Univ.-Prof. Dr. H.-Chr. Langowski

Prüfer der Dissertation:

1. Univ.-Prof. Dr. Th. Becker
2. Univ.-Prof. Dr. A. Delgado, Friedrich-Alexander-Universität, Erlangen-Nürnberg

Die Dissertation wurde am 03.07.2014 bei der Technischen Universität München eingereicht und durch die Fakultät Wissenschaftszentrum Weihenstephan für Ernährung, Landnutzung und Umwelt am 03.02.2015 angenommen.

Acknowledgements

First of all, I would like to express my gratitude to Prof. Dr. Thomas Becker to give me the opportunity to develop this thesis at his chair within wide scientific freedom. The constructive scientific discussions contributed to the successful completion of this research and to the confidence that nothing is difficult.

I want to thank the examining committee, the chairmen Prof. Dr. Horst-Christian Langowski and Prof. Dr. Antonio Delgado, for accepting this responsibility, as well as for their time and effort in reviewing the thesis. Additionally, I would like to thank Prof. Dr. Antonio Delgado and the entire foam-cluster fellows, for the great co-operation throughout the last years.

Dr. Mohamed Hussein deserves my special appreciations, for his friendship, his loyalty, his support, our discussions and disputes, but most of all for his supervision raising the invaluable gift of independent research. Thanks a lot to my colleagues providing comfort and sweets in work.

Thanks to Ludwig Boltzmann.

And last but not least I want to thank my parents for everything.

Munich, June 2014

Simone Chriemhilde Mack

Publications

Peer reviewed publications

1. Mack, S., Hussein, M. A., Becker, T.: Multicomponent phase transition kinetics in cereal foam - Part I: Developing a lattice Boltzmann model. *Microfluidics and Nanofluidics* (2014). DOI: 10.1007/s10404-014-1410-2.
2. Mack, S., Hussein, M. A., Becker, T.: Multicomponent phase transition kinetics in cereal foam - Part II: Impact of microstructural properties (2014). DOI: 10.1007/s10404-014-1420-0.
3. Mack, S., Hussein, M. A., Becker, T.: On the Theoretical Time-Scale Estimation of Physical and Chemical Kinetics Whilst Wheat Dough Processing. *Food Biophysics* 8(1) (2013), 69-79. DOI: 10.1007/s11483-013-9285-4.
4. Mack, S., Hussein, M. A., Becker, T.: Tracking the thermal induced vapor transport across foam microstructure by means of micro-sensing technology. *Journal of Food Engineering* 116(2) (2013), 344–351. DOI 10.1016/j.jfoodeng.2012.11.015.
5. Mack, S., Hussein, M.A., Becker, T.: Examination of thermo-physical and material property interactions in cereal foams by means of Boltzmann modeling techniques. *Microfluidics and Nanofluidics* (2013). DOI: 10.1007/s10404-013-1157-1.
6. Mack, S., Hussein, M. A., Becker, T.: Modeling flavor development in cereal based foams under thermal treatment. *Procedia Food Science* 1 (2011), 1223-1230. DOI:10.1016/j.profoo.2011.09.182.
7. Mack, S., Hussein, M. A., Becker, T.: Investigation of Heat Transfer in Cereal based Foam from a Micro-scale Perspective using the Lattice Boltzmann Method. *Journal of Non-Equilibrium Thermodynamics* 36 (2011), 311-335. DOI 10.1515/JNETDY.2011.019.

Conference contributions***Oral presentations***

1. Mack, S., Hussein, M. A., Becker, T.: Modellierung thermo-physikalischer Prozesse in Proteinschäumen unter Berücksichtigung der Phasenübergänge mittels Lattice-Boltzmann-Methoden. Jahrestreffen der ProcessNet-Fachgruppe Lebensmittelverfahrenstechnik 2013. Quakenbrück, Germany, 2013.
2. Mack, S., Hussein, M. A., Becker, T.: Thermo-physical Investigations in life-science based foams by means of Lattice Boltzmann Method: Impact of material properties. 16th IUFOST. Foz do Iguacu, Brazil, 2012.
3. Mack, S., Hussein, M. A., Becker, T.: Ermittlung der mikrophysikalischen Prozesse in getreidebasierten Erzeugnissen während des Backprozesses mittels numerischer Modellierung und Micro-Sensing. 1. Frühjahrstagung des WIG. Freising, Germany, 2012.
4. Mack, S., Hussein, M. A., Becker, T.: Micro-sensing of moisture and temperature distribution in thermally processed multiphase systems and modelling the diffusion kinetics using Lattice-Boltzmann methods. ECCE / ECAB, Berlin, Germany, 2011.
5. Mack, S., Hussein, M. A., Becker, T.: Numerical Modeling of Heat and Mass Transfer in Water Vapor Saturated Micro Bubble Systems. DECHEMA-Jahrestagung der Biotechnologen und ProcessNet-Jahrestagung 2010. Aachen, Germany, 2010.
6. Mack, S., Hussein, M. A., Becker, T.: Innovative Optimizations of the Heat Transfer Rate in Bread during the Baking Process from a Micro-scale Perspective using the Lattice-Boltzmann Method. 3rd International Symposium on Biothermodynamics. Bologna, Italy, 2010.

Poster presentations

7. Mack, S., Hussein, M. A., Becker, T.: Development of a lattice Boltzmann multiphase method and its application to model evaporation-condensation based heat transfer, ESBES + ISPPP 2012. Istanbul, Turkey, 2012.
8. Mack, S., Hussein, M. A., Becker, T.: Modeling flavor development in cereal based foams under thermal treatment. 11th International Congress on Engineering and Food, ICEF11. Athens, Greece, 2011.

Contents

Abstract	5
Zusammenfassung	6
1. Introduction	7
1.1 A sense of scale.....	7
1.2 Impact of foam microstructure.....	24
1.3 Thesis outline.....	28
2. Summary of results (thesis publications)	31
2.1 Paper summary.....	31
2.2 Paper copies.....	34
2.2.1 On the theoretical time-scale estimation of physical and chemical kinetics whilst wheat dough processing.....	34
2.2.2 Tracking the thermal induced vapor transport across foam microstructure by means of micro-sensing technology.....	45
2.2.3 Examination of thermo-physical and material property interactions in cereal foams by means of Boltzmann modeling techniques.....	53
2.2.4 Multicomponent phase transition kinetics in cereal foam – Part I: Developing a lattice Boltzmann model.....	62
2.2.5 Multicomponent phase transition kinetics in cereal foam – Part II: Impact of microstructural properties.....	70
3. Discussion	80
4. References	92

Abstract

Cereal foam microstructure is current matter of research due to global continuous growth in the bakery industry involving increased industrial processing. Enlightening thermo-physical processes and their relation to micro-structural properties is closely linked to economic requirements offering the possibility to optimize the heating process. The complexity of interacting phenomena impedes the explicit inference to particular bio-chemical or physical processes occurring at micro-scale whilst thermal treatment. Experimental investigation, especially at the microscopic length scales of interest, is limited but can be used to deliver indirect insight in occurring processes. The power of the Lattice-Boltzmann Method is in the fact that complicated thermo-physical processes can be analyzed in complex structures independent or coupled at each time- or length-scale of interest. With a focus on heat transfer optimization, the working hypothesis is termed *“coupled heat and mass transfer proceeds in the scope of cyclic evaporation-condensation processes in foam microstructures”*. Thus, the main objectives of the thesis are to investigate if evaporation-condensation occurs inside the microstructure, to examine the influence on macro-heat transfer and to determine the impact of material properties to investigate optimized conditions for enhanced heat transfer. In a first step, heat and vapor flow through the structure is determined by sensing technique to deliver insight in the macro-framework of temperature and humidity distribution. The numerical investigation of coupled heat and mass transfer processes, with associated phase transitions, in relation to cereal foam microstructure are held by means of Lattice-Boltzmann modeling techniques. The results confirm the working hypothesis and furthermore contribute to enlighten sophisticated structure, –material properties, –heat and mass transfer dependencies. In addition, the use of numerical methods delivers the possibility to visualize formerly hidden processes at bubble-scale without interfering in the process.

Zusammenfassung

Die Mikrostruktur getreidebasierter Schäume steht aufgrund des globalen, kontinuierlichen Wachstums der Backwarenindustrie, sowie steigenden industriellen Fertigung zunehmend im Interesse der Wissenschaft. Dabei sind Einblicke in thermo-physikalische Prozesse sowie deren Bezug zu mikrostrukturellen Eigenschaften, hinsichtlich der Optimierung des Erhitzungsprozesses, von hohem industriellem Interesse. Die Komplexität interagierender Phänomene erschwert explizite Rückschlüsse auf die jeweiligen mikro-skaligen bio-chemischen oder physikalischen Prozesse, die während thermischer Behandlung auftreten. Experimentelle Untersuchungen sind, insbesondere in den mikroskopischen Längenskalen die hierbei von Interesse sind, nur beschränkt anwendbar. Diese können jedoch eingesetzt werden um indirekt Rückschlüsse auf ablaufende Prozesse zu ziehen. Die Lattice Boltzmann Methode bietet den Vorteil, komplizierte thermo-physikalische Prozesse in komplexen Strukturen, gekoppelt oder unabhängig voneinander, in der jeweiligen Zeit- oder Längenskala zu analysieren. Im Fokus dieser Arbeit steht die Optimierung der Wärmeübertragung mit der Arbeitshypothese *„gekoppelter Wärme- und Massentransport vollzieht sich im Rahmen zyklischer Verdampfungs- und Kondensationsprozesse in der Mikrostruktur von Schaum“*. Die Hauptzielsetzungen umfassen die Ermittlung von Verdampfungs- und Kondensationsprozessen in der Mikrostruktur, deren Einfluss auf die makroskopische Wärmeübertragung, sowie die Auswirkung der Materialeigenschaften hinsichtlich verbesserter Wärmeübertragung. In einem ersten Schritt wurde der Wärme- und Wasserdampftransport durch die Struktur experimentell ermittelt, um Einblicke in die makro-skalige Temperatur- und Feuchtigkeitsverteilung zu erhalten. Die numerische Betrachtung des gekoppelten Wärme- und Massentransports, sowie den damit verbundenen Phasenübergangsprozessen in Relation zur Mikrostruktur des Schaumes wurde mittels Lattice Boltzmann Modellierung durchgeführt. Die Ergebnisse bestätigen die Arbeitshypothese und tragen dazu bei, Beziehungen zwischen Struktur- und Materialeigenschaften sowie Wärme- und Massentransfer aufzuklären. Zusätzlich ermöglicht der Einsatz numerischer Methoden verborgene Prozesse innerhalb der Gasblasen zu visualisieren ohne den Prozess zu beeinflussen.

1. Introduction

1.1 A sense of scale

Fundamentals of sophisticated process analysis require a detailed process understanding. To get an impression of potential analyzing tools, as well as process optimization, the driving physical phenomena of the process have to be clearly identified, objecting to avoid any misinterpretation. In general, any material, and its associated physical processes inside, can be considered from various length scale perspectives. Despite the fact that micro-processes always reflect on the macro properties, the entity of different scales of length allows the consideration of processes, due to the occurrence at different length scales, decoupled from each other (Leuzzi et al., 2008). Besides the spatial separation, the incidence of processes occurring at different time-scales confirms the decoupling feasibility due to the fact that processes with small length scales tend to be associated to small time scales, and vice versa (Markowski et al., 2010). The view-scale to analyze a process thereby heavily influences the gathered cognition. Discussing this assumption requires a survey through the different length scales of the process, hence, in the case of this work: the thermal treatment of cereal foam.

A distinction can be drawn between the length scales of the occurring thermo-physical processes and the length scales of the structural features of the material. In fluid mechanics, the length scales are clearly subdivided in macroscopic- and microscopic-scales (Chung, 2007). According to this definition, bulk materials, such as gases or liquids, pertain to the macro or continuum state, which is on a smaller length scale composed of interacting particles, constituting the micro states of the bulk (Hemminger, 2012). Figure 1.1 shows the classification of different length scales in combination to the modeling techniques being applicable in the respective length scale. In the following, numerical modeling techniques tools will be discussed for the relevant length scales, with respect to cereal foam under thermal treatment. Furthermore a link to sensing techniques is provided. Being aware of the fluid mechanical classification of scales, material characteristics can be sub-divided in different length scales according to SI-units, which will be elaborated in more detail in following sections, additionally.

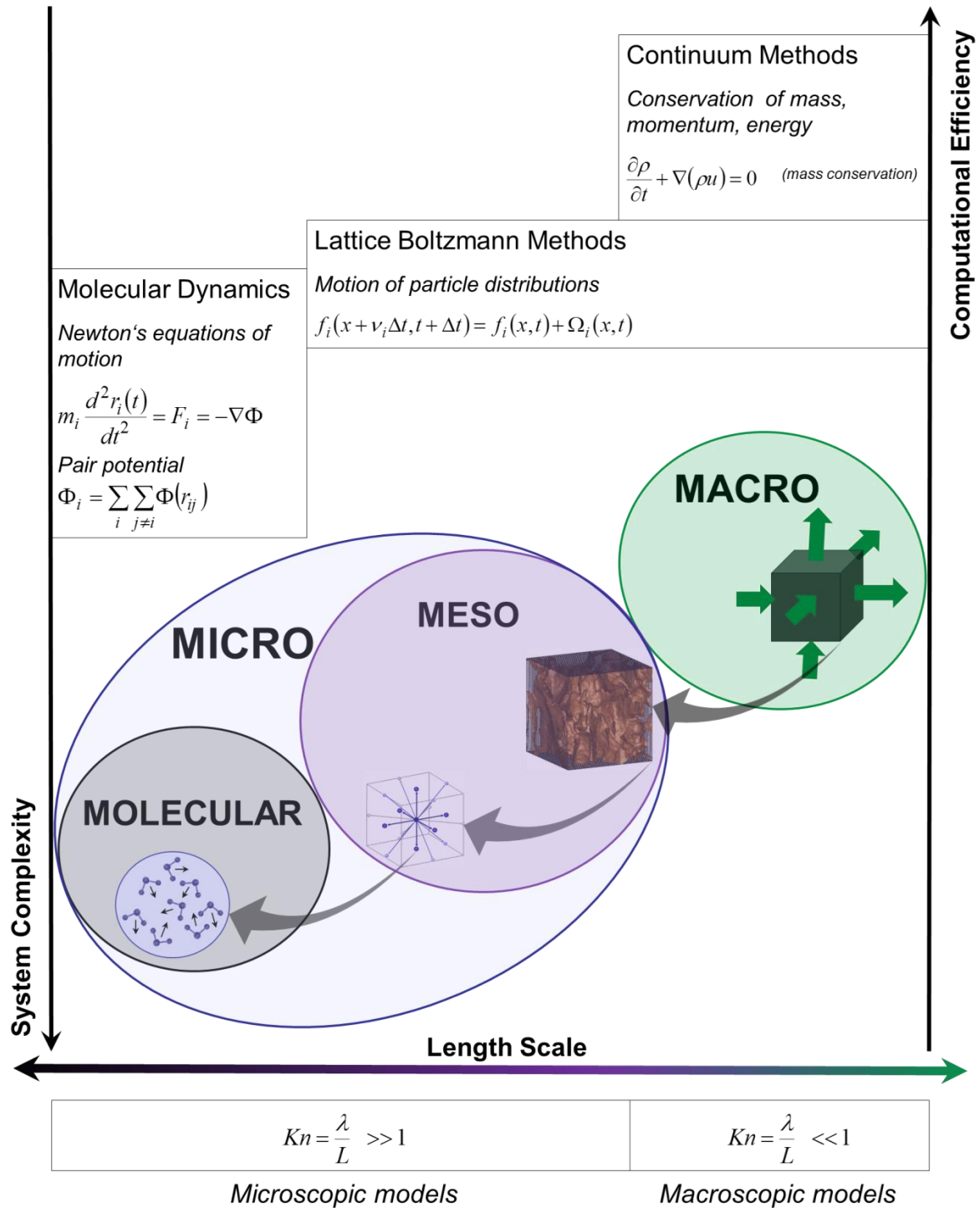


Figure 1.1 The division of macro- and micro- length scales follows the Knudsen number regime, where macroscopic models can be applied for $Kn \ll 1$ and microscopic models for $Kn \gg 1$ (Chung, 2007). Macro represents the bulk and continuum methods can be applied, whereas the micro state of the bulk is composed of interacting molecules in the molecular regime and the dynamics are described by molecular dynamics. The meso-scale bridges the molecular and the macro-scale due to statistical treatment resulting in coarse grained distribution functions of interacting molecules.

As shown in figure 1.1, the dimensionless Knudsen number indicates a general division line between both length scales, thus microscopic models can be applied for a Knudsen number $\gg 1$ and macroscopic models for a Knudsen number $\ll 1$ (Chung, 2007; Cosgrove, 2010). The Knudsen number Kn represents the ratio of the mean free path λ of molecules to the physical characteristic length L of a system (Cengel, 2007; Jiji et al., 2009),

$$Kn = \frac{\lambda}{L} = \frac{k_B T}{\sqrt{2} \pi \sigma^2 P L} \tag{1-1}$$

Calculating Kn for an ideal gas includes the Temperature T , the Boltzmann constant k_B ($k_B = 1.38066 \cdot 10^{-23}$ J/K), the molecule diameter σ and the pressure P (Nguyen et al., 2002), thus the ratio of kinetic energy to the macro-momentum energy. If the free mean path of the molecules is large in comparison to the characteristic length of the system, the system refers to continuum regime (Cosgrove, 2010). The macro scale is related to the bulk state of the system and continuum methods can be applied. The micro-scale can be subdivided in molecular states, where motion of molecules can be described by molecular dynamics (MD), and the meso-scale, which results from coarse graining of single molecules, to calculate mean values for mass and momentum density (Wolf-Gladrow, 2005). A more detailed classification of flow regimes according to the Knudsen number can be given as shown in figure 1.2.

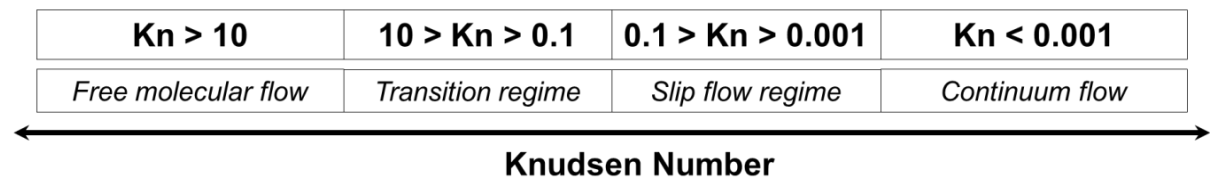
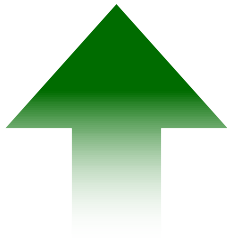


Figure 1.2 Flow regime related to the dimensionless Knudsen number of the system (Kakac et al., 2005)

For a Knudsen number of 1, collisions among molecules and collisions of molecules to the wall are at a similar length scale. In this regime two different flow regimes are present, and the transition regions are given by the change from Knudsen diffusion to viscous flux, which is the slip flow regime, and the transition from Knudsen diffusion to molecular diffusion, which is the transition regime (Pletney, 2007).



MACRO LENGTH SCALE...

In the macro-scale, materials are considered as bulk, and are therefore by definition independent of micro-scale effects (Jiji, 2009).

The micro-scale composition of discrete molecules is disregarded due to the proportionally large scale averaging of micro-scale properties (Sonntag, 2009).

Thermo-physical processes can be described by partial differential continuum equations based on the classical laws of mass, momentum and energy conservation (Kukudzhanov, 2013). Representative, the continuity equation can be given in differential form by

$$\frac{\partial \rho}{\partial t} + \nabla(\rho u) = 0 \quad (1-2)$$

Where, ρ is the fluid density, t is the time and u is the flow velocity vector field. The continuity equation expresses, that the density is locally conserved, and is only affected by a flow with velocity u (Nield, 2006). Macroscopic thermodynamics, and thus continuum laws, are based on the concept of local thermodynamic equilibrium (Rohsenow et al., 1998; Bellomo et al. 2007). Meaning that even though a system is globally far away from equilibrium it is locally in quasi-equilibrium states (Sonntag, 2009; Manneville, 2010). The assumption of local thermodynamic equilibrium is fundamental to describe the spatio-temporal progression of thermo-dynamical quantities by partial differential equations connecting the state of the system at each point (Manneville, 2010), with the consequence to deliver averaged macro-scale descriptions (Brennen, 2005).

Classical computational fluid dynamics (CFD), such as the finite element method, or the finite volume method deliver an approximated solution of the set of differential equations numerically describing continuum processes (Saha et al., 2011). Plenty of work exists delivering profound outline on the classical continuum mechanics (Hoffmann, 2000; Chung, 2007; Reddy, 2008; Kukudzhanov, 2013), thus to present it in detail is non-essential and beyond the purpose of this work. Drawing a first conclusion, macro descriptions are an approximation over the considered length and

locally the micro-information remains absent. Nonetheless, the luxury of the continuum length scale is the fact that objects are visible for the human eye and the possibility is given to observe or measure processes directly (Reif, 1965).

Concerning cereal foam, a macro-scale description shows its relevance in the range of cm. Thus, macroscopic quantities such as the temperature distribution can be determined by the use of sensing tools inside the foam during processing, as shown by several researches for the proposed cereal foam (Purlis et al., 2009 a,b; Zanoni et al., 1993). The examination of the macroscopic moisture distribution is considerably more challenging. High temperature gradients, associated with vaporization of present dough water, yields to difficulties of an accurate identification of the absolute amount of moisture. This becomes crucial as indicated by contradicting results of previous work presented in literature, presented in the following section. Generally two procedures were conducted to analyze the moisture distribution in cereal foam, destructive methods and inline sensing. Destructive methods, as cutting the foam at several time steps and analyzing the absolute moisture content was carried out (Zanoni et al., 1993). Finding, that moisture content decrease in the crust but remains constant throughout the crumb (Zanoni et al., 1993). Applying the same methodology, but achieving contradictive results as an initially increase of moisture in the middle of the foam and additionally equalizing of moisture content (Wagner et al., 2007). Under similar procedure, an increase in the center was detected whilst the absolute moisture content in the whole crumb remains constant (Purlis et al., 2009a). The contradictive results can be explained by the limitation of such procedure according to measurement uncertainties due to material instabilities and evaporation processes. Sensing the moisture content arise the challenge, that most humidity sensors are not applicable in the required small size, and even more severe, not functioning in the high temperature and humidity range. One approach was carried out by the use of a Near Infrared (NIR) sensor, showing that initially the moisture content decreases in the center, but passing a temperature of 70 °C the moisture content increases towards the coldest spot (Thorvaldsson et al., 1998). In conclusion the determination of moisture content and its distribution is still remaining a difficult challenge leading to counteracting results. In addition to experimental analysis,

several numerical investigations were carried out to determine heat and mass transfer, following the continuum description of cereal based products (de Vries et al., 1989; Zanoni et al., 1993; Therdthai et al., 2002; Datta et al., 2005; Purlis et al., 2009 a,b). The presented continuum models accounted for simultaneous heat and mass transfer, where the presence of processes such as evaporation-condensation were implemented as averaged functions (Purlis et al., 2009). In addition, structural changes, such as expansion (Datta et al. 2005), or chemical kinetics, such as browning and starch gelatinization (Zanoni et al., 1995 b,c) were addressed in recent studies.

Certainly continuum considerations are sufficient if insight in macroscopic characteristics is requested. Nonetheless, various engineering applications require a more detailed look. For instance, biotechnological processes combine complex multi-physics (Berthier et al., 2010), therefore the set of governing continuum equations explaining the processes becomes too complicated for most numerical techniques, according to non-linearity as well as the presence of multiple length and time-scales of the partial differential equations to be considered (Succi et al., 2002). Multiple length scales increase the amount of quantities to be considered, as well as the complexity of process descriptions and interactions amongst them (Wilson, 1979). Perceiving that the foam consists of different components, the void fraction as well as the foam lamellas, is certainly not surprising. Nonetheless, taking such details into account, leads to increasing complexity from a process description point of view. Material properties may be well established experimentally for the bulk, but taking the different sub-components (foam lamellas and bubbles) into account, raises the sum of properties to be considered to a much higher quantity. Thus, material parameters of the lamellas have to be investigated, as well as the gases and their properties being present in the void fraction. Such considerations face limitations due to required measurements at small length scales, specifically challenging during processing. Drawing a conclusion, providing sophisticated insight in heat transfer related processes and taking micro-scale effects into account, it is insufficient to consider the material as bulk. Therefore, the structural relevant length scales of the cereal foam microstructures have to be defined, and are summarized in figure 1.3.

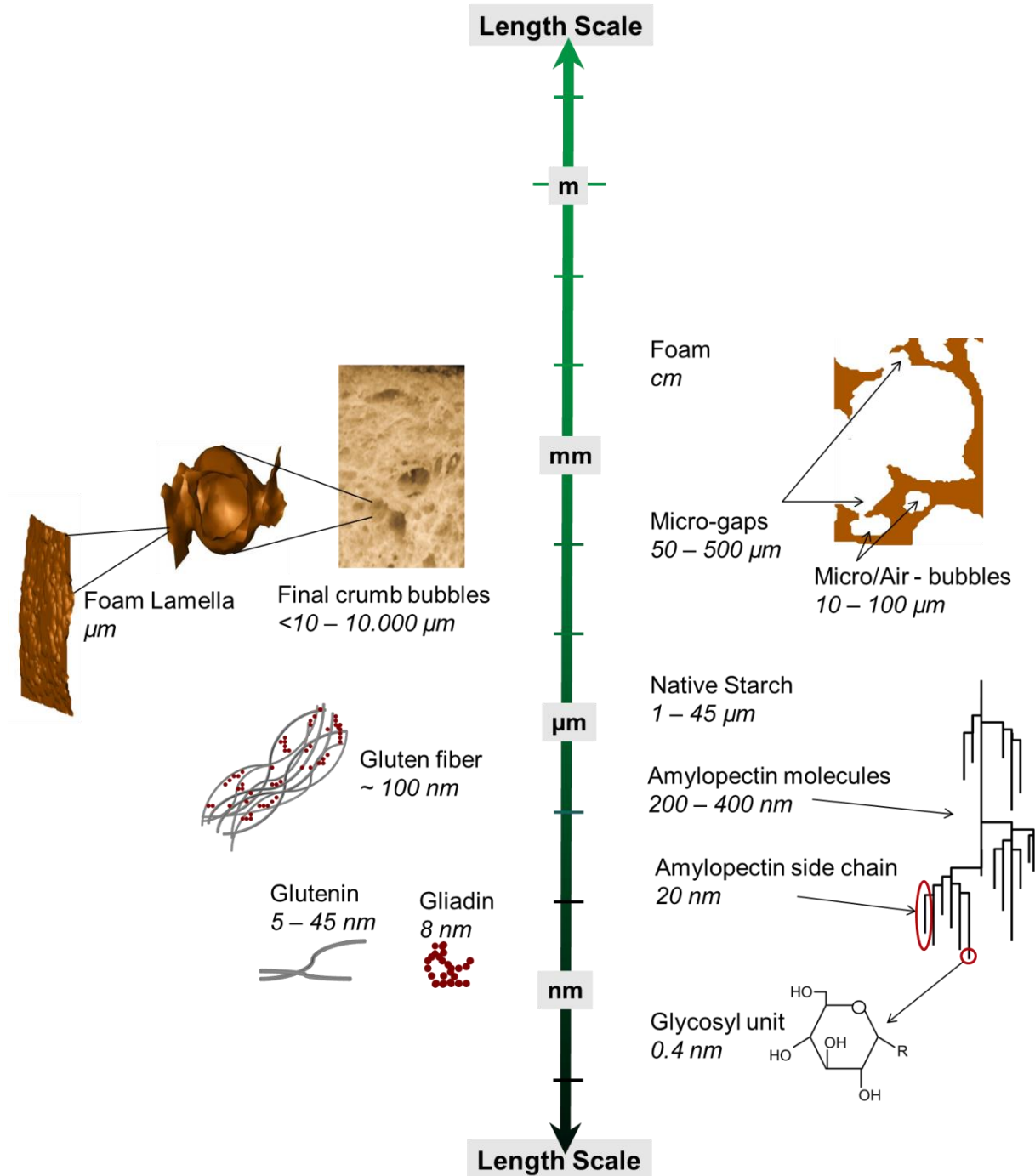


Figure 1.3 Length scales of cereal foam microstructures covering SI-length scales from cm to nm. The microstructural characteristics as foam lamella and foam bubbles, is illustrated, as well as the composition of the lamella, consisting of gluten and starch (Wahlund et al., 1996; Buleon et al., 1998; Kulp et al., 2000; Chinachoti et al., 2001; Liu et al., 2003; Hannah et al., 2008; BeMiller et al., 2009; Gilbert et al., 2009; Miguel et al., 2013).

Depending on technological conditions, as raw material properties, mixing or fermentation time, foam bubbles are spherical and intact or to a rising degree interconnected (Vanin et al., 2009; Gan et al., 1990). The void fraction of fermented dough consists of fermentation gases and to a minor degree of air, embedded during mixing, resulting in air bubbles size in a range of 10 – 100 μm (Liu et al. 2003).

In the fermentation step bubbles are forced to expand, according to developing fermentation gases, and thus increasing pressure, yielding to an interconnected void fraction (Gan et al., 1990). According to the increasing pressure and the constitution of the lamella by means of viscoelasticity, the lamella ruptures and foam bubbles are executed to coalescence (Sroan et al., 2009; He et al., 1992). The thereby generated micro-gaps connecting the bubbles are generally in the range of 50 – 500 μm , but can also reach a size of more than 1 mm (Chinachoti et al., 2001). In addition to the foam bubbles, there exist micro-bubbles, with sizes of 10 – 100 μm , being embedded inside the lamella (Chinachoti et al., 2001). These micro-air-bubbles remained from the mixing step, unable to expand due to pressure related resistances, according to the fact that larger bubbles have lower internal pressure and thus being favorable to expand (Cauvain, 2000). After processing, including fermentation, forming, and thermal treatment, the final developed crumb has a bubble size ranging from <10 – 10,000 μm (Liu et al., 2003). Bubbles are surrounded by visco-elastic foam lamellas, where the lamellas have a diameter in the range of micrometer (Liu et al., 2003). Foam lamellas consist mainly of a gluten-starch network, whereby starch granules are embedded, and with increasing fermentation time more tightly covered by gluten (Cauvain, 2000; Liu et al., 2003). The diameter of native starch in wheat flour is in the range 1 – 45 μm (Kulp et al., 2000), where around 60 % of the starch granules have a size of less than 10 μm (Liu et al., 2003). At a further level of the decreasing length scale, starch is composed of amylopectin molecules with diameter 200 – 400 nm, where amylopectin side chains have an average diameter of 20 nm (BeMiller et al., 2009). Amylopectin is composed of glycosyl units having as size of 0.4 nm (BeMiller et al., 2009). Fermentation gas holding capabilities and visco-elasticity of wheat dough are linked to gluten (Cauvain, 2000). Glutenin and gliadin fractions associate to micro-fibrillar structures, being in the range of 5 – 8 nm,

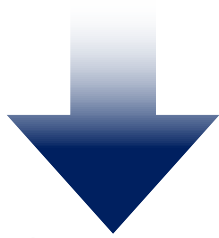
clustering to macro-fibrillar structures of up to 500 nm, where optimally kneaded dough captures 2-3 μm thick glutenin fibrils (Chinachoti et al., 2001). At such length scales, secondary bonding forces, as ionic or hydrophobic bonds play an important role (Chinachoti et al., 2001). The size of starch granules directly affects the lamella diameter, which is in the range of micrometer, thus of adequate thickness to contain starch granules, where around 60 % of the starch granules have a size of less than 10 μm affording the opportunity to stabilize foam lamellas (Liu et al., 2003). On the contrary, if starch granules are larger than the lamellas, they tend to induce instabilities and bubble coalescence (Liu et al., 2003). In addition, if mainly composed of gluten, lamella thickness can decrease below 2 μm (Liu et al., 2003).

A more generalized classification of the length scales in cereal foam microstructures is given by Gilbert, see table 1 (Gilbert et al., 2009).

Table 1.1: Summary of lengths in the dough depending on the process step (Gilbert et al., 2009)

Section of Structure	Size
Gas bubbles	10^{-4} m
Lamellas	10^{-5} m
Degraded starch granules due to enzyme attack	10^{-6} m
Gluten fibers embedding the starch granules	10^{-7} m
Long protein molecular chains	10^{-8} m
Proteins made of amino acids	10^{-9} m

MICRO LENGTH SCALE...



The previously elaborated micro-structural characteristics of cereal foam can be determined by various imaging techniques:

micro-computed tomography (μ CT) (Bellido et al., 2006; Dietrich et al., 2012), fluorescence fingerprint imaging (Kokawa et al., 2012), or confocal laser scanning microscopy (CLSM) (Jekle et al., 2011). For instance, μ CT imaging offers the possibility of non-invasive insight in the product, and was used to determine the bubble size distribution in wheat dough (Bellido et al., 2006). Thus, structural properties of the cereal foam, and the corresponding length scales, are quite well established due to a wide spread amount of imaging techniques and the opportunity to measure structural characteristics (Bellido et al., 2006; Le-Bail et al., 2011).

Analyzing the thermo-physical processes occurring at decreasing length scales experimentally is considerably more complex. The arising challenge is composed of two main features, associated to the length scales: (i) sensing limitations, and (ii) non-similarity of micro- and macro-scale processes.

At first instance, as shown in previous sections, determining macro- temperature distribution, as well as macro- and micro-structural properties by imaging techniques, is feasible. Certainly, determining absolute local moisture content and corresponding humidity fluxes remains challenging inside the foam lamellas or foam bubbles respectively, due to the small length scales in the range of μ m. Likewise, determinations of thermo-physical effects are heavy to conduct at a length scale in the range of bubble or lamella size, extreme conditions and therefore unknown physical mechanisms. Extreme conditions are given by means of high temperature and humidity gradients, present under thermal treatment of the cereal foam, facing sensing technology limitations in combination to the extreme small sized sensor requirements. At the state of current sensing technology, a macro-scale temperature or humidity measurement is covering an area of mm – cm range, thus averaging void fraction and lamellas is practicable, and can give insight in macro- heat and mass transfer processes. But delivering insight in the processes inside a single bubble or a single lamella, by means of inline sensing during thermal processing, is still limited,

due to the fact that smallest commercially available sensors are in the size range of 2 – 3 mm (Crawford et al., 2008).

Addressing heat transfer measurements at smaller scales, several micro-scale thermometry techniques exist, for instance: thermography, modulated or pulsed heating source, thin-film thermocouples, thin-film micro-bridges, optical techniques, nanometer-scale thermocouples (typically used together with atomic force microscope), photo-thermal techniques, or scanning thermal microscopy (resolving surface temperature on nanometer length scales), transient thermo-reflectance technique (monitoring transport phenomena on a picosecond time scale) (Sungtaek et al., 1999; Bejan et al., 2003). Despite these examples, a measurement technique combining ultra-short time- and length scales is a remaining challenge (Bejan et al., 2003). In addition, the measurement techniques given above may be helpful to deliver insight in small scale heat transfer processes in a range of nm – μm in specific applications (Crawford et al., 2008), but are of limited practicability to determine temperature inside a single bubble, or lamella, of cereal foam during processing and thermal treatment.

The second point to be addressed thoroughly is the non-similarity of micro- and macro-scale phenomena (Jiji et al., 2009). In micro-systems, the ratio of surface forces to volume forces increases by one half, thus, surface forces, such as adhesion, friction, electrostatic and Van der Waals forces, dominate (Berthier et al., 2010; Crawford et al., 2008). Consequently, with decreasing characteristic length of an object, the surface area per volume increases, meaning that heat transfer through interfaces is of higher importance in the micro-scale (Cengel, 2007). In addition, visco-elasticity, hydraulic resistance and capillarity effects become more important in a micro domain, whereas inertia and gravity are of minor importance (Berthier et al., 2010). At further decreasing length scales, thus being in a SI-unit range of nm, intermolecular and atomic forces become dominant (Crawford et al., 2008). Concerning heat transfer, it could be shown that the thermal conductivity of a specific material is suitable in the range of meters to microns, but can differ heavily for thin films in a range of nanometers (Bejan et al., 2003; Jiji et al., 2009). Micro-scale physical effects become significant at small length-scales, where the mean free path

of the energy carriers is comparable to the physical length of the considered system (Cengel, 2007). Consequentially, further crucial characteristic of micro-scale heat transfer is that the **thermo-physical properties are dependent on the microstructure** of a material (Cengel, 2007).

As elaborated in previous sections, distinction between macro- and micro-scale can be given by a classification according to the dimensionless Knudsen number for heat transfer (Jiji et al., 2009). If the mean free path is much smaller in comparison to the characteristic length, heat transfer is macroscopic, and thus, follows Fourier's heat diffusion theory (Anderson, 2008). On the contrary, if the mean free path of molecules is similar, or larger than, the physical length of the system, or if the time-scale of the process is comparable, or smaller than, the relaxation time of energy carriers Fourier's law fails (Saha et al., 2011). In that case, the concept of Knudsen diffusion is feasible to account for diffusion problems. For Knudsen numbers in the range of greater than 1, macro-scale descriptions are of insufficient use, since continuum mechanics fail to define the processes and other physical descriptions are required to explain the thermo-physical processes (Bejan et al., 2003). Nonetheless, energy transfer, conducted in the micro-scale by energy carriers as phonons, electrons, molecules and photons can be related to macro-scale described by continuum equations, even though the physics of each energy carrier is different (Rohsenow et al., 1998). Micro-states of a system being consistent with its macroscopic properties are described in thermodynamics and statistical mechanics following different approaches, as given by Boltzmann, Gibbs, the Landauer formalism, the Green-Kubo formalism, radiation analogies, the Schrödinger equation, the Maxwell equation, amongst others (Rohsenow et al., 1998; Jiji et al., 2009; Beisbart et al., 2011). A distinction is drawn between statistical mechanics, providing static probabilities, and quantum mechanics, providing dynamic probabilities (Beisbart et al., 2011).

The field of quantum mechanics has the objective to explain atomic structure, the behavior of matter at atomic or subatomic length scales, and possible relations to macroscopic properties (Rae, 2002). Such molecular descriptions advance in perspective to resolve thermo-physical processes in nanostructures, numerically

solved by lattice dynamics, molecular dynamics (MD), or Monte Carlo simulations (Bejan et al., 2003). Additionally, there exist hybrid technologies to combine features from each method (Attig et al., 2004).

Molecular dynamics uses Newton's equations of motion and interacting potentials, as given by Lennard-Jones, to solve a system of interacting molecules (Saha et al., 2011). Newton's equation of motion is given as:

$$m_i \frac{d^2 r_i(t)}{dt^2} = F_i = -\nabla \Phi \quad (1-3)$$

Where m is the mass, r the distance between molecules, t the time, F the force, and Φ the pair potential is given as:

$$\Phi_i = \sum_i \sum_{j \neq i} \Phi(r_{ij}) \quad (1-4)$$

The method can be used under equilibrium or non-equilibrium conditions, where the latter is applied more frequently (Yip, 2005). In general, MD is used to study the structure and dynamics of macromolecules (e.g. proteins, nucleic acids,...) (Meller, 2001), phase transition processes including liquid-vapor phase equilibrium, or capturing the statistics on the molecule number evaporated and condensed (Landry et al., 2007). Tracking individual molecules or atoms, related to super-transient time-scales of femto- to nanoseconds, yields, even though approximation and simplifications are included, to incredible computational effort and limited accuracy (Meller, 2001; Bejan et al., 2003; Saha et al., 2011). In practice, MD-simulations can cover motion of molecules driven processes only locally in their specific relatively short time-scales, delivering insight in interactions among molecules, rather than in their macro-scale dynamics (Chen et al., 1994; Roco et al., 2010).



MESO LENGTH SCALE...

The term meso-scale is defined as the intermediate size, or length scale, between two length scales (Antonietti et al., 2004).

The impact of meso-scale descriptions is crucial since it acts as a spatial linkage of classical continuum and quantum mechanics (Hemminger, 2012). Despite the link of both length scales, functionality, visible on a macro-level, is ruled by meso-scale characteristics rather than the atomistic states of the system (Hemminger, 2012). Even though the direct descriptions of single molecule interactions become insignificant, the challenge is to span several time and length-scales (Bagchi, et al., 2010). Pertaining between continuum and molecular descriptions, the kinetic theory acts as a basis for multi-scale fluid descriptions (Bernaschi et al., 2009). The kinetic theory thereby delivers sophisticated insight in micro-scale effects or related transport phenomena, and as well links the micro-state of a system, given by motions and collisions of its atoms and molecules, to its macro-states (Jiji et al., 2009). Molecules are regarded as hard spheres at ideal gas conditions, thus quantum-mechanical effects are insignificant, and gases considered to be composed of interacting particles (Ge et al., 2007).

The kinetic theory was developed to provide a dynamical description of heat, transferred by kinetic energy of molecules in motion, before statistical mechanics was established to solve systems for many particles (Beisbart et al., 2011). The dynamical state of the system can be described by the location x and momentum p of each particle at a given time t (Sukop et al., 2006). Worth to mention that one mm^3 of air contains 10^{16} molecules (Succi, 2001). According to the enormous quantity of particles occupied in space, statistical treatment is required, statistical mechanics gives a probability distribution function $f(x,p,t)$ to find a particle with a defined location and momentum (Sukop et al., 2006).

Macro-scale heat transfer can be described by the heat diffusion equation. Certainly the applicability of the heat diffusion equation is limited in the micro-scale due to the non-equilibrium characteristics of micro- heat transfer (Cengel, 2007; Sungtaeket al.,

1999). To understand micro-scale processes at non-equilibrium conditions, non-equilibrium thermodynamics have to be employed (Rohsenow et al., 1998).

To anticipate, the kinetic theory is not applicable under non-equilibrium conditions, since it follows the assumption of local thermodynamic equilibrium (Rohsenow et al., 1998). Boltzmann solved that. The basic idea was to show how a system under non-equilibrium conditions reaches equilibrium state, and Ludwig Boltzmann proved, according to the H-Theorem, that any non-equilibrium distribution function is the equilibrium Maxwell-Boltzmann distribution in the limit of time (Beisbart et al., 2011).

In comparison to continuum equations, the Boltzmann transport equation is dependent on the statistical distributions of energy, rather than temperature dependent equations (Bejan et al., 2003). Furthermore, the Boltzmann equation can account for all types of particles following a statistical distribution, gas molecules, phonons, photons, electrons, ions (Bejan et al., 2003; Rohsenow et al., 1998). Likewise the concept of the kinetic theory, the Boltzmann equation describes the motion of a rarefied gas, being composed of interacting particles, by a particle density distribution function (Sukop et al., 2006).

The Boltzmann equation, without external forces, is given by equation 1-5, where the collision among particles is implemented via the collision term Ω (Succi, 2001).

$$\frac{\partial f}{\partial t} + \nu \nabla f = \Omega \quad (1-5)$$

Where, f is the particle distribution function, t is the time, ν is the particle velocity, and Ω is the collision term. The original collision term of the Boltzmann equation is highly complex, embedding usually non-linear scattering rates, achieving an analytical solution of Boltzmann equation is thus considerable challenging (Aristov, 2001), therefore several analytically as well as numerically approximate solutions have been presented. Convenient approach to linearize this term can be done by a relaxation-time approximation (Bejan et al., 2003; Rohsenow et al., 1998).

Thus, for local equilibrium equation 1-5 reaches:

$$\frac{\partial f}{\partial t} = -\frac{f - f_0}{\tau} \quad (1-6)$$

Where, f_0 describes a state of local equilibrium. The non-equilibrium distribution f is thus (Rohsenow et al., 1998):

$$\int_{f(0)}^{f(t)} \frac{\partial f}{f - f_0} = \int_0^t -\frac{1}{\tau} \partial t \rightarrow \frac{f(t) - f_0}{f(0) - f_0} = e^{-\frac{t}{\tau}} \rightarrow f(t) = (f(0) - f_0)e^{-\frac{t}{\tau}} + f_0 \quad (1-7)$$

With proceeding time the distribution function approaches f_0 . Consequently, if a system is in a non-equilibrium state, the collisions restore equilibrium (Rohsenow et al., 1998), following an exponential decay (Bejan et al., 2003). The Boltzmann equation allows calculations of micro particle-particle interactions, and furthermore, macroscopic properties can be derived from the Boltzmann equation (Rohsenow et al., 1998). For instance, the conservation of mass, momentum and energy, is given by equations 1-8 to 1-10, relating the particle distribution function to macroscopic density, momentum and specific internal energy (Succi, 2001).

$$\rho = \sum f_i \quad (1-8)$$

$$\rho u = \sum v_i f_i \quad (1-9)$$

$$\rho e = \frac{1}{2} \sum (v_i - u)^2 f_i \quad (1-10)$$

Where, ρ is the macroscopic density, u the flow velocity, v the particle velocity in i^{th} direction f the particle distribution function and e is the internal energy. Therewith, Boltzmann provides a link from micro- to macro length scales. Advantageous is the incorporation of micro-scale effects and the applicability to derive macro-properties from the micro-states, even under conditions if continuum descriptions fail (Hussein et al., 2010). Quantum-mechanical effects among the particles can be neglected for thermodynamic equilibrium conditions if the mean particle distance is larger than the thermal de Broglie wavelength (Spickermann, 2011). Worth to mention additional simplifications to the derivation of Boltzmann's equation, like the presumption that only binary elastic collisions among similar particles are considered, and that collisions lead to a directional change rather than accelerated particles (Zwanzig, 2001). In computational fluid dynamics, the Lattice Boltzmann Method (LBM) gives a discrete formulation of the kinetic theory, distinguished to classical CFD methods

which deliver discrete approximations of partial differential equations to each infinitesimal volume element of the fluid (Mohamad, 2011). Numerically, the lattice Boltzmann Method discretizes the Boltzmann equation in time and space on a defined lattice (Zhang et al., 2010). At each lattice site x , the particle distribution function $f_i(x, t)$ is given, and during each time step Δt the particles move according to a set of discrete velocities v to the nearest lattice site $x+v_i\Delta t$ (Zhang et al., 2010; Chen et al., 1994). Subsequently, at the new lattice site, particles collide, which is addressed in the collision term, and a new particle distribution function is computed (Chen et al., 1994). According to a single-time relaxation approximation, the corresponding lattice Boltzmann equation is given as (Zhang et al., 2010):

$$f_i(x + v_i\Delta t, t + \Delta t) - f_i(x, t) = \Omega_i(f) \quad (1-11)$$

The collision term accounts for the rate of change towards equilibrium, according to the relaxation time τ , which is related to the fluid viscosity (Chen et al., 1994). The lattice Boltzmann equation allows recovering of correct hydrodynamics by applying the least amount of kinetic information (Succi et al., 2002). Essential features of molecular dynamics are combined by coarse graining of particle interactions, obeying a good approximation of continuum equations and macroscopic quantities (Chen et al., 1994). Thus, the LBM bridges the gap between micro- and macro-scales, and consequently, providing a meso-scale approach (Monaco et al., 2007). From a computationally point of view it is more efficient than MD (Saha et al., 2011), since particle distribution functions are considered, rather than single molecules. Drawing a first conclusion shows that both, macro- as well as molecular descriptions are insufficient to deliver insight in thermo-physical processes at the length scale of interest, namely the cereal foam microstructure. Micro-scale dynamics and the linked small-scale physics are following highly non-linear functions which cannot be described by continuum models (Succi et al., 2002). Continuum descriptions are not applicable to provide insight into the microstructure and the associated processes, whereas molecular dynamics are delivering too much information on a too small length and time scale which reflects to high computational costs (Tielemann, 2006).

1.2 Impact of foam microstructure

The challenge to determine characteristic thermo-physical processes through the cereal foam is owed to their complex structure-material property interactions. As elaborated in chapter 1.1, limitations to analyze thermo-physical properties, by means of sensing whilst cereal foam processing, in the micro-scale still remain. In addition, the investigations showed that thermo-physical properties are depending on the microstructure, and therewith on micro-scale properties. The basic question as well as the arising challenge is thus: **the incidence of thermo-physical and material property interactions in cereal foam microstructures.**

Recent researches show that transport properties are depending on the microstructure (Hussein et al., 2010; Yazdchi et al., 2011; Wang, 2012). A study addressing the macroscopic permeability of periodic fibrous porous structures, which is depending on microstructural effects, was carried out by the use of finite element methods, validated with theoretical and numerical data (Yazdchi et al., 2011). The effects of microstructural properties (fiber shape, aspect ratio, orientation) were determined for a broad range of porosities and showed that permeability is depending on these micro-structural parameters (Yazdchi et al., 2011). Likewise, it could be shown that the porous structure type, such as granular, fibrous or network has a significant influence on electro-osmotic permeability (Wang, 2012). The network structure is favorable at low porosity, reaching highest permeability due to the surface to volume ratio, whereas at high porosity the granular structure yields to highest permeability due to the lower shape resistance (Wang, 2012). The latter results are based on numerical simulations by the use of lattice Boltzmann methods and indicate the impact of microstructures on transport properties.

Relating the impact of cereal foam microstructure on thermo-physical properties, little research was done thus far. Nonetheless, the conducted studies showed the impact of the microstructure on the heat transfer (Zanoni et al., 1995a; Hussein et al., 2010). According to Zanoni, bread macro-structure was distinguished between crumb and crust, and experimental measurements showed that their thermal diffusivities are functions of porosity (Zanoni et al., 1995a). A difference between crumb and crust

was detected, which may be related to variations of apparent density, specific heat and thermal diffusivity of both regions (Zanoni et al., 1995a). In a further study, the influence of porosity was determined by the use of lattice Boltzmann methods in an artificial porous system, representing cereal dough (Hussein et al., 2010). It could be shown that increasing porosity results in more quick heat spread through the system according to the different material properties (Hussein et al., 2010). Nonetheless, real micro-structural characteristics were not taken into account, which would be necessary to estimate their impact on the heat transfer. Additionally, the differentiation of crumb and crust density shows the impact of different structural properties on the heat transfer (Zanoni et al., 1995a), allows first insights, but inappropriately, in both regions the microstructure additionally is not uniform across the characteristic length of the foam (Cauvain et al., 2006). According to the non-uniform microstructure, macroscopic quantities are not equal across the macroscopic length scale (Gray, 2002). Therefore, foam density is depending on the ratio of void fraction to lamella fraction, rather than its local distribution or the occurrence of structural different regions. A macro-description does not account locally on the specific characteristics of the foam, such as bubble size, lamella thickness, thermal diffusivity of the lamella or thermal diffusivity of bubble content. Contrariwise, macro-descriptions implement such structural features as averaged functions. However, taking a step deeper into the micro-scale one can consider that variation of the structural constitution of a single foam lamella contributes to local uncertainties. For instance, the bulk density of the foam can have the similar value, thus the amount of void fraction remains constant, even though bubble size distribution or lamella thickness may be different at the micro-scale.

Thermo-physical properties for cereal foam, considered as bulk, are quite well established (Rask, 1989), but thermo-physical properties of microstructural parameter are insufficiently discussed in literature. Bear in mind the example of heat transfer through a section of cereal foam microstructure, a macro-description may offer the value for temperature, but averaged for the whole micro-section. Thus, in a continuum description, micro-scale effects remain invisible. For instance, the thermal diffusivity is a macro quantity, depending on the density, the thermal conductivity and

the specific heat of the bulk, as shown in equation 1-12.

$$\alpha = \frac{k}{\rho c} \quad (1-12)$$

Where k is the thermal conductivity, ρ is the density and c is the specific heat capacity. Theoretically, variations of thermal conductivity, density as well as specific heat lead to a higher thermal diffusivity through the bulk and thus, influence heat transfer. Related to cereal foam, the thermal conductivity, as well as specific heat is depending on the material constitution and its water content (Purlis, et al., 2009b). Varying the density from a micro-structural perspective can be conducted by means of bubble size distribution, and likewise lamella constitutions, as its thickness, presence of air inclusions or micro-gaps, connecting the bubbles to an increasing degree or not at all. The prior described variations account at the micro-scale, but are hidden at macro-scale, and even worse, different micro-scale structural constitutions can lead to the same macro quantity due to averaging. Argumentum e contrario, micro-parameter variations can be used to influence macro quantities.

Remaining the question of the nature of the driving underlie thermo-physical processes, as well as the impact of structural constitution from a micro-scale perspective. In theory, determining the heat flux separately through void fractions and through the lamellas would provide a defined picture of the underlying processes through the microstructure. From this local micro-description the global macro quantities can be determined, and additionally the impact of microstructural characteristics could be identified. As elaborated previously, the water content has an influence on the heat transfer, given by continuum descriptions (Zanoni et al., 1995a; Purlis, et al., 2009b). Remaining the question of the micro-structural dependency, thus the role of water inside the lamellas, inside the bubbles, fluxes through both of them, interactions with the material, and finally the impact on the microstructure and the heat transfer. Experiments, carried out with μ CT imaging, showed that steaming conditions in the oven ambient has an influence on the structure and the properties of bread crust (Le-Bail et al., 2011). Lower steaming yields to a thinner crust and higher permeability for moisture than for higher steaming (Le-Bail et al., 2011). Thus the results show the correlations of thermo-physics related to micro-structural properties.

On the contrary to external steaming, whilst thermal treatment, temperature gradients develop yielding to evaporation of water from the foam to the oven ambient (Kotoki et al., 2010). Evaporation to the surrounding implies that evaporation processes may as well play a role inside the microstructure. Recent researches state repeatedly the theory of the possible occurrence of evaporation-condensation based heat transfer through cereal foam (Sluimer et al., 1987; Sablani et al., 1998; Purlis et al., 2009a), where the assumption is as follows:

Under the influence of thermal energy, water evaporates at the warmer side of the foam bubble from the lamella, thereby absorbing latent heat of vaporization. The vapor moves through the foam bubble, condenses at the colder side of the bubble, thereby setting free the latent heat of vaporization, as illustrated in figure 1.4.

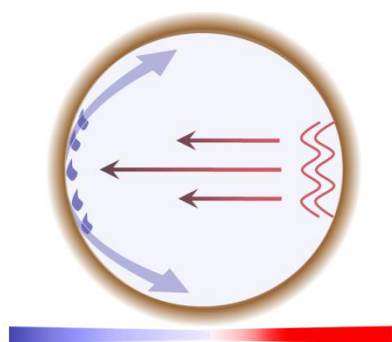


Figure 1.4 Sketch of evaporation condensation mechanism. A single foam bubble is exposed to a temperature field from the right hand side (red). Inside the bubble lamella water vaporizes under the influence of heat, moves through the bubble and condenses at the colder side (blue). Depending on the conditions additional backflow may occur, indicated by blue arrows. (Sluimer et al., 1987; Sablani et al., 1998; Purlis et al., 2009a)

From a straight physical point of view the theory of evaporation-condensation (E-C) is certainly meaningful, and thus lead to the application of continuum models, implementing this process as averaged functions in heat transfer simulations of cereal foam (Thorvaldsson et al., 1999; Purlis et al., 2009a,b). Nonetheless, the specific conditions in combination to complex interacting processes under thermal treatment limited thus far to proof the existence of E-C. In addition, the quantitative impact of this process on the overall heat transfer is unknown and interactions of such processes related to microstructural properties remain unidentified, but would certainly contribute to enlighten the micro-scale characteristics of the heat transfer as well as processes proceeding inside single foam bubbles. In conclusion, the theoretical investigations show that micro-structural characteristics have an influence on the heat transfer through cereal foam. And thus, micro-structural variations may be used to examine the impact, as well as an optimized micro-state of the system, for improved heat transfer in the whole process.

1.3 Thesis outline

The previous chapters gave an introduction to relevant length scales of cereal foam microstructures as well as corresponding sensing and modeling techniques. The survey showed that hidden micro-property details constitute the basis for bulk material properties (Attig et al., 2004), and that diverse micro-states of a system may affect the heat transfer.

A central role in science is attributed to experimental procedures, providing fundamental knowledge on physical processes (Meller, 2001). Nonetheless, under a large instance of conditions it is impossible to conduct the required measurements, and theories are required to explain the related processes (Attig et al., 2004). In that case numerical modeling and simulation attracts notice to use basic physical principles to link measurements and theories (Meller, 2001; Attig et al., 2004). A further benefit of modeling techniques is the possibility to support proper interpretation of measurement results (Roco et al., 2010). In addition, modeling and simulation is usually faster, less expensive and allows numerous parameter variation studies without the effort arising during experimentation (Robinson, 2004). Related to cereal, examining thermo-physical properties by means of in-line sensing during processing, is limited due to processing barriers to macro-scales. Thus, theoretical and numerical investigations are required to deliver insight and analyze underlying processes.

At first instance process-relevant time- and length-scales have to be identified to elaborate which method is best suiting and if micro-scale heat transfer effects have an influence on the process (Rohsenow et al., 1998). The choice of the length-scale to be considered is fundamental for the numerical tool to be applied and the gained insight in the process. If neglecting the presence, or the composition, of the lamella of starch and protein and other ingredients as well as the starch granule of amorphous and crystalline lamellas and amylopectin chains (Liu et al., 2003) respectively, then in conclusion, from a straight structural point of view, dough microstructure is in the range where continuum descriptions could be applied according to the Knudsen number classification. In addition, worth to mention, that foam lamellas are

sufficiently thick to be independent of micro-scale heat transfer effects, which may be induced by the mean free path of molecules with respect to the lamella diameter. Nonetheless, in any porous medium, the macro-scale is much larger than the pore diameter, and in addition, macro-quantities may not remain the same over the whole macro length scale (Gray, 2002). Thus far, numerical investigations on heat transfer and mass transfer have been conducted based on continuum descriptions, averaging the specific micro-heat transfer phenomena in continuum partial differential equations and neglecting the characteristic micro-structural features of the cereal foam. In several researches the occurrence of evaporation-condensation based heat transfer is described theoretically and implemented in numerical models based on continuum descriptions (Thorvaldsson et al., 1999; Purlis et al., 2009a,b). Additionally, for systems in non-equilibrium state, or when gradients exist among the micro-scale properties, it is complicated to reach a macro description of the thermodynamic processes (Gray, 2002). Despite the fact that methods to study non-equilibrium nonlinear processes exist, they are limited by the nature of the mathematical models (Aristov, 2001). Furthermore, processes during thermal treatment, as phase changes, or diffusion through the microstructure, are hidden micro-scale processes, and the necessity remains to identify and visualize thermo-physical processes from a length-scale perspective below continuum descriptions.

The survey, given in the previous chapters, arises several basic questions:

- *Which thermo-physical processes occur inside a single foam bubble?*
- *Is evaporation and condensation based heat transfer of relevance in cereal foam microstructures under thermal treatment?*
- *Does the microstructure have an influence on the heat transfer?*
- *How can thermo-physical and material property interactions be defined?*

These fundamental research questions are closely linked to application based requirements of industry. Global growth in the bakery industry (Pan, 2012), in combination to increasing energy costs require innovative process optimization inquiries. In the bakery industry a considerable part of the consumed energy is

required for the baking process. In order to contribute to reduce energy consumption by means of saving energy, time and costs, there is the demand of optimization technologies to improve the heat transfer rate inside the product without affecting product quality. The relevance is specifically crucial in large sized industrial production, with high through put. Thus, the significance to deliver insight in the correlation of cereal foam microstructures and thermo-physical phenomena, their impact as well as the potential of heat transfer optimization is evidentiary.

In conclusion, this work has the main objective to investigate numerically the heat and mass transfer processes at bubble length-scale, thus delivering insight in so far hidden processes. Conventional continuum methods are limited according to the spatio-temporal range of the processes to be considered. Furthermore, the possibility to treat non-equilibrium processes based on particle dynamics in complex structures makes the LBM a promising alternative to conduct the required numerical investigations in the meso-scale (Aristov, 2001). Thus, cover the relevant features of microstructural properties and thermo-physics in macro- and micro-scales, respectively. In summary, the following points are addressed in this work:

- (i) Theoretical investigation of thermo-physical processes occurring in cereal foam microstructures under thermal treatment and the determination of their relevant length and time scales
- (ii) Experimental determination of heat and mass transfer through cereal foam microstructures
- (iii) Development of physical- and mathematical algorithms describing the thermo-physical processes
- (iv) Development of a numerical tool to conduct physics-based simulations
- (v) Visualization of thermo-physical processes inside foam microstructures
- (vi) Parameter variation studies to elaborate impact of microstructure on optimized heat transfer through the foam

2. Summary of results (thesis publications)

2.1 Paper summary

Part 1 – A review

On the theoretical time-scale estimation of physical and chemical kinetics whilst wheat dough processing

In order to establish sophisticated insight in the complex interacting physical and chemical processes occurring under the influence of heat requires a fundamental knowledge of their characteristics. Therefore, this review gives an outline on the main physical and chemical processes in relation to heat transfer from macro- to micro-scale. In addition to the specific length-scale considerations, each process follows a characteristic time-scale being of impact on limitations or acceleration of related processes. The characteristic times are calculated, related to each other and their dominance, influence as well as interactions are discussed. Thus, the detailed knowledge allows an estimation of the impact of each process from a micro-scale description to the macroscopic state. The gained time and length-scale relationship is fundamental to proceed to establish the heat and mass transfer relevant phenomena inside cereal foam microstructure, to set up a meaningful measurement device and to develop an appropriate numerical tool to model these processes.

Part 2 – Sensing the scenery

Tracking the thermal induced vapor transport across foam microstructure by means of micro-sensing technology

Following the basic question if evaporation-condensation based heat transfer plays a significant role, the vapor distribution was measured during the heating process. For this purpose, a small scale (3 mm x 3 mm) sensor was positioned inside the foam and temperature as well as relative humidity was logged simultaneously throughout the cross-section of the loaf. The procedural method of the measurement device covers the humidity amount in the gas phase, thus allowing the determination of the

vapor flux through the microstructure. The results show that in the end of baking the highest humidity level is found at the coldest spot of the loaf. Together with the convergence towards a 100 °C temperature level the conclusion can be drawn that indeed evaporation-condensation takes place yielding to mass transport towards the coldest spot. In addition, the measurement results are used to provide the initial conditions of the foam for the numerical part. Nonetheless, even though the small size of the sensor, it is still not capable to deliver insight into the vapor distribution inside a single bubble and thus providing evidence only indirectly at macro-scale. The challenge, to determine the vapor flux at the micro-scale and if evaporation or condensation locally occurs, still remains.

Part 3 – Numerical investigations

Based on the findings of the previous parts, and with the objective to complete the missing links which are not feasible by measurements, numerical investigations are carried out to examine and visualize the thermo-physical processes at micro-scale. Therefore, the lattice Boltzmann method is used, which is predestined to bridge micro- and macro- scales (Sukop et al. 2001).

Examination of thermo-physical and material property interactions in cereal foams by means of Boltzmann modeling techniques

In this study, the coupled heat and mass transfer through cereal foam is addressed by means of diffusion. The modeling domain is based on μ CT images of breads crumb, hence delivering a realistic virtual foam microstructure. The computational domain is divided in 2 components, the foam lamella and the foam bubbles respectively. Such classification allows distinguishing the specific material properties for each component, being aware to be dependent on averaged macro-properties, and thus considering the process from a micro-scale point of view. The developed lattice Boltzmann model covers thermal and vapor diffusion and the simulation results deliver insight in the related heat and vapor flux through the microstructure. In addition, variations of the thermal diffusivity of the foam lamella shows that the possibility is given to improve heat transfer by parameter variations.

Multicomponent phase transition kinetics in cereal foam – Part I: Developing a lattice Boltzmann model

The diffusion model of the previous study is extended to address phase transitions occurring under specific temperature and partial vapor pressure conditions. Therefore, two additional sink and source terms are implemented in the lattice Boltzmann diffusion equation. The term added to the mass diffusion equation, accounts for the phase transition of water vapor to its condensate, whereas the other term added to the heat diffusion equation addresses the additional energy transfer depending on the amount of transitioned phase. Furthermore the evaporation from the foam lamella, as well as the re-evaporation from the condensate and the related absorption of latent heat is considered. The numerical model is validated with a test case based on experimental data from literature, examining the evaporation of a water droplet, and showed quite well accuracy.

Multicomponent phase transition kinetics in cereal foam – Part II: Impact of microstructural properties

The objective of this study is the application of the developed phase transition LBM to cereal foam under thermal treatment, covering three minor goals: (i) does evaporation-condensation take place under the given specific conditions, and how does evaporation-condensation then affect the heat transfer; (ii) parameter variations to determine how micro-structural properties influence the heat transfer; and last but not least (iii) to visualize the thermo-physical phenomena inside the foam bubbles.

The simulation results show that evaporation-condensation occurs and that this process indeed increases the heat transfer rate. Furthermore it could be shown that changing the foam microstructural properties, by means of porosity, permeability and thermal diffusivity, yields to increased heat transfer. Additionally, the simulation results support process understanding from a micro-scale perspective and make formerly, for the human eye, hidden processes visible.

2.2 Paper copies

2.2.1 On the theoretical time-scale estimation of physical and chemical kinetics whilst wheat dough processing

Food Biophysics (2013) 8:69–79
DOI 10.1007/s11483-013-9285-4

REVIEW ARTICLE

On the Theoretical Time-Scale Estimation of Physical and Chemical Kinetics Whilst Wheat Dough Processing

Simone Mack · Mohamed A. Hussein · Thomas Becker

Received: 26 April 2012 / Accepted: 31 January 2013 / Published online: 17 February 2013
© Springer Science+Business Media New York 2013

Abstract During processing of complex multiphase systems several processes occur on different time and length scales simultaneously and influencing each other. To establish the main relevant driving process, time-scale analysis is an important tool in physics. This work outlines the physical and chemical kinetics occurring during cereal based foam processing and contributes to enlighten the impact of different characteristic times. Such analysis becomes beneficial if detailed micro-scale description of the whole process is required which may be used for process optimization. With regard to the latter, an important tool is numerical modeling where a sophisticated knowledge of the processes, time and length scales is required to produce realistic results. The time scale estimation shows the impact of each process on the whole macro scale behavior of the system and gives a critical review of previous physical and mathematical models and the related simulation approaches.

Keywords Time-scale analysis · Cereal foam · Thermo-physics · Numerical modeling

Nomenclature

α Thermal diffusivity; [m^2/s]
 c_p Heat capacity; [J/kgK]
 C Concentration; [mol/m^3]
 C_0 Initial concentration; [mol/m^3]
 D Mass diffusivity; [m^2/s]
 D_{eff} Effective mass diffusivity; [m^2/s]
 δ Constrictivity; [-]

E Evaporation rate; [$\text{kg}/\text{m}^2/\text{h}$]
 E_a Activation energy; [kJ/mol]
 ε Porosity; [%]
 G Gelatinized starch fraction; [-]
 H Height; [m]
 h Heat transfer coefficient; [$\text{W}/\text{m}^2\text{K}$]
 h_v Enthalpy of vaporization; [J/kg]
 J Diffusion flux; [$\text{mol}\cdot\text{m}^2/\text{s}$]
 K Thermal conductivity; [W/mK]
 K_c Mass transfer coefficient; [m/Pas]
 k Kinetic reaction rate constant; [$1/\text{s}$]
 k_0 Reaction frequency factor; [$1/\text{s}$]
 k_g Permeability; [m^2]
 K_v Viscoelastic constant; [-]
 λ Mean free path; [m]
 L Characteristic length; [m]
 μ Viscosity; [Pas]
 n Reaction order; [-]
 P Pressure; [Pa]
 Q Extent of gelatinized starch; [$\text{mW}/100\text{mg}$]
 ρ Density; [kg/m^3]
 R Universal gas constant; [J/molK]
 r Radius; [m]
 RH Relative humidity; [%]
 σ Surface tension; [N/m]
 T Temperature; [K]
 T Tortuosity; [-]
 t Characteristic time; [s]
 τ Relaxation time; [s]
 v Velocity; [m/s]

S. Mack (✉) · M. A. Hussein · T. Becker
Group of (Bio-) Process Technology and Process Analysis, Faculty of Life Science Engineering, Technische Universität München, Weihenstephaner Steig 20, 85354 Freising, Germany
e-mail: s.mack@wzw.tum.de
URL: wzw.tum.de/bgt/

Introduction

In complex biotechnological processes the physical phenomena are usually occurring in the micro-scale, being

responsible for the macro-scale behavior of the process. During thermal treatment the processes become even more complex due to the thermal sensitivity of the properties such as pressure, humidity, surface tension, viscosity and chemical reaction kinetics. In addition, the phenomena in complex physical processes are occurring at different time and length scales [1], making a detailed description and mathematical modeling challenging. Profound knowledge of the characteristic time scale of each process, either in macro or micro-scale, helps to understand how micro- or even nano-scale phenomena interact to assemble to a macro-process. Nonetheless, one remaining challenge is to link the micro-scale to the product and its specific properties [2]. Furthermore the driving process of several parallel running processes can be determined regulating the phenomena observed in the macro-scale, what can be used for process optimization.

Even though sensing technology advanced rapidly in the past decades it is still challenging to determine especially the micro phenomena experimentally due to the lack of appropriate sensing technology with the required specific conditions. Applying sensors inside the loaf during the baking process demands for low mass, small size and applicability to high temperature and humidity ranges. Sample applications are humidity measurement by means of NIR [3] or micro-sensing [4]. The resolution time of the latter is in the range of ms, whereas the NIR probe delivers immediately measurement results due to the measurement being based on light absorption and reflection [5]. Drawback is that the measurement techniques are in general influencing the process or product destructive, especially when the governing problem occurs in the micro-scale. A promising alternative is to model the processes, allowing an easy parameter variation study to enlighten the impact of each property without interrupting, influencing, or destroying the product. The impact of different length scales becomes important when choosing the right modeling method. In the macro-scale a continuum description of the flow fields based upon the Navier–Stokes equations is adequate. Nevertheless, this approach is only valid until the dimensionless Knudsen number, see Eq. 1, is smaller than 0.1, with λ as the mean free path in m of the molecules and L as the characteristic length in m.

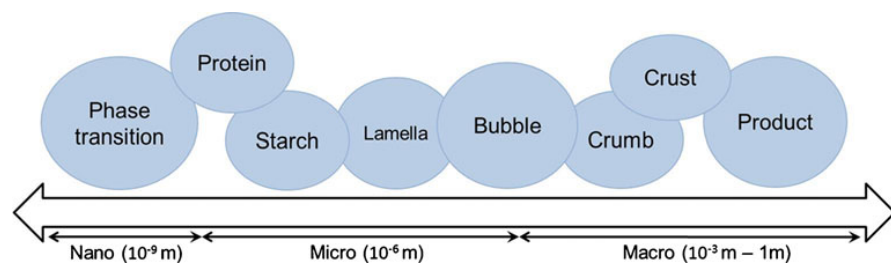
$$Kn = \frac{\lambda}{L} \quad (1)$$

In the meso-scale, particle dynamics such like the lattice Boltzmann Method (LBM) can be applied, considering that gases are composed of interacting particles. The LBM allows an easy derivation of macroscopic conservation properties based on the micro-scopic properties to be solved. In the nano-scale molecular modeling recently has the luxury of significant progress and can be used to simulate

molecule interactions, but due to the small time and length scales of the processes to be considered, the immense computational effort of such calculations is still limiting the application. Considering typical cereal foam consisting of a protein-starch network with CO₂ bubbles, the different scales can be seen in Fig. 1.

Modeling a Complex process requires the time-dependent change of the properties to be resolved. As soon as more than one process is considered in the model the right time scale has to be chosen carefully since it is not always easy to determine the driving process and the corresponding characteristic time. In order to monitor the process at the right time scale and prevent to lose any information. Worth to mention that, besides the importance to be aware of the time-scales involved in the process, modeling in food systems require a multi-scale, multi-physics and as well non-linear and dynamic descriptions [6]. Mechanical Modeling by the use of Finite Element Methods, can be used to deliver insight in the texture of food and the structure-function relationships, as shown by the review of Guessma et al. [7]. Nonetheless, the linked simplifications of the food microstructure requires alternative process modeling tools to cover the detailed thermodynamic, structural, bio-chemical and mechanical features of the food systems [8]. The SAFES (systematic approach to food engineering systems) methodology, as presented by Fito et al., incorporates all relevant features in combination to the complexity of the food systems [8]. Vasconcelos et al. [9] reconstructed a two-dimensional foam structure from an image segment and compared the results to a simulation. In their study about coarsening they faced two timescales, the first time is linked to surface tension and viscous dissipation, the second timescale is driven on gas permeability and foam polydispersity and controls the coarsening rate. Concerning liquid foams, the characteristic time of the processes is for the first time fractions of a second, and for the second time in the order of minutes or hours [9], hence being challenging to combine both times in one model or to choose which is of main impact. In another study, Xiao et al. [10] analyzed theoretical- and numerically multiphase subsurface flows in porous media. The analysis comprises solitary wave run-up/drawdown of pore pressure diffusion and propagation of the saturation front. The analysis showed the existence of different timescales for each process, and the coupling of the processes was analyzed due to comparison of the time scales of pore pressure diffusion and saturation front propagation. Drawback of the study is that the analysis is based on the average quantities of the whole system, meaning that the situation in the local scales can be different [10]. Concerning cereal based foams, Hailemariam et al. [11] proposed a mathematical model for the isothermal growth of bubbles in an extrusion process including a time scale analysis of the processes linked to

Fig. 1 Different length scales occurring in the model multiphase system



bubble dynamics. The bubble growth described by the Maxwell model has two characteristic times, related to the diffusion and to the momentum transfer. Theoretically, both times can be applied in the model to non-dimensionalize the equations, dependent on the dominant process. Since it is not always obvious which process is dominant, a process characteristic time was introduced in the numerical analysis and based on different characteristic times for each process the driving phenomena was elaborated in several case studies [11].

This work focuses on the different physical and chemical processes occurring under the influence of heat in a cereal based foam. The processes discussed in this study include: (a) Heat and mass diffusion; (b) Expansion and bubble dynamics; (c) Bio-chemical reactions; which are described from a macro and micro-scale perspective to get detailed insight in the characteristics of the process. Characteristic time scales are assembled, estimated for a control volume of the model material, and used to enlighten the linkage and impact of the processes on each other and on the final product. Besides the theoretical description and time-scale analysis of the processes, the objective of this study is to demonstrate their impact on modeling and to give a critical review on the modeling progresses in the related field.

Dimensional Analysis

Physical modeling requires a dimensional analysis, this is done by the application of dimensionless numbers used to up/down-scale the process to the computational domain, ensuring that the physical phenomenon occur at a real ratio. Dimensional analysis is a basic tool to estimate the impact of several characteristic parameters affecting the whole process [11]. The analysis can be based on length or time scale, whereas the time-scale plays an important role when determining the time step of the computational model.

In the macro-scale, surface forces are proportional to surface area and volume forces are proportional to the volume, special concern has to be taken into account in micro-physics, where with a decreasing length scale surface forces tend to dominate volume forces. The latter is reasoned by an increasing ratio between surface forces and volume forces by 1/L [12]. In micro-systems, inertia and

gravity become less important and capillarity, interface phenomena and viscoelasticity start to become more dominate for the system [12]. For the proposed model foam this is of impact in narrow pores, at the interface and inside the cell wall. The model cereal based foam encompasses the whole length scale: diffusion processes in the macro-scale, phase transition/diffusion and chemical reactions in the micro-scale, and molecular interactions in the nano-scale. The process related dimensionless numbers are summarized according to the occurring processes in Table 1.

Thermo-Physical Processes—Reflection from Macro- to Micro-Scale

The temperature change in cereal based foams effects the material properties significantly and induces several complex bio-chemical and -physical reactions each of them linked to each other and influencing each other. Macro-scale processes are governed by phenomena occurring in the micro-scale. Cumbersome is the fact that different micro-scale processes can lead to the same macro-scale behavior. Depending on the demands and the application, a macro-scale description of the process may be sufficient, but ensuring detailed understanding of the macro-processes requires an accurately observation of the micro-scale phenomena and their linkage, thus enabling an optimization of the whole process. Characteristic time of each micro-scale process supports the estimation on the driving process and their interleaving. Figure 2 gives a brief impression on the processes of the model cereal based foam occurring under thermal treatment.

The foam consists of a visco-elastic cohesive starch-gluten network containing CO₂ bubbles produced by yeast or other foaming agents. Worth to mention, that additionally flour components such as pentosan, lipids or proteins are required to achieve specific dough rheology properties, rather than simple starch-gluten mixtures [13, 14]. This could also be shown by a study carried out based on X-ray computed microtomography [15]. The results showed that the void phase is stabilized by liquid film walls, and thus additional minor components are required to obtain the characteristic bread structure [15]. Further work should be done to determine the specific interfacial properties of such

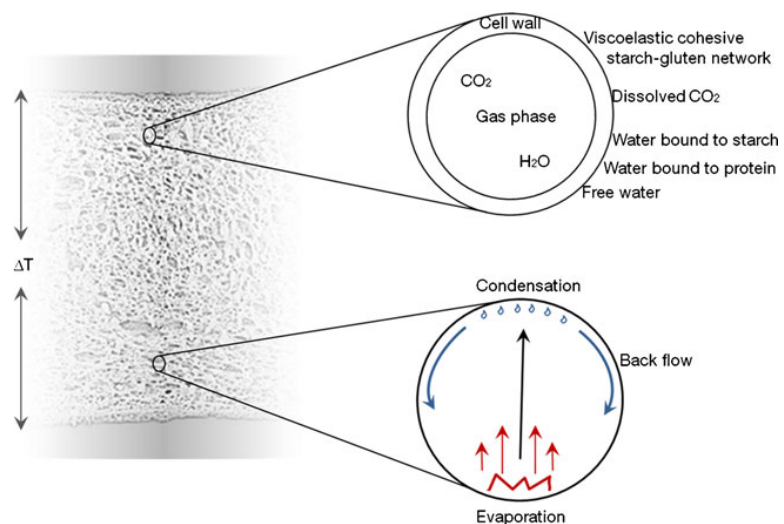
Table 1 Process related dimensionless numbers

Dimensionless number	Equation	Description
Elasticity number	$El = \frac{Wi}{Re} = \frac{\mu\tau}{\rho L^2}$	Proportional to (elastic force)/(inertial force)
Elasto-capillary number	$Ec = \frac{\tau\sigma}{\mu L}$	Combining elastic and capillary effects as compared to viscous stresses
Fourier	$Fo = \frac{\alpha t}{L^2}$	Ratio of heat conduction rate to the rate of thermal energy storage
Biot	$Bi = \frac{hL}{K}$	Ratio of the heat transfer resistances inside of and at the surface of a body
Damköhler	$Da = \frac{kC_0^n}{C_0} t = k * C_0^{n-1} t$	Reaction time scales vs. transport phenomena
Jakob	$Ja = \frac{\Delta T c_p}{h_v}$	Plays an important role during liquid–vapor phase change
Knudsen	$Kn = \frac{\lambda}{L}$	Ratio of means free path to characteristic length
Ohnesorge	$On = \frac{\mu}{\sqrt{\rho L \sigma}}$	Ratio of viscous forces to inertial and surface tension forces
Weissenberg	$Wi = \frac{\tau v}{L} = \tau \dot{\gamma}$	Ratio of viscous to elastic forces

minor compounds as well as to use X-ray technology to get deeper insight in the rheological properties of expanding dough [15]. Water is existing bound to starch and proteins and a marginal amount free. Proving time regulates the amount of CO₂ development being responsible for final product structure, pore size and pore size distribution. Under non-isothermal conditions, when heat is applied the properties of the material change significantly. In the macro-scale, the material undergoes a temperature dependent transformation process, the former porous visco-elastic dough matrix develops to crust and crumb, the latter following a solidification front towards the middle [16–18]. This transformation and solidification process is reasoned mainly by starch gelatinization and protein denaturation, accompanied by local bubble expansion, coalescence, densification and collapse [19]. Further characteristics, mainly in the crust are the water loss and the development of flavor and color compounds due to the higher temperatures in the outer layers. Exposed to heat, the temperature in the crust converges to the oven temperature, reasoned by the quick

evaporation of water. The resulting lack of water required for starch gelatinization and protein denaturation affects the rheological properties, by means of limited bubble growth and deformability [20]. Thus yielding to smaller sized bubbles, and a more dense structure compared to the crumb structure [19]. Heat transfer through conduction is limited due to the porous character, therefore heat transfer in such material is known to depend mainly on evaporation-condensation processes inside the pores [16, 17, 21], resulting in a maximum temperature of 100 °C in the crumb region. Heat transfer is directly linked to mass transfer, increasing temperature yields to mass transfer due to evaporation to the outside and according to a pressure driven flow based on evaporation-condensation towards the coldest spot of the material [21]. The evaporating water from the semi-liquid dough matrix to the pores moreover yields to a displacement of CO₂ from the pores to the surrounding. The mass transfer processes on their part influence the structure, from a macro-scale point of view the whole material expands—until the rigid crust is set, which is limiting

Fig. 2 Processes occurring in the cereal based foam under thermal treatment



expansion. From a micro-scale point of view the bubbles expand due to gases, depending on the visco-elasticity of the cell walls and the gas retention possibility accompanied by cell wall thinning until the cell walls rupture due to over pressure [20]. A non-invasive method to determine crumb structure is given by microcomputed tomography [22]. Bubble size distributions were analyzed for two different dough consistencies, stiff dough and slack dough respectively. The results give insight in bubble size distributions and show the impact of dough consistency, thus small bubbles in the slack dough, deform to a greater extend then in the stiff dough. To get more detailed insight in the microstructure and to quantify gluten, starch and bubble distributions in dough a method based on fluorescence fingerprint was developed [23]. The combined applied imaging technique allows insight in different mixing stages and furthermore the extraction of quantitative parameters of the structure [23].

In the further sections the processes are described more detailed from a thermo-physical and chemical point of view associated to the specific timescales and applied models for relevant characteristics of each process. The properties of the model multiphase system are summarized in Table 2.

Thermo-Physical and Chemical Processes Under Thermal Treatment

Thermal Flux

The temperature distribution inside the material is of main impact for this review since all the discussed phenomena are temperature dependent. The thermal distribution inside the material was measured and modeled in several researches

Table 2 Thermo-physical properties of model cereal based foam. Diffusion coefficients are given for a temperature of 100 °C

Process	Value	Unit	Reference
Moisture diffusivity crumb	$9.0 \cdot 10^{-8}$	[m ² /s]	[24]
Moisture diffusivity crust	$2.5 \cdot 10^{-8}$	[m ² /s]	[17]
Mass diffusivity CO ₂ dough	$7.4 \cdot 10^{-10}$	[m ² /s]	[25]
Thermal diffusivity vapor	$1.92 \cdot 10^{-5}$	[m ² /s]	[26]
Thermal diffusivity crumb	$5.0 \cdot 10^{-7}$	[m ² /s]	[27]
Thermal diffusivity crust	$3.8 \cdot 10^{-7}$	[m ² /s]	[27]
Thermal diffusivity solid	$1.6 \cdot 10^{-7}$	[m ² /s]	[26]
Frequency factor	$2.8 \cdot 10^{19}$	[1/s]	[28]
Activation energy	1.39	[kJ/mol]	[28]
Surface tension	$4.0 \cdot 10^{-2}$	[N/m]	[25]
Density liquid	$1.4 \cdot 10^3$	[kg/m ³]	[29]
Viscosity dough	$2.2 \cdot 10^7$	[Pas]	[30]
Moisture diffusivity bubble	$2.0 \cdot 10^{-5}$	[m ² /s]	[26]
Moisture diffusivity solid	$3.0 \cdot 10^{-9}$	[m ² /s]	[26]

[16, 17, 27, 31] but since the characteristic temperature distribution is dependent upon the specific recipe and baking conditions, it becomes cumbersome to easily compare the different results. Heat transfer through conduction is known to be limited and mainly driven by energy transfer based on evaporation-condensation. In general, the mathematical models developed to describe heat transfer were applied averaging the micro-scale properties of the material [27, 32, 33], e.g. Purlis et al. [17] included the appearance of evaporation-condensation inside the pores in the equation accounting for the thermal conductivity for the whole loaf.

In addition heat transfer can be described based on the thermal diffusivity of the material. The thermal diffusivity relates the thermal conductivity to the density and specific heat capacity of a material:

$$\alpha = \frac{K}{\rho \cdot c_p} \tag{2}$$

Where α represents the thermal diffusivity in m²/s, K is the thermal conductivity in W/mK, ρ is the density in kg/m³ and c_p is the specific heat capacity in J/kgK. For non-dimensionalization, the Fourier number which relates the heat conduction rate to the rate of thermal energy storage, can be used, the see Table 1. In combination with the Biot number transient heat transfer can be characterized.

Zanoni et al. proposed different thermal diffusivities for crumb, Eq. 3, and crust region, Eq. 4, since porosity and thermo-physical properties differ significant in these two regions [27]:

for crumb

$$\alpha = \exp(0.01\varepsilon - 15.25) \tag{3}$$

for crust

$$\alpha = \exp(0.0062\varepsilon - 15.30) \tag{4}$$

Where ε is the porosity in %.

Certainly, this gives insight in the macro-behavior of heat transfer, but to really understand the underlying processes a micro-scale description is recommended. To overcome the application of averaging methods, the temperature flux through the material can be considered based on the different thermal diffusivities of each phase [34, 35]. Distinguishing the thermal diffusivities for the gas phase inside the pores and the solid dough phase surrounding the pores gives a more realistic insight in the phenomena from a micro-scale point of view and shows the impact of different properties of the phases. Such procedural method yields to the observation that heat transfer through the porous phase proceeds much quicker than through the solid phase, reasoned by the differing thermal diffusivities and the evaporation condensation. Nonetheless, further work

should be done to explicitly implement evaporation and condensation effects, thus allowing a realistic description of thermo-physical processes occurring inside the microstructure. In addition further investigations should emphasize on the determination of thermal diffusion coefficients of thin lamellas, where experimental data is required to model related processes.

Mass Flux

Mass flux is the rate of mass flowing across a specific area ($\text{kg}/\text{m}^2\text{s}$). Several different mass flux processes occur in the present problem, see Fig. 3: (a) mass transfer from the liquid dough phase towards the gas bubble according to concentration gradients (CO_2 and water vapor), decreased solubility (CO_2), and a higher evaporation rate (water vapor) due to higher temperatures; (b) mass transfer through the cell walls, due to concentration gradients (CO_2 and water vapor); (c) through the connected gas phase/inside the bubbles to reach equilibrium with the surrounding; (d) pressure driven flux due to evaporation.

Depending on the properties of interest the mass flux can be described by Fick’s law or Darcy’s law. Fick’s law is given by Eq. 5, and defines the mass flux according to a concentration gradient including the molecular mass.

$$J = D\nabla C \tag{5}$$

Where J is the diffusion flux in molm^2/s , D is the specific diffusion coefficient of the material in m^2/s and C is the concentration in mol/m^3 .

Hussein et al. used Fick’s first law of diffusion to determine the moisture flux from the dough surface to the surrounding depending on the temperature difference [34].

$$J = -D\nabla C = K_C(P_{\text{Dough}}(T_{\text{Dough}}) - P_{\infty}(T_{\infty})) \tag{6}$$

K_C mass transfer coefficient in m/Pas , P is the water partial pressure in dough and ambient in Pa , and T is the temperature

in K . Similar to the thermal flux, the Fourier number for mass transfer can be used for non-dimensionalization.

In general, Fick’s first law is an acceptable assumption for the mass flux from the surface to the surrounding, nevertheless, several authors stated that gas movement in porous media can also be described by Fick’s first law [36, 37]. In the presence of a porous network with moisture flow through, the structural characteristics have to be taken into account to assure a realistic description of the process. One possibility in micro-porous systems is the correction of the diffusion coefficient D by the constrictivity δ , porosity ϵ and tortuosity T of the material yielding to an effective diffusion coefficient [34].

$$D_{\text{eff}} = \frac{D\epsilon\delta}{T} \tag{7}$$

Another possibility to define the mass flux mathematically is based on Darcy’s law, see Eq. 8, which describes the gas flux through a porous media according to pressure gradients [36, 38]:

$$J = -\rho_g \frac{k_g}{\mu_g} \frac{\partial P}{\partial s} \tag{8}$$

Where k_g is the permeability in m^2 , ρ is the gas density in kg/m^3 , μ the gas viscosity in Pas and P the pressure in Pa .

Under the influence of heat the main mass transfer to be considered is the vapor flux. Transfer of CO_2 is of major importance in the pre-baking step proving and of impact for the structural properties of the final product. Leavening kinetics was implemented in a mathematical model to describe bubble expansion in a cereal microsystem during fermentation [31]. Mass fluxes of carbon dioxide as well water vapor, were addressed in their model yielding to a combine diffusion–reaction scheme. Several mathematical models are existing concerning the proofing step [25, 30, 39]. Additional work should be done to transfer these models to the baking step, considering the combined and certainly interacting mass fluxes of carbon dioxide, water vapor and flavor compounds.

Phase Transition

Considering heat and mass transfer by diffusion is acceptable in a simplified macro-or meso-scale description of the process. Nevertheless, on a decreasing length scale and accounting for a realistic physical representation, the processes can not only be described by diffusion processes. Diffusion coefficients are temperature dependent, another impact of a temperature gradient on mass flux are phase transition processes as evaporation and condensation of water. Applying such process to a single pore in the model material water evaporates in higher temperature regions from the pore wall and latent heat of vaporization is

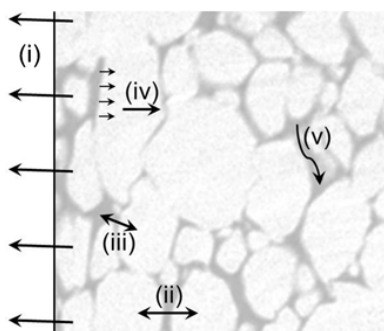


Fig. 3 Mass flux of water vapor and CO_2 (i) to the surrounding; (ii) through cell wall; (iii) cell wall–bubble; (iv) inside bubble (v) within cell wall

absorbed. Phase transition processes where latent heat is involved are first-order phase transitions. Increasing pressures acts as a driving force for vapor through the pore, ceasing in condensation at lower temperature regions, geometrical on opposite side of the pore, thereby setting free the latent heat of vaporization [16, 17]. This process is known as the heat pipe principle and is used to explain the quick spread of heat through foam-like materials in the presence of water. Justification of the theory is given by experimental studies showing that heat transfer in a leavened dough proceeds much faster than in gas free dough [40]. This is contradictive to the fact that gas pores acting as insulating elements should yield to increased heat transfer in non-leavened dough, the opposite is the case therefore energy transfer based on evaporation-condensation becomes crucial. Furthermore, during the cyclic evaporation-condensation process energy is absorbed or released in the system, resulting in a limited temperature of 100 °C, as long as free water is available. Such property of the model system is presented in several publications, determined experimentally [17, 33].

Evaporation and/or condensation induce the development of an interface between liquid and vapor region. This interface is located between the transition phase next to the bulk liquid and the so called Knudsen-layer in the vapor region, which is at a non-equilibrium state [41]. Local equilibrium in the vapor phase is reached in the far-field vapor region. Significance of the phase transition process is given by the fact that the previous subdivisions of occurring phenomena are physically described by different governing equations. The transition region, including the determination of the boundary conditions at the interface may be solved by molecular dynamics (MD), the non-equilibrium region as well as vapor flow across the interface can be solved by micro/meso-scale- and the equilibrium region by macro-scale-approaches [41]. Quite challenging is the determination of evaporation and condensation coefficients, which can be done by MD-simulations, although it is hard to verify the results with experiments since there are different time and length scales existing and being essential for phase change phenomena. Published results scatter largely between more than one hundred times [41] thus making it difficult to assign the characteristic transition time. Studies about the vapor-liquid interface displacement showed that transition time for water vapor is 7 μs, whereas the mean free time of water vapor molecules is 8 ns [41].

Huang et al. modeled the moisture transport during baking, an assumption made in their model was that the phase change occurs at a much shorter time scale than the diffusion, where the diffusive time scale was said to be in the order of 10³ s [24]. Applying both processes in one model, the time step has to be chosen carefully. To ensure instantaneous phase change, the time scale for the phase change should be smaller than the time step sizes and the time step

size should be much smaller than the diffusive time scale [24]. To non-dimensionalize phase transition processes, the Jakob number plays an important role, see Table 1.

Besides the transitions of water liquid to its vapor and vice versa, phase transitions play an important role in starch-water systems. Under the influence of heat, and as well in the presence of water, an order–disorder phase transition occurs in the starch granule [42]. To go more into detail, this gelatinization process covers the loss of crystallinity, heat uptake, hydration and swelling of the granule [42]. Likewise, several researches have been conducted to characterize processes such as glass transition, melting or network formation of starch and gluten in relation to their thermal, mechanical and structural features [43]. These properties can be measured by the use of differential scanning calorimetry (DSC), dynamics mechanical analysis (DMA), thermomechanical analysis (TMA), Thermodielectrical analysis (TDEA), or electron spin resonance (ESR) amongst others [43]. A remaining challenging task for further research in this direction may be the implementation of the water uptake dependent processes of the starch granules combined with protein denature inside the foam lamella in relation to lamella permeability and water diffusion processes.

Bubble Dynamics

Depending on the specific material properties foams have a firm fixed structure or are exposed to dynamic processes yielding to structural changes. The characteristic bubble dynamics in the model cereal based foam can be subdivided in three parts: the proving step, the heating step and the cooling/storing step. Whilst proving, the bubbles expand under iso-thermal conditions according to the yeast (or other leaving agents) activity and proving time, as a consequence cell walls get thinner until they get interconnected, yielding to an open porous network. A 3 dimensional finite element method was developed to analyze the proofing step, accounting for bubble expansion and coalescence [44]. The results allow insight in the development of a cellular structure of the dough and show furthermore satisfactory results in comparison to experimental data [44].

Under the influence of heat, the bulk material expands within the first minutes until crust sets [20]. The macroscopic expansion rate was studied by Zanoni et al. [33] where the relative height of the loaf was expressed by:

For $t < 1,140$ s:

$$\frac{H_t}{H_0} = 1.07 + (9.2 \cdot 10^{-4} t) \tag{10}$$

For $t < 1,800$ s:

$$\frac{H_t}{H_0} = 2.61 - (4.5 \cdot 10^{-4} t) \tag{11}$$

Where H_0 is the initial height and H_t is the height at time t [33]. Critical is that these expansion rates are given depending on baking time and not on temperature, so a comparison to experiments under different conditions is not possible. Wagner et al. determined the oven rise expansion rate for different baking temperatures, e.g. at $T=182\text{ }^\circ\text{C}$ the expansion rate was 2,4 mm/min, for lower temperatures, the rate was slower and crust formation was to a lesser extent [45]. In several studies the bubble growth dynamics were described and modeled for gas bubbles in a viscoelastic liquid, in general the gas inside the bubble was assumed to behave according to the ideal gas law [46]. Therefore the rate of diffusion from liquid to gas phase was used in combination with Henry's law to relate the gas concentration at the interface. Bubble expansion/gas diffusion is then reasoned by a concentration gradient in the liquid yielding in a flux from liquid to gas phase [46]. Since the ideal gas law is a very rough estimation it would be recommended that laws describing real gases are applied to get a better insight in the real pressure flux. Jefferson et al. modeled the pressure-driven growth of a single bubble in dough and fracturing according to the previous mentioned processes. Time scale calculations lead them to the conclusion that the surface tension time scale is too long to have an effect on the collapse of fractured bubbles. Unfortunately this time scale estimation was not presented in their publication. Having a look at more than one bubble in a viscoelastic fluid, the processes become even more complex. Expansion of bubbles inside the material follows a temperature dependent expansion and solidification front towards the center. Due to increased temperature the gases inside the bubbles expand, restricted by crust setting and solidification of cell walls at a temperature range of 65–75 °C according to starch gelatinization and protein denaturation. Further impact on the bubble dynamics has the limited expansion space, yielding to local densification and collapse induced by expanding neighbor bubbles and crust setting [19]. In the end of baking the cell walls get more permeable for gases yielding to slight shrinkage of the whole material, nevertheless the structure got solidified and no dynamic processes occur anymore. In the cooling and storing phase the bubble dynamics are restricted to the ongoing water loss and retrogradation of the starch yielding to a slow overall shrinkage. Evidently the structural dynamics are occurring at different time scales and strongly depending on the heat treatment of the product. The characteristic time scales for the macro-scale processes are minutes/hours for the proving step, minutes for the heating step, and days for the cooling/storage step.

Having a more detailed look at the micro-scale phenomena the time-scales shift tremendously. In general, foams are almost always at quasi-equilibrium because the cell walls equilibrate on a very short time-scale after a mechanical perturbation. The time scale of a perturbation of an interface

exposed inertia and surface tension is described by the surface tension time [11]:

$$t_R = \sqrt{\frac{\rho R^3}{\sigma}} \tag{12}$$

The time taken by a perturbed interface to regain its shape against the action of viscosity is the capillary time [12]:

$$t_T = \frac{\mu R}{\sigma} \tag{13}$$

Where ρ is the density in kg/m^3 , R is the bubble radius in m, μ is the viscosity in Pas and σ is the surface tension in N/m. In this context, the dimensionless Ohnesorge number relates the viscous to inertial and the surface tension forces [12] and indicates the impact of viscosity which is larger with increasing Ohnesorge numbers.

Another phenomena affecting cell walls is the higher pressure in smaller bubbles tending to force gas to pass towards bigger bubbles at lower pressure. Nonetheless, this is depending on permeability of the cell walls to present gases and the time scales of the processes depend on the diffusion mechanism at the boundary. The effect called coarsening has two time scales, the first time scale is depending on surface tension and viscous dissipation and is for liquid foams in a time scale of fractions of seconds. The second time scale is depending on gas permeability and foam polydispersity and is responsible for the characteristic coarsening rate and is in the range of minutes or hours for liquid foams [9].

According to Arefmanesh et al. [46] the bubble growth and its characteristic time can be related to diffusion, see Eq. 14 and momentum transfer, which is given by the Rayleigh collapse time Eq. 15 [47].

$$t_D = \frac{R_0^2}{D} \tag{14}$$

Where R_0 is the initial bubble radius in m and D is the mass diffusivity in m^2/s .

$$t_{RC} = 0.915R \left(\frac{\rho_L}{P_{G0}} \right)^{\frac{1}{2}} \tag{15}$$

Where R is the bubble radius in m, ρ is the density in kg/m^3 and P is the pressure in Pa.

The ratio of the time scales of the prior study [46] are varying between 10^{-4} and 1 and the mass transfer time scale always being smaller or equal to the momentum transfer time scale. In general, both of them can be used to scale the time step size. Commonly Eq. 14 is used if mass transfer is dominant and Eq. 15 is used if momentum transport is dominant [11].

Cereal dough is a non-Newtonian fluid and the viscoelastic properties are responsible for the structural development and the gas holding possibilities. The viscoelasticity is in this respect of impact for expansion and collapse processes since viscoelastic effects tend to retard collapse [11]. Viscoelasticity can be characterized by a relaxation time and describes the time for the configuration change of the material [12]. The most commonly rheological measurement technologies as well as the structure-function relationships in bread making are reviewed by Dobraszczyk et al. [48]. The rheological characteristics are related to the gluten polymer properties being of major impact of visco-elasticity [48]. Furthermore, additional ingredients as well as different operating conditions have an effect on the rheology [49]. Several dimensionless numbers can be applied such as the elasto-capillary number, the elasticity number or the Weissenberg number, see Table 1.

Zhang et al. studied dough viscoelasticity in relation to the effect of temperature and elaborated the corresponding relaxation time which is given by Eq. 17 [32].

$$\tau = 9 \left(\frac{2}{\pi} \arctan \left(\frac{T - 65}{2} \right) + 1 \right) + 2 \tag{17}$$

Due to the solidification with increasing temperature viscoelasticity changes and relaxation time was reported to change from 2 s in wet dough to 20 s after baking [32].

Bubble growth characteristics and the impact of the time scale was mainly studied under iso-thermal conditions and gives already insight in the processes. Nonetheless, thermal treatment increases the complexity of the bubble dynamics and time-scale analysis from a micro-scale perspective and is still a challenging remaining future task.

Chemical Reactions

Time of chemical reactions is depending on several influencing factors like temperature, pH and medium, making it difficult to establish a characteristic time scale. In general, based on the reaction kinetics, the time scale for the gelatinization process can be estimated according to the time of a reaction of first order (Eq. 18):

$$t = \ln \frac{C_0}{C} k \tag{18}$$

Where C is the concentration in mol/m³ and k is the reaction rate constant in 1/s.

Main chemical reactions occurring in the model foam are starch gelatinization, protein (gluten) denaturation, and color and flavor development. Main impact of starch gelatinization is the amount of free water and temperature. Starch is absorbing water used for starch granules swelling, and gelatinizing at temperature ranges from 65 to 75 °C.

Gelatinization temperature is of importance since gelatinization restricts further bubble expansion, this temperature range is specific for each flour type, but is also affected by the heating rate. When the heating rate is increased from 5 to 25 °C/min, there is a shift in the swelling of starch granules at higher temperatures [50]. This effect becomes obvious in the crust, where due to the higher heating rate and the lack of water due to heavy evaporation to the surrounding starch gelatinization proceeds only partially [20]. Considering chemical reactions non-dimensional, the Damköhler number can be applied, which relates the reaction time scales to transport phenomena.

Only few studies were carried out to determine the starch gelatinization kinetics in the proposed model foam [51] and are all based on the assumption that starch gelatinization follows irreversible first order kinetics [28, 52].

$$(1 - G) = \exp(-kt) \tag{19}$$

With

$$G(t) = \left[1 - \frac{Q(t)}{Q_{\max}} \right] \tag{20}$$

Where G is the gelatinized starch fraction, k is the reaction rate constant in 1/s, Q is the heat uptake, and t is the time in s. K depends on temperature according to Arrhenius equation:

$$k = k_o \exp \left(- \frac{E_a}{RT} \right) \tag{21}$$

K_o is the reaction frequency factor in 1/s, E_a is the activation energy in kJ/mol, R is the gas constant in J/molK, and T is the absolute temperature in K.

Zanoni et al. [28] determined the kinetics of the starch gelatinization process as a function of heating temperature and time and the results showed that no gelatinization occurred below 65 °C and that with increasing temperature the extent of gelatinized starch increased. A comparison of heating time and temperature shows that at 70 °C G is equal to 0.39 after 180 s, whereas the same value is reached at 79 °C after 20 s [28].

The gelatinization process is accompanied with protein denaturation, at a temperature range of around 65 °C, where water is set free. For the gluten coagulation it is essential that the lower the water content, the higher the denaturation temperature of proteins [20]. Likewise the starch gelatinization, the time scale of gluten denaturation is not well reported in literature. For proteins systems in general the time scale reported is 10 ns at a length scale of 10 μm [1]. The knowledge of these time scales would help to understand and optimize the whole process since especially starch gelatinization is heavily linked to the solidification, therewith change in permeability effecting diffusion and end of baking.

Table 3 Estimated characteristic times for model cereal based foam at T=100 °C

Description	Characteristic time
Rayleigh collapse time $t_{RC} = 0.915 \left(\frac{\rho_l}{P_{G0}} \right)^{\frac{1}{2}}$	$5.4 \cdot 10^{-5}$ s
Surface tension time $T_R = \sqrt{\frac{\rho R^3}{\sigma}}$	$2.1 \cdot 10^{-3}$ s
Diffusion time $t_D = \frac{R^2}{D}$	
Moisture diffusivity crumb	2.7 s
Moisture diffusivity crust	10.0 s
Moisture diffusivity bubble	$1.3 \cdot 10^{-2}$ s
Moisture diffusivity solid	83.3 s
Thermal diffusivity crumb	$5.0 \cdot 10^{-1}$ s
Thermal diffusivity crust	$6.6 \cdot 10^{-1}$ s
Thermal diffusivity bubble	$1.3 \cdot 10^{-2}$ s
Thermal diffusivity solid	1.6 s

Time Scale Estimation

From the analysis in the previous sections it can be seen that multiple time scales are associated to the whole process. To compare the time scales of each separate process, the characteristic times are calculated for a control area, with radius 0.0005 m at a temperature of 100 °C, according to the corresponding equations as given in Table 3. The characteristic time for phase transition of water vapor is reported in literature with a value of 7 μs [41]. In addition, the characteristic times for heat and mass diffusion processes, as well as bubble collapse and surface tension, are calculated according to literature values of thermo-physical properties of the proposed cereal based foam, which are summarized in Table 2.

Figure 4 shows the time-line for both, macroscopic as well as microscopic processes and thus allows a direct comparison of the involved processes and their impact on each other.

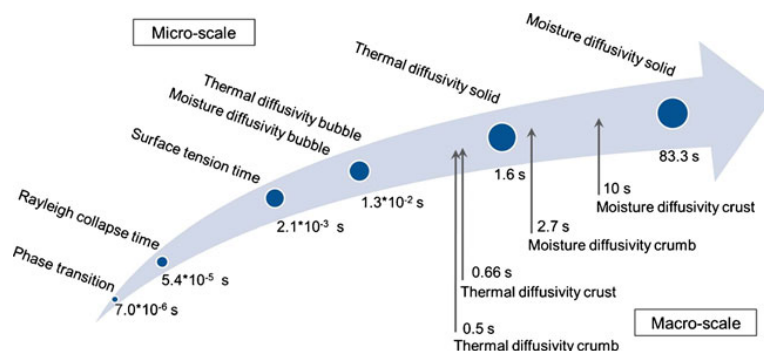
The moisture as well as the thermal diffusion processes in the cell wall (in Fig. 4 labeled as solid) and through the crumb and crust occur on a much larger time scale than inside the bubbles. This leads to the conclusion that the

moisture as well as the thermal diffusion rate is governed by the gaseous phase and limited by the solid cell walls. The thermal diffusivity is of impact for the heating rate of the whole system, from the time scale analysis it can be seen that the thermal diffusivity of vapor is 2 orders of magnitude higher than the thermal diffusivity in the cell walls. The higher required time for moisture diffusion inside the crust, in comparison to crumb, is reasoned by the different structural properties. The crust structure has a higher density, having smaller bubbles and thus acting as a barrier for moisture diffusion [17]. With 0.66 s, the thermal diffusion proceeds slightly slower in the crust than in the crumb, where the estimated time is 0.5 s. On the one hand, this might be explained by the absence of evaporation-condensation heat transfer in the crust, due to the lack of water [53]. On the other hand, following the assumptions of Zanoni et al., the increased thermal diffusion in the crumb may be reasoned by the different structural properties such as heat capacity and density, rather than evaporation-condensation [27]. The quick distribution of temperature is hence mainly driven by the heat transfer through the bubbles. Thus, these processes can be considered separately. The coupling of several processes is only of impact if they occur in the same time range [10]. The moisture diffusivity inside the bubble is in a similar time scale to the surface tension time, therefore both processes are directly linked to each other. In contrast, collapse proceeds on smaller time scale and is therefore limited by diffusion and surface tension.

Conclusion

The characteristic time scales are discussed and related to the multi-physics in cereal based foam under thermal treatment. The time scale estimation shows the coupling of processes from macro- to micro-scale and gives an impression on the governing processes. The largest time scales are occurring for macro-scale diffusion processes in crumb and crust and the smallest discovered time scale is for phase transition of water liquid to water vapor. Bubble dynamics,

Fig. 4 Time-line showing different time scales in macro- and micro-scale



such as bubble collapse, occur on a very small time scale, but is limited by diffusion and surface tension. Several researches have been done in the past to determine heat and mass transfer problems in cereal foams. Drawbacks are that they mainly focused on averaged macro phenomena of the system. Thus a deeper insight in the linkage of the processes from micro-scale point of view was disregarded in the past. Still challenging is the determination of characteristic times of chemical processes since they occur on very small time scales and is heavily influenced by environment conditions such as temperature, pH and medium. In addition it is difficult to determine the characteristic time of processes as e.g. phase transition and the relaxation time of a bubble wall in a multi bubble system. To fulfill such requirements, micro-sensing and micro-modeling approaches are promising tools especially against the background of increasing sensing technology in the micro-scale and computational power. To accomplish numerical modeling of a complex material in combination with multi-thermo-physical processes such time scale analysis is of impact to choose the best timescale to obtain stable solutions. In general each time can be used, but based on the latter, it is reasonable to choose the smaller time scale.

References

1. B. Bagchi, C. Chakravarty, *Curr. Trends Sci.* **75**, 67–78 (2009)
2. J.M. Aguilera, *J. Sci. Food Agric.* **86**, 1147–1155 (2006)
3. K. Thorvaldsson, C. Skjöldebrand, *Lebensm.-Wiss. u. Technol.* **31**, 658–663 (1998)
4. S. Mack, M.A. Hussein, T. Becker, *J. Food Eng.* **116**(2), 344–351 (2013)
5. K. Thorvaldsson, C. Skjöldebrand, *J. Food Eng.* **29**, 13–21 (1996)
6. N. Perrot, I.C. Trelea, C. Baudrit, G. Trystram, P. Bourguin, *Trends Food Sci. Technol.* **22**, 304–314 (2011)
7. S. Guessma, L. Chaunier, G. Della Valle, D. Lourdin, *Trends Food Sci. Technol.* **22**(4), 142–153 (2011)
8. P. Fito, M. LeMaguer, N. Betoret, P.J. Fito, *J. Food Eng.* **83**, 173–185 (2007)
9. I.F. Vasconcelos, I. Cantat, J.A. Glazier, *J. Comput. Phys.* **192**, 1–20 (2003)
10. H. Xiao, Y.L. Young, J.H. Prévost, *Int. J. Numer. Anal. Methods Geomech.* **34**, 1935–1959 (2010)
11. L. Hailemariam, M. Okos, O.A. Campanella, *J. Food Eng.* **82**, 466–477 (2007)
12. J. Berthier, P. Silberzan, *Microfluid. Biotechnol.* Artech house Norwood (2010)
13. S. Uthayakumaran, M. Newberry, N. Phan-Thien, R. Tanner, *Rheol. Acta.* **41**, 162–172 (2002)
14. J. Lefebvre, *Rheol. Acta.* **45**, 525–538 (2006)
15. P. Babin, G. Della Valle, H. Chiron, P. Cloetens, J. Hozzowska, P. Pernot, A.L. Reguerre, L. Salvo, R. Dendievel, *J. Cereal Sci.* **43**, 393–397 (2006)
16. K. Thorvaldsson, H. Janestad, *J. Food Eng.* **40**(3), 167–172 (1999)
17. E. Purlis, V.O. Salvadori, *J. Food Eng.* **91**, 428–433 (2009)
18. A.H. Bloksma, *Cereal Foods World.* **35**, 228–236 (1990)
19. D.R. Jefferson, A.A. Lacey, P.A. Sadd, *Appl. Math. Model.* **31**, 209–225 (2007)
20. F.M. Vanin, T. Lucas, G. Trystram, *Trends Food Sci. Technol.* **20**, 333–343 (2009)
21. S.S. Sablani, M. Marcotte, O.D. Baik, F. Castaigne, *Lebensm.-Wiss. u.-Technol.* **31**, 201–209 (1998)
22. G.G. Bellido, M.G. Scanlon, J.H. Page, B. Hallgrímsson, *Food Res. Int.* **39**, 1058–1066 (2006)
23. M. Kokawa, K. Fujita, J. Sugiyama, M. Tsuta, M. Shibata, T. Araki, H. Nabetani, *J. Cereal Sci.* **55**, 15–21 (2012)
24. H. Huang, P. Lin, W. Zhou, *SIAM J. Appl. Math.* **68**(1), 222–238 (2007)
25. P. Shah, G.M. Campbell, S.L. McKee, C.D. RIELLY, *Trans. IChemE.* **76**(C), 73–79 (1998)
26. S. Mack, M.A. Hussein, T. Becker, (ECCE/ECAB, Berlin, Germany, 2011)
27. B. Zanon, C. Peri, R. Gianotti, *J. Food Eng.* **26**, 497–510 (1995)
28. B. Zanon, A. Schiraldi, R.A. Simonetta, *J. Food Eng.* **24**, 25–33 (1995)
29. J. Fan, J.R. Mitchell, J.M.V. Blanshard, *J. Food Eng.* **23**(3), 337–356 (1994)
30. A. Cordoba, *J. Food Eng.* **96**, 440–448 (2010)
31. B. de Cindio, S. Corra, *J. Food Eng.* **24**, 379–403 (1995)
32. J. Zhang, A.K. Datta, *AIChE J.* **51**, 2569–2580 (2005)
33. B. Zanon, C. Peri, *J. Food Eng.* **19**, 389–398 (1993)
34. M.A. Hussein, T. Becker, *Food Biophys.* **5**(3), 161–176 (2010)
35. S. Mack, M.A. Hussein, T. Becker, *J. Non-Equilib. Thermodyn.* **36**, 311–335 (2011)
36. A.K. Datta, *J. Food Eng.* **80**, 80–95 (2007)
37. W. Zhou, *Int. J. Comput. Fluid Dyn.* **19**(1), 73–77 (2005)
38. L. Zhang, T. Lucas, C. Doursat, D. Flick, M. Wagner, *J. Food Eng.* **80**, 1302–1311 (2007)
39. E. Chiotellis, G.M. Campbell, *Trans. IChemE.* **81**(C), 194–206 (2003)
40. P. Sluimer, C.E. Krist-Spit. 355–363 (Ellis Horwood, Chichester, 1987)
41. S. Fujikawa, T. Yano, M. Watanabe. (Springer Berlin, 2011)
42. J.W. Donovan, *Biopolymers.* **18**, 263–275 (1979)
43. L. Slade, H. Levine, *J. Food Eng.* **24**, 431–509 (1995)
44. J. Bikard, T. Coupez, G.D. Valle, B. Vergnes, *J. Food Eng.* **85**, 259–267 (2008)
45. M. Wagner, S. Quellec, G. Trystram, T. Lucas, *J. Cereal Sci.* **48**, 213–223 (2008)
46. A. Arefmanesh, S.G. Advani, *Rheol. Acta.* **30**, 274–283 (1991)
47. G.F. Oweis, J. Choi, S.L. Ceccio, *Acoust. Soc. Am.* **115**(3), 1049–1058 (2004)
48. B.J. Dobraszczyk, M.P. Morgenstern, *J. Cereal Sci.* **38**, 229–245 (2003)
49. H. Mirsaedghazi, Z. Emam-Djomeh, S.M.A. Mousavi, *Int. J. Agric. Biol.* **10**, 112–119 (2008)
50. B.K. Patel, K. Seetharaman, *Carbohydr. Polym.* **65**, 381–385 (2006)
51. T.D. Karapantsios, E.P. Sakonidou, S.N. Raphaelides, *Carbohydr. Polym.* **49**, 479–490 (2002)
52. M. Turhan, S. Gunasekaran, *J. Food Eng.* **52**(1), 1–7 (2002)
53. U. de Vries, P. Sluimer, A.H. Bloksma, *Cereal Sci. Technol. Sweden.* 174–188 (1989)

2.2.2 Tracking the thermal induced vapor transport across foam microstructure by means of micro-sensing technology

Journal of Food Engineering 116 (2013) 344–351



Contents lists available at SciVerse ScienceDirect

Journal of Food Engineering

journal homepage: www.elsevier.com/locate/jfoodeng

Tracking the thermal induced vapor transport across foam microstructure by means of micro-sensing technology

S. Mack*, M.A. Hussein, T. Becker

Group of (Bio-) Process Technology and Process Analysis, Faculty of Life Science Engineering, Technische Universität München, Weihenstephaner Steig 20, 85354 Freising, Germany

ARTICLE INFO

Article history:

Received 20 June 2012

Received in revised form 22 September 2012

Accepted 20 November 2012

Available online 7 December 2012

Keywords:

Micro-sensing

Humidity distribution

Cereal foam

Bread baking

Thermo-physics

Blockage factor

ABSTRACT

In thermally processed multiphase systems such as cereal based foam, the material characteristics as well as the thermo-physical processes are of major impact on the internal heat transfer rate. Improving and optimizing this production step would contribute to an enormous amount of energy saving, considering the high demand on bakery products in the world. Bread baking is a high complex process and the determination of the included processes and their relevance is not simple, since the main processes are occurring in the micro-scale. Heat transfer in cereal based foam is expected to depend mainly on the evaporation–condensation mechanism, therefore it is crucial to determine heat and mass transfer phenomena inside the bread. Due to the hazardous surrounding conditions, such as high temperature and humidity it becomes challenging to find applicable sensors working reliable under such conditions. This study shows the application of micro-sensors to examine temperature and humidity distribution inside the foam during heating and gives insight in the impact of water vapor on the heating rate due to evaporation–condensation.

© 2012 Elsevier Ltd. All rights reserved.

1. Introduction

Cereal based foam consists of a solid and a gaseous component. Simplified, the solid component can be described as a starch–gluten network, where water exists free as droplets, associated to starch and bound to protein (gluten). The gas component develops during a fermentation period according to yeast metabolism and consists mainly of CO₂, besides some fermentation by-products which will be neglected in this study due to their minor amount. During the baking step, the foam undergoes several tremendous changes (Purlis and Salvadori, 2009):

- Structural changes: elevated temperatures cause evaporation of CO₂ and water vapor and therewith expansion of the gas bubbles and the whole material, restricted by the characteristic elasticity of the dough (Zhang and Datta, 2005).
- Water transport: evaporation to the surrounding and evaporation–condensation based pressure driven flow toward the coldest spot (Wagner et al., 2007).
- Starch gelatinization and protein denaturation, associated with water absorption and release, yielding to solidification of the structure (Zanoni and Peri, 1993).
- Crust formation (Vanin et al., 2009).

- Chemical reactions such as browning reactions or flavor development (Zanoni et al., 1995).

In cereal based foam, heat transfer is known to depend mainly on the evaporation condensation-mechanism (Thorvaldsson and Janestad, 1999; Purlis and Salvadori, 2009; Sablani et al., 1998). This assumption grew based on the findings of (De Vries et al., 1989), who determined that heat transfer in fermented dough is much quicker than in unfermented dough. Since the porous structure should cause insulating properties, the quicker heat spread was expected to depend on the present water transferring the heat according the heat pipe principle (Sluimer and Krist-Spit, 1987). When the dough is heated, heating up the gas pores yields to evaporation of water at the warmer side and re-condensation on the colder side, thereby cyclic absorbing and setting free the latent heat of vaporization (Wagner et al., 2007), see Fig. 1.

Facts counting for this theory are the plateau of 100 °C reached in the end of baking, since temperature is not rising as long as there is still water present to evaporate.

From a physical point of view this process should lead to an increase in pressure driven moisture toward the coldest spot of the loaf (Thorvaldsson and Janestad, 1999; Purlis and Salvadori, 2009). Besides the evaporation–condensation driven mass transfer, vapor transport through the open porous structure occurs depending on total pressure gradients in the gas phase of the foam following Darcy's law, which describes the pressure dependent discharge rate through a porous medium. In addition, water gradients in the

* Corresponding author. Tel.: +49 08161 71 3661; fax: +49 08161 71 3883.
E-mail address: s.mack@wzw.tum.de (S. Mack).

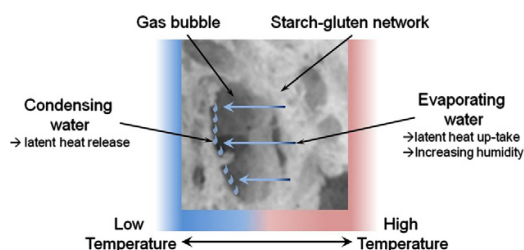


Fig. 1. Basic structure of the cereal based foam consists basically of a starch–gluten network and gas bubbles. Liquid dough water is evaporating toward the bubble, absorbing latent heat of vaporization which yields condensation at the colder side of the bubble and thereby setting free the latent heat.

continuous liquid phase are responsible for moisture migration by diffusion according to Fick's law.

Gradient-driven evaporation from the surface of the dough occurs under isothermal conditions until equilibrium is reached and elevated at higher temperatures due to the dependency of the saturation vapor pressure on the temperature. At higher temperatures air can contain more humidity than at lower temperatures. This can be explained by the fact that a higher temperature means more energy is provided to the system supplying water molecules with energy to overcome the bindings and evaporating, therewith increasing the partial vapor pressure (Valson and Bharat, 2011).

Determining such processes experimentally is challenging due to the high temperature, complex interacting and coupled mass transfer processes. In general 2 main approaches exist to measure the moisture content, destructive methods, where the dough is cut during baking and the amount of water is analyzed, and inline sensing.

The first approach was carried out by cutting bread samples in several unique pieces with increasing baking time and determined the moisture content. Their results showed that water content decreases in the crust, but remains constant throughout the crumb with a value of 44% (Zanoni and Peri, 1993). Unquestionable is the fact that a decrease in moisture occurs from the crust due to the close vicinity to the high temperature surrounding yielding to increased evaporation. At the same time the high dehydration rate in the crust yields to incomplete starch gelatinization and increased heating rate, being responsible for denser pores, different structural properties, acting as a water evaporation barrier from crumb to the surrounding. Thus making sense that crumb moisture content remains the same, but nonetheless it is questionable if the used method (Zanoni and Peri, 1993) is sensitive enough to detect small changes inside the crumb. A similar method was used (Wagner et al., 2007), but contradictive to the previous elaborated findings, they detected an increase in water content in the bread center after 4 min after the beginning of baking and equalizing to the initial value after 7 min baking when temperature reached to 65 °C (Wagner et al., 2007). The authors came to the conclusion that the evaporation–condensation mechanism even takes place when the pores are not connected. Undesirably invasive measurement destroys the material, and especially at elevated temperatures it is self-evident that destructing the material yields to increased evaporation making reasonable results doubtful, as can be seen in the contrary results (Wagner et al., 2007; Zanoni and Peri, 1993). The same method was used (Purlis and Salvadori, 2009), and again, different results in the crumb were achieved. The whole crumb maintained the same water content like the dough, but an increase in the center was detected throughout the whole process. Their conclusion was that evaporation–condensation takes place

during the whole baking time, and is not depending if structure is opened or closed (Purlis and Salvadori, 2009).

Another approach was proposed to measure the water content by the use of a Near Infrared (NIR) probe (Thorvaldsson and Janestad, 1999). Unfortunately their results did not contribute to enlighten the moisture distribution, because their results showed that below the structural change temperature of 70+–5 °C the water content in the center decreased, but as soon as this temperature level has passed, water content in the center rose toward the coldest spot. The authors explained this by the evaporation–condensation mechanism which accounts for vapor transport from warmer regions toward the coldest spot (Thorvaldsson and Janestad, 1999). The initial decrease of water is explained by the oven rise, whereas the “real” water content may stay the same. Water is said to be prevented from moving due to the closed structure below 70 °C. Furthermore, the transport was said to rely on the temperature gradient, and water transport stops when the temperature reaches 100 °C. Drawback of their study is the problem of calibrating the NIR to measure the moisture content. An approach to overcome this problem was carried out by reheating rolls, therefore excluding the initial dough phase (Wählby and Skjöldebrand, 2001). In the crust, the moisture content decreased almost linearly until zero, whereas the moisture content in the center decreased in the beginning and then equalized at a water content of 40+–5 g water/g dry matter. The method may have overcome the dough calibration problem, but nevertheless, the results are again contrary to all the previous findings. Nevertheless the application of inline sensing is favorable to cutting since it is nondestructive. On the other hand, the advantage of destructive methods is that the whole water content can be determined.

The objective of this study is to determine the humidity distribution in cereal based foam whilst baking by micro-sensing.

The application of miniature sensors gives the advantage to examine vapor transport at a small scale together with minimal destruction of the foam structure. Furthermore, the impact of water vapor on the heating rate is estimated to investigate the effect of evaporation–condensation heat transfer.

2. Materials and methods

2.1. Dough preparation and baking conditions

The wheat dough is prepared based on a standard recipe using 1000 g flour (Schapfenmühle, Ulm, Germany, german type 550), 590 g water (based on 14% flour humidity), 13 g dry yeast (Instant yeast Fermipan red, species: *Saccharomyces cerevisiae*, Casteggio Lieviti srl, Casteggio, Italy), 18 g salt (Salt, iodized (minimum 0.0025% potassium iodate), Südsalz GmbH, Bad Friedrichshall, Germany) and 30 g malt (Ulmer Spatz, Ulm, Germany). The ingredients are mixed for 1 min at 25 Hz and kneaded for 6 min at 60 Hz in a spiral kneader (Model SP-12, DIOSNA Dierks & Söhne GmbH, Osnabrück, Germany) and placed for 20 min in a fermentation trunk (Wachtel Stamm GmbH, Hilden, Germany) at a temperature of 30 °C and a humidity of 80%. After this rest, the dough is formed to pieces of 600 g and placed in covered baking forms with the dimensions 250 × 120 × 76 mm (BÄKO Marken und Service eG, Bonn, Germany). In this step, the humidity sensors are placed inside the dough to prevent posterior destruction of the structure. Afterward, the loaf has a second rest for 75 min in the fermentation trunk, at same conditions as previously mentioned. The loaf is baked in a convection oven (Model SCC-61, Rational AG, Landsberg am Lech, Germany) for 60 min at a temperature of 180 °C. The volume of the baking chamber is 197 L, and the rotations of the fan are 5001/min.

2.2. Micro-sensing of humidity and temperature distribution

The humidity and temperature distribution inside the loaf is measured with a detecting element (RFT-XXS), which is applicable at temperatures up to 120 °C and relative humidity of 100% and its dimensions are 3 mm diameter, and 12 mm length. The individually calibrated micro-sensor (SHT21, Sensirion, Switzerland) is composed of a band gap temperature sensor and a capacitive humidity sensor. The sensors' accuracy tolerance in terms of relative humidity has a value of +/-2.0% RH, repeatability is +/-0.1% RH, hysteresis is +/-1% RH and response time is 8 s. For temperature measurement the accuracy tolerance is +/-0.3 °C, repeatability is +/-0.1 °C and response time is 30 s.

Relative humidity is defined as the ratio of present humidity to the maximum possible humidity at the given temperature. In another expression, as shown in Eq. (1) the relative humidity is the ratio of the partial water vapor pressure to the saturated vapor pressure (Sonntag, 2003).

$$RH_w(t) = \frac{P}{P_w(t)} * 100\% \tag{1}$$

where RH is the relative humidity [%], P is the partial vapor pressure [kPa], and P_w(t) is the saturation vapor pressure [kPa].

In a closed system, the relative humidity is 100% when equilibrium is reached. The drawback occurring here is that the proposed material is not a closed system and equilibrium conditions will never be reached. At each temperature level, there is a maximum amount of water vapor which can be held by air, represented by the maximum partial vapor pressure. In a closed system at constant temperature, both evaporation and condensation are in equilibrium at the temperature dependent specific partial vapor pressure, which is the saturated vapor pressure. The characteristic behavior of relative humidity can be described as follows: During cooling, the partial pressure will stay constant for a whilst, simultaneously the relative humidity will increase due to the decreasing saturation vapor pressure. Vice versa, during heating the relative humidity will decrease since the saturation vapor pressure increases. But since the proposed system has a water source (the solid dough parts), more molecules will overcome the energy required for evaporating and therefore the relative humidity will increase during baking.

The absolute humidity is defined as the ratio of the mass of water vapor per volume. Relating it to the relative humidity of the system, the absolute humidity d [g/m³] is given by Eq. (2).

$$d = 216.7 * \frac{RH}{100\%} * \alpha * \exp\left(\frac{\beta * T}{\lambda + T}\right) \tag{2}$$

where RH is the relative humidity [%], T is the temperature [°C] and the coefficients α = 6.112 [kPa], β = 17.62 [-] and λ = 243.12 [°C].

In each baking trial one sensor is placed inside the dough during the forming step, therefore the sensor is moving together with the bulk during fermentation induced expansion. The dough is rolled out, the sensor is placed in the middle, left and right sides of the flat dough are folded to form a loaf. Since baking is performed in a closed baking form, and the final height of the loaf is reached after fermentation, and due to the high viscosity of the dough structure, sensor position changes that are of minor significance. The position of the sensor is varied in each trial to gain insight in the distribution throughout the whole cross-section of the loaf, where each position is repeated 3 times. After baking, the position of the sensors is measured manually. The probe is connected via a cable to a data logger (humilog 325, Driesen + Kern GmbH, Germany), and measurement reading is every 2 s. Besides the temperature and humidity measurements, the average water loss is determined during baking via weighing (Sartorius 3100 S-G, Sarto-

rius AG, Göttingen, Germany) in another series of experiments. Therefore, the loafs are taken out of the oven and weighed with a sampling rate of 10 min.

After the baking step, the loafs are cooled down at room temperature and reheated again under the same conditions as the baking step (60 min, 180 °C). This procedure is carried out to deliver deeper insight into the humidity flux, on one hand to compare the same loaf at different initial moisture contents. And on the other hand to be independent of possible structural changes since structure is fixed in the reheating step.

2.3. Blockage factor

Even though inline sensing is favorable to a destructive method, the inclusion of the sensor inside the material is affecting the measurement. Therefore, the blockage factor was calculated.

A blockage factor calculation is important to get a feeling of the impact of how the sensor influences the flow field and therewith the measurement itself. The moisture flux is partially blocked by the sensor, thus interacting in real flow conditions. Nevertheless this influence should be as small as possible, that is why the smallest sensor available on the market fulfilling the operating conditions was chosen for the measurement.

In a 3 dimensional space, the blockage factor can be calculated as follows (Sahini, 2004), Eq. (3), where A is the area in m².

$$\phi = \frac{A_{Sensor}}{A_{Loaf}} \tag{3}$$

The loaf has a cross section area of 0.019 m², and the sensor has a diameter of 4 mm, with the given values, the blockage factor for the whole material is 0.00264.

The time scale analysis for the proposed phenomena clearly shows that the mass flux through the medium is mainly driven by the flow through the gas phase. Thus, the above estimation is acceptable from a macro-scale point of view, since the gas phase exists of a continuous network of connected bubbles. It is recommended that the blockage should be less than 5%, otherwise a blockage correction should be applied (Sahini, 2004).

3. Results and discussion

3.1. Humidity and temperature distribution

The big advantage of the experimental set-up is that the relative humidity and temperature sensor are combined in one miniature probe, allowing simultaneous measurement of both properties at the same time at the same place. To get insight of the vapor diffusion through the loaf, measurements were carried out throughout the whole middle-cross section of the loaf. Humidity was measured in combination with the temperature at several spots inside the loaf. The experimental set-up is illustrated in Fig. 2.

Challenging in such measurements is that the relative humidity is depending on the vapor pressure, and that the saturation vapor pressure is temperature dependent. If there is a specific amount of water vapor in a closed system, the relative humidity will decrease with increasing temperature due to the temperature dependent saturation pressure. If a water source is present in the closed system and temperature is increased to a higher level, then water will evaporate until again the equilibrium is reached. Important to note is that reaching equilibrium is lagging behind the saturation pressure increase. In an open system, the equilibrium will not be reached due to the high mass diffusivity of water vapor. To get a better understanding of the humidity measurements, the dough is first considered as a closed system to apply the thereby gathered knowledge to the real measurements.

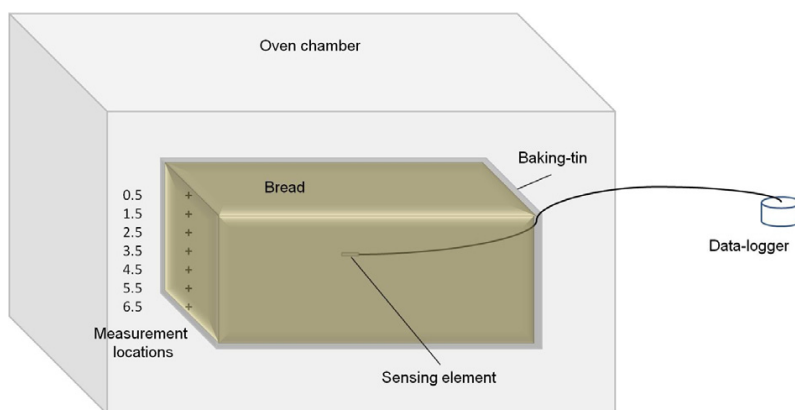


Fig. 2. Sketch of the experimental set-up. Measurement points inside the loaf marked with a cross; distances from the top are 0.5, 1.5, 2.5, 3.5, 4.5, 5.5, and 6.5 cm.

After fermentation, the dough has an average temperature of 27.4 °C with a standard deviation of 0.75 and a relative humidity of 92.6% with a standard deviation of 0.68. Based upon the initial values the absolute humidity is calculated according to Eq. (2). Initial Absolute humidity is 88.6 g/m³, which means that this is the amount of water molecules present in the gas phase at a temperature of 27.4 °C. If the loaf would be a closed system and no water would evaporate from the solid dough phase, then this initially absolute humidity would be equal to the maximum amount of water vapor in the gas phase. Based upon this assumption the related relative humidity for every temperature can be calculated and the results are shown in Table 1.

Theoretically, if no water would evaporate from the solid dough phase, the measured relative humidity in the gas phase would be around 14% in the end of baking due to the temperature dependent change in water vapor saturation pressure. Therefore the difference between the really measured relative humidity and the theoretically estimated relative humidity of 14% is the evaporated water vapor from the solid dough phase.

The results of the simultaneously measured temperature and humidity distribution are shown in Fig. 3. Measurement points are vertical cross-wise through the loaf. Humidity is represented here as the difference of initially measured relative humidity and the measured relative humidity at time *t*, allowing more precise comparison of humidity distribution at the different locations.

Respectively, for both properties, temperature and relative humidity gradient, results can be distinguished in two phases, the initial phase covering around 1/3 of the whole baking time, where a sharp increase of temperature is obligatory and the temperature progression is following sigmoid behavior in all locations followed by a second phase covering the last 2/3 of baking time,

Table 1
Theoretical relative humidity of 88.6 g/m³ water vapor at temperatures from 0 °C to 100 °C.

T [°C]	P _w [kPa]	P [kPa]	RH [%]
0	6.1	0	0
28	37.7	34.5	91.5
30	42.3	37.2	87.9
40	73.7	51.2	69.5
50	123.5	66.1	53.5
60	199.9	81.8	40.9
70	314.0	98.3	31.3
80	479.5	115.6	24.1
90	713.9	133.7	18.7
100	1038.5	152.6	14.7

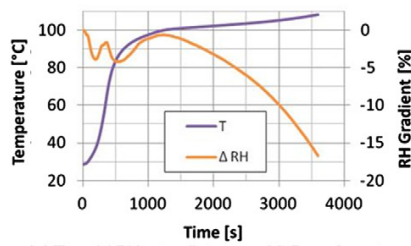
where the temperature reaches a plateau of around 100 °C. Only in a distance of 0.5 cm the temperature leaves the plateau level and increases up to 108 °C. The plateau develops due to continuous evaporation–condensation, limiting the maximum reachable temperature to 100 °C. In a distance of 0.5 cm, the water evaporates quickly to the surrounding, where the lack of water vapor allows the increase in temperature. The evaporation to the surrounding can be seen in the progression of the relative humidity in this location which is decreasing significantly after a temperature of around 98 °C is reached. At this location, the standard deviation of temperature is 5.3 °C and for relative humidity it is 12.1%. The big deviation may be reasoned by the close vicinity to the crust and the ambient. Comparatively, the standard deviation at the other locations in the crumb is much smaller, see Table 2.

In comparison to the progression at the other measuring points, the relative humidity is not exceeding the initial value. At the other locations, the RH is higher at the end of baking compared to the initial value, but to a different degree for each measurement point. It can be seen that the highest gradient is reached at 4.5 cm from the top, which is equal to the coldest spot, but not the center of the loaf.

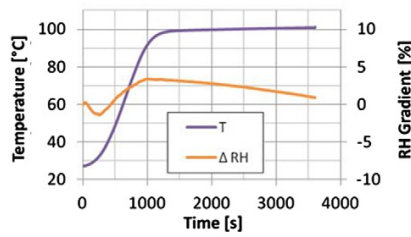
In the first part, the RH is generally first decreasing, followed by an increase according to the increase of temperature. As soon as the relative humidity plateau in the second part is reached, the RH is decreasing slightly and following the characteristic trend of each location.

The behavior in the initial stages may be induced by the oven rise. During oven rise, structural changes occur caused by gas bubble expansion and compression, and the previously closed structure opens and becomes available for simplified diffusion processes through the material. Therefore the former “closed system” with a specific amount of water vapor molecules is suddenly increasing its volume, yielding in a decrease of RH due to the same amount of water vapor molecules in a bigger volume. Certainly, equilibrium is favorable, but requires some time to adapt to the new situation, this is where the RH starts to increase according to the increasing temperature. Increasing temperature yields to increased evaporation of water molecules from the solid dough to the gas phase.

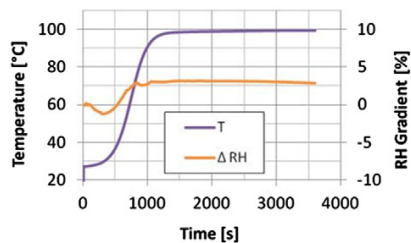
Whilst in the second part the humidity is decreasing in each location, the trend in the 4.5 distance point is conversely, indicating that the vapor is diffusing toward the coldest spot. Since this increase in the middle region of the loaf is very small, the absolute humidity is calculated giving a closer link to the actual amount of water vapor in each location. the measured values at the end of



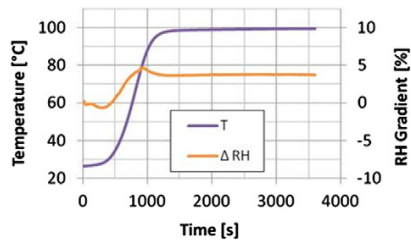
(a) T and ΔRH at a distance of 0.5 cm from top



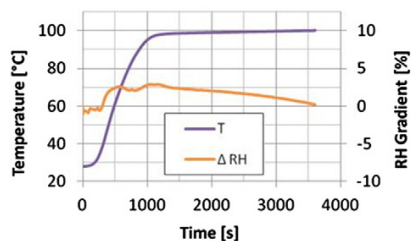
(b) T and ΔRH at a distance of 2.5 cm from top



(c) T and ΔRH at a distance of 3.5 cm from top



(d) T and ΔRH at a distance of 4.5 cm from top



(e) T and ΔRH at a distance of 6.5 cm from top

Fig. 3. Measurement results of temperature and relative humidity at several locations from 0.5–6.5 cm from top, showing the differing progression of relative humidity in each location.

baking, the real values as well as the gradient of each parameter are plotted in Fig. 4. As already seen in Fig. 3, the humidity is the highest in the location of lowest temperature.

Table 2

Temperature and relative humidity values at the end of baking.

Location [cm]	STD T [°C]	STD RH [%]
0.5	5.3	12.1
1.5	0.3	0.7
2.5	1.4	3.7
3.5	0.2	0.9
4.5	0.3	0.7
5.5	1.0	3.4
6.5	0.2	0.4

The gradient is calculated and is shown to exclude measurement variations and misinterpreting of the results due to these variations. The results show that in 0.5 cm distance to the ambient (at the top of the loaf) the loss of water vapor is immense, -100.9 g/m^3 . The situation is different in the bottom of the loaf, the absolute humidity there rose about 1.4 g/m^3 .

Unfortunately it is not possible to determine how much the water vapor has evaporated to the surrounding and how much it has evaporated from the solid dough to the gas phase in the dough. The reason that the value in the bottom is much higher than in the top is reasoned by the restricted contact to the ambient limiting moisture diffusion to the outside. In the middle of the loaf, the values for RH and absolute humidity are higher than those in the outer regions. This may be due to lagged evaporation to the ambient reasoned by the bigger distance, or by evaporation condensation based pressure driven flux to the coldest spot.

Indications that evaporation–condensation pressure driven flux that occurs inside are given by:

1. The absolute humidity as well as the relative humidity are higher at location 4.5 than in 3.5 (which is the center). Therefore the humidity is the highest at the coldest spot. If the higher humidity content would only be reasoned by the higher temperature then the humidity at 3.5 should be higher since it can be expected that both locations are not exposed to the moisture loss at this stage of baking.
2. In Fig. 3, there is a slight increase in RH detectable in the location 4.5 (in the second part of baking).
3. In Fig. 3, there is an increase in RH detectable in the location 3.5 followed by a decrease, which indicates that this vapor is flowing to the inside (in the second part of baking).

To get deeper insight in the impact of water vapor and evaporation–condensation on the heating rate, the baked bread was reheated after cooling and the results are shown in Fig. 5.

Comparing the baking and the reheating curves directly, see Fig. 5, the comparison shows that the baking curve follows a more

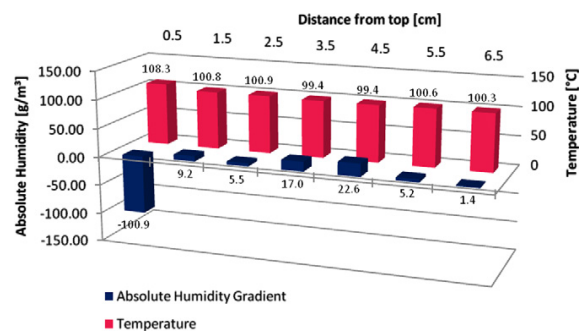


Fig. 4. Absolute humidity gradient at measurement locations showing the values at the end of heating.

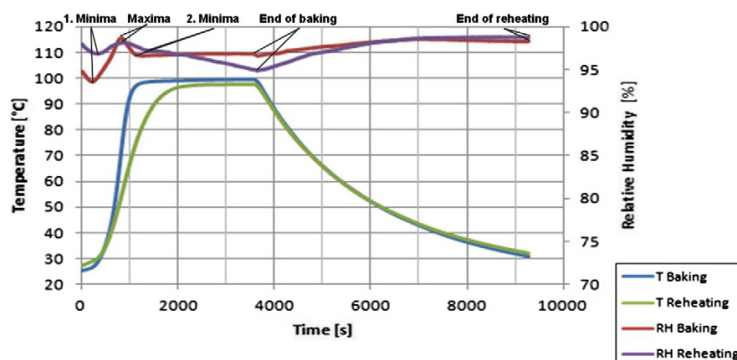


Fig. 5. Relative humidity and temperature distributions for baking and reheating at the location 4.5 cm from top.

step increase than the reheating. This can be explained by the less amount of water. This effect becomes crucial when a temperature of 56 °C is reached. The quicker temperature increase is reasoned by the evaporating water which accounts based on evaporation–condensation on an increased heating rate. The according heating rates are shown in Fig.6.

During both heating steps, the RH curve shows the same trend in the first part, just with a different amplitude, reasoned by the less amount of water in the reheating step. In addition, the maxima and minima of the relative humidity curve show similar behavior, the corresponding values are given in Table 3.

The first minimum is reached after around 5 min which is equal to the range of time oven rise takes place. In this period the relative humidity is decreasing due to an increase in volume. Even though the structure is already fixed in the reheating process and no bub-

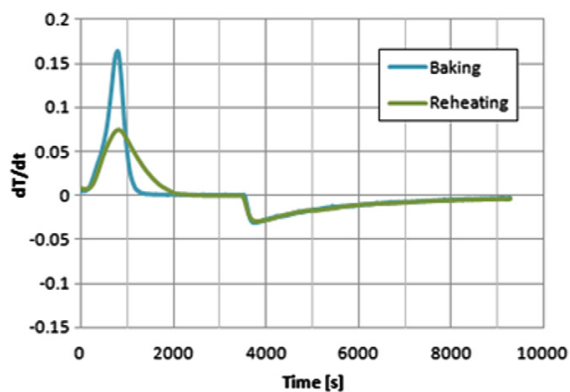


Fig. 6. Comparison of dT/dt of baking and reheating, showing that in the initial stage of heating temperature increase proceeds much quicker than in the reheating step.

ble dynamics occurred a slight increase in the volume takes place due to internal gas expansion. In the baking trial, the relative humidity maximum is reached at a temperature of 76 °C which is the temperature range where starch is gelatinizing, subsequently, the relative humidity is decreasing, which may be explained by the water up-take of the starch gelatinization process. The second minimum is reached at a temperature of 96.4 °C. At this stage the biochemical reactions like starch gelatinization and protein denaturation are already finished and the structure got solidified. The significance of starch gelatinization on heat and mass transfer mechanisms during baking is due to the complexity of interfering processes which is not easy to determine, but the presented results indicate their relevance on heat and mass transfer. From now on the relative humidity is slightly increasing, which may be reasoned by evaporation–condensation based mass transport. Comparatively, in the reheating curve the relative humidity is decreasing at this stage due to the minor amount of water present yielding to increased diffusion to the surrounding due to immense vapor pressure differences.

The contrariwise characteristics of relative humidity during baking and reheating, when the temperature plateau is reached, are resulting in a RH gradient of 1.9% for baking and reheating in the end of baking. Interesting enough that despite this difference, the RH humidity during cooling reaches an almost equal value. As soon as the temperature effect is not ostensibly affecting the RH progression, the hygroscopic properties of the bread become significant which means that after cooling when the system reaches equilibrium temperature as well as its relative humidity, the relative humidity in the product is depending on the hygroscopy of the crumb, independent of the moisture content (at least in the small difference range analyzed here).

Another interesting point to mention is that the maximum temperature in the reheating phase is lower than that in the baking trial, 99.4 °C in the baking, and 97.9 °C in the reheating step. This experiment was repeated 4 times and showed always the same characteristics.

Table 3
Temperature and relative humidity values at the minima and maxima of the relative humidity curve shown in Fig. 5.

Baking	Time [s]	T [°C]	RH [%]	RH [%]	T [°C]	Time [s]	Reheating
1. Minimum	296	27.8	92.2	96.8	29.9	326	1. Minimum
Maximum	852	76.7	98.7	98.2	57.4	868	Maximum
2. Minimum	1180	96.4	96.7	97.4	81.4	1258	2. Minimum
End of baking	3600	99.4	96.8	95.0	97.9	3600	End of reheating
End of cooling	9236	31.2	98.3	98.8	31.2	9510	End of cooling

To magnify the different heating rates, the slope of both temperature curves is plotted in Fig. 6.

The slope is calculated according to finite difference scheme for second order accuracy as shown in Eq. (4), with a sampling frequency of 50 points.

$$\frac{\partial T}{\partial t} = \frac{T_{i+1} - T_{i-1}}{2 * \Delta t} \tag{4}$$

This illustration shows clearly the difference of the heating rate with different amounts of water. The peak of heating rate is reached simultaneous, but the amplitude is lower and broadened in the reheating case. From the difference of baking and reheating the impact of evaporation condensation can be estimated and at which time this process becomes the driving process for heat transfer. According to Eq. (5), the latent heat describes the amount of energy required for a phase change (Sonntag, 2003).

$$Q_V = m_V L_V \tag{5}$$

where *m* is the mass of water [kg] evaporated from the crust <100 °C, *L* is the latent heat of vaporization 2260 [kJ/kg] (Sonntag, 2003).

The heat stored as latent heat as given in Eq. (5), in the baking case, there is Δ*m* of 128.9 g more water vapor inside the system, resulting in Δ*Q* of 291.2 kJ more heat available to transfer heat by evaporation–condensation.

3.2. Water loss

Whilst baking and as well during cooling water evaporates from the loaf to the surrounding. Fig. 7, shows the water loss during baking, in the end of baking the mass of the loaf reduced about 20.6%. This value is quite high compared to literature values where the water loss during baking is stated to be in the range of 10–12% (Purlis and Salvadori, 2009).

Likewise Fig. 6, d*W*/d*t* is presented in Fig. 8, showing that maximum water loss occurs in the initial stages. This can be explained by the non-developed crust at the beginning of baking resulting in increased evaporation from the dough. As soon as the crust is developed, water evaporation is decreased.

The big amount of evaporated water may be reasoned by the baking conditions of relatively low temperatures and long baking time. During cooling the water loss is additionally 1.1%. During cooling the water is evaporating according to the concentration gradient differences with the ambient. During baking water vapor in the baking atmosphere has the positive effect of increased heat transfer toward the system, during cooling the evaporation has a refrigerating effect, which is also known as evaporative cooling. Such effect yields to 10% heat removing from the system for 1%

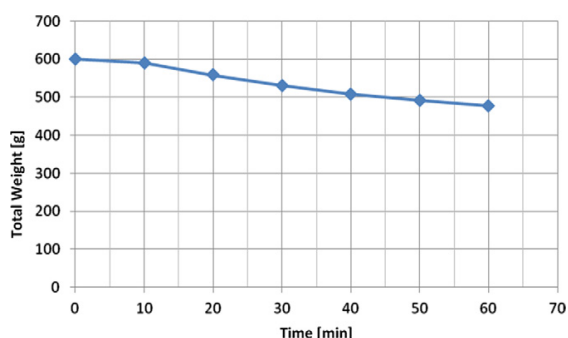


Fig. 7. Recorded water loss during baking with a sampling rate of 10 min.

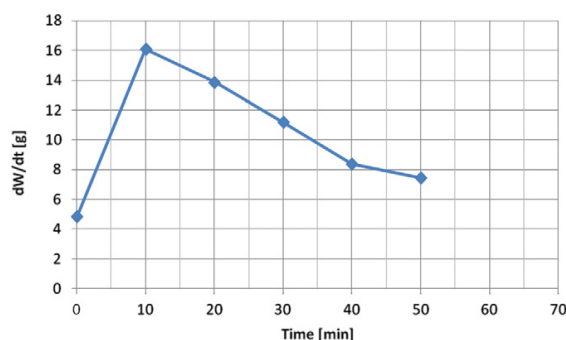


Fig. 8. d*W*/d*t* of baking, showing that in the initial stage of heating water loss proceeds much quicker than in the final stages.

Table 4 Water loss values for baking, reheating and the cooling steps and baking and reheating.

	Weight loaf [g]	Water loss [%]
Initial	600.0	0.0
Δ baking	123.7	20.1
Δ reheating	40.6	8.6
Δ cooling (after baking)	5.3	1.1
Δ cooling (after reheating)	3.1	0.7

water loss (Chung and Pfost, 1967). The water loss for each process stage is summarized in Table 4.

4. Conclusion

The literature survey as well as the presented results of this study, are showing clearly the challenge to measure the water content during baking, reasoned by the complexity of the system and the available measurement technology. Nevertheless, this study gives further insight in the vapor flux during the process. The high temperature conditions inside the product going along with structural changes lead to conditions where measurements of relative humidity become even more challenging due to the sensitivity of relative humidity on temperature changes. Despite this fact the results show the repeatability of the measurements and thus allowing realistic interpretation of the vapor flux through the inner product. Due to the high standard deviations near the crust conclusions can be drawn that the time range of crust setting is majorly influencing the vapor release to the surrounding. The results of the measurements are in agreement with the literature, and even more, they bridge the gap between the mismatching results of (Wagner et al., 2007) and (Thorvaldsson and Janestad, 1999; Purlis and Salvadori, 2009; Zaroni and Peri, 1993). In fact there is a decrease of humidity in the first 7 min of baking, and in fact there is afterward a change in the trend. Furthermore it could be shown that there is an increase of water vapor in the coldest spot of the loaf. First results are gathered to show the impact of the amount of available water vapor on the heating rate, which is increased if more water vapor is present. The presented results not only show the vapor flux through the product, but moreover lead to the conclusion that the amount of vapor has indeed an influence on the heating time required. Further work should be done with varying the amount of water added during dough preparation to compare this effect during baking. In addition, to measure the actual absolute humidity in the gas as well as in the solid components for water liquid and water vapor would a favorable objective to clearly

know what is really going on in the system, but it is doubtful to get an inline measurement system fulfilling this dream in the near future. Such drawback could be compensated by the application of numerical methods to simulate and visualize the processes for which there is until now no possibility to measure directly.

References

- Chung, D.S., Pfost, H.B., 1967. Adsorption and desorption of water vapor by cereal grains and their products part I. Heat and free energy changes adsorption and desorption. *Transaction ASAE* 10, 549–551.
- De Vries, U., Sluimer, P., Bloksma, A.H., 1989. A quantitative model for heat transport in dough and crumb during baking. In: *Cereal Science and Technology in Sweden, Proceedings of an International Symposium*, p. 174.
- Purlis, E., Salvadori, V.O., 2009. Bread baking as a moving boundary problem part 1: mathematical modelling. *Journal of Food Engineering*, 422–434.
- Sablani, S.S., Marcotte, M., Baik, O.D., Castaigne, F., 1998. Modeling of simultaneous heat and water transport in the baking process. *Lebensmittel-Wissenschaft & Technologie*, 201–209.
- Sahini, D. (2004). Wind tunnel blockage corrections: computational study. Master Thesis, Texas Tech University.
- Sluimer, P., Krist-Spit, C.E., 1987. Heat Transport in Dough During Baking. Ellis Horwood, Chichester, UK, pp. 355–368.
- Sonntag, R., 2003. *Fundamentals of Thermodynamics*. Wiley.
- Thorvaldsson, K., Janestad, H., 1999. A model for simultaneous heat, water and vapour diffusion. *Journal of Food Engineering*, 167–172.
- Valsson, S., Bharat, A., 2011. Impact of Air Temperature on Relative Humidity – A study. *Architecture – Time Space & People*.
- Vanin, F.M., Luca, T., Trystram, G., 2009. Crust formation and its role during bread baking. *Trends in Food Science & Technology*, 333–343.
- Wagner, M., Lucas, T., Le Ray, D., Trystram, G., 2007. Water transport in bread during baking. *Journal of Food Engineering*, 1167–1173.
- Wählby, U., Skjöldebrand, C., 2001. NIR Measurements of moisture changes in foods. *Journal of Food Engineering* 47, 303–312.
- Zanoni, B., Peri, C., 1993. A study of the bread-baking process. I: a phenomenological model. *Journal of Food Engineering*, 389–398.
- Zanoni, B., Schiraldi, A., Simonetta, R., 1995. A Naive model of starch gelatinization kinetics. *Journal of Food Engineering*, 25–33.
- Zhang, J., Datta, A.K., 2005. Transport processes and large deformation during baking of bread. *Bioengineering, Food, and Natural Products*, 2569–2580.

2.2.3 Examination of thermo-physical and material property interactions in cereal foams by means of Boltzmann modeling techniques

Microfluid Nanofluid
DOI 10.1007/s10404-013-1157-1

RESEARCH PAPER

Examination of thermo-physical and material property interactions in cereal foams by means of Boltzmann modeling techniques

S. Mack · M. A. Hussein · T. Becker

Received: 20 July 2012 / Accepted: 7 November 2012
© Springer-Verlag Berlin Heidelberg 2013

Abstract Cereal foam is a high complex material undergoing several temperature-dependent processes under thermal treatment, such as phase transitions, biochemical reactions and structural changes. Simultaneous heat and mass transfer plays an important role to investigate optimization studies in cereal-based foams. In porous media such as cereal foams, thermal conduction is of minor impact on the overall heat transfer, since the major part of heat is transferred through the gas phase filled with water vapor. This becomes evident comparing the thermal diffusivities of solid and gaseous components of the foam, where the difference is in the order of five magnitudes. The objective of this study is to model the coupled heat and mass diffusion processes in cereal-based foam under thermal treatment by means of Lattice Boltzmann methods. The proposed model is then used to perform parameter variation studies, showing the impact of material property changes offering the possibility on optimizing heat transfer through the foam.

Keywords Numerical modeling · Lattice Boltzmann · Simultaneous heat and mass transfer · Cereal foam

List of symbols

A Thermal diffusion coefficient
 Ω Collision operator
 τ Relaxation time
eq Equilibrium

f Particle distribution function
 v Velocity
 c Lattice speed of sound
 x Space coordinate
 e Direction vector
 w Weight factor
 ρ Density
 C Concentration
 Fo Fourier number
 L Characteristic length
 t Time
 D Mass diffusion coefficient

1 Introduction

Numerical modeling of heat and mass diffusion inside foam is a quite challenging task due to the complexity of the structure and processes occurring in the micro-scale. Classical continuum mechanics are describing the flow as a continuum by solving the Navier–Stokes equations. Such methods are known as macro-scale methods. They offer a powerful tool to model fluid flow if only a continuum description of the process is required. If more detailed insight in the microphysics of the flow is the objective, such methods are not recommended, since they fail in for low Knudsen numbers (Hussein 2010). Comparatively, the LBM is a meso-scale method. The advantage of the LBM is that the macroscopic flow is modeled in the spatio-temporal range where the flow originally happens on the particle level. As further plus, the Navier–Stokes equations and therewith the macroscopic flow properties can be recovered from the LBM equations bridging micro and macro scales (Succi 2001).

S. Mack (✉) · M. A. Hussein · T. Becker
Group of (Bio-) Process Technology and Process Analysis,
Faculty of Life Science Engineering, Technische Universität
München, Weihenstephaner Steig 20, Freising,
85354 Munich, Germany
e-mail: s.mack@wzw.tum.de

Published online: 26 February 2013

 Springer

Concerning cereal-based foam, numerical simulations of heat and mass transfer were mainly carried out by the use of continuum approaches (Purlis and Salvadori 2009; Zaroni and Peri 1993; Zhang and Datta 2006). Drawback of such studies is that the micro-scale properties are not taken into account directly and that even the foam structure is regarded as a continuum. To get detailed insight in the physical phenomena occurring on the pore level, the LBM offers the possibility to model such processes from a particle level. Challenging remains the combination of diffusion through porous structures in non-isothermal processes.

One possibility to account for the micro-structural properties of porous media is to apply effective diffusion coefficients. Xuan et al. (2010) developed a method to predict effective mass diffusivities of fluids in porous media (Xuan et al. 2010). They applied their LB-Model in 2 and 3 dimensions to regular and randomly structured porous media. The results show that they are in agreement with analytical Maxwell equation at low diffusivity gradients between grains and fluid (Xuan et al. 2010). Another approach to implement the porosity in a LB-model was carried out by Guo and Zhao (2002), by including the effect of porosity in the equilibrium distribution function (Guo and Zhao 2002). In addition, Darcy’s equation was included by the use of an additional force term. The presence of the force term allowed interactions between the fluid and the medium. For validation, several benchmark test cases were carried out in 2 dimensions and showed satisfactory results (Guo and Zhao 2002). Drawback of the proposed method is that the application is limited to isothermal single-phase fluid flows.

To account for thermal effects, McNamara et al. (1997) presented a three-dimensional multi-speed thermal LB-scheme achieving a temperature-scale by choosing the Boltzmann factor k to be unity. Beneficial to previous thermal LBM, the proposed method produces stable results without the restriction of the Prandtl number equal to one (McNamara et al. 1997). In another study, an additional distribution function is used to introduce temperature effects besides the standard distribution function for the velocity field (Guo and Zhao 2005). The method was used to simulate convective heat transfer in porous media for several applications. Hussein et al. applied the LBM to model simultaneous heat and mass diffusion in bread during baking in a simplified foam structure. In their simulations, heat transfer from the oven is ambient towards the bread as well as moisture loss due to diffusion to the surrounding was investigated (Hussein and Becker 2010).

The present study has the objective to examine SHMT in more realistic foam structures as well as accounting for mass diffusion processes from the solid foam component towards the gas component. Both points are investigated in

this study, where the foam structure is generated based on μ CT images and evaporation processes through the foam are considered. Furthermore, a parameter variation study is carried out to determine the impact of material properties on overall heat and mass transfer with the objective to optimize the baking process.

2 Materials and methods

2.1 Lattice Boltzmann method

The Lattice Boltzmann Method (LBM) is a numerical method considering fluid flow based on particle–particle interactions. Since the calculation of real particle–particle interactions would lead to heavy computation effort and time, due to the high amount of particles in a specific volume, the LBM considers the particles as a particle distribution function (Succi 2001).

The main equations of the LBM are based on Boltzmann’s equation, shown in Eq. (1) without external forces, which describes a particle distribution function f with time evolution on (Succi 2001).

$$\frac{\partial f}{\partial t} + v \nabla f = \Omega \tag{1}$$

where f is the particle distribution function, t the time, v is the particle velocity and Ω is the collision operator.

Discretizing the Boltzmann equation in time and space on a discrete lattice yields to the discrete Lattice Boltzmann equation, Eq. (2), for single-phase single-component fluid flow (Succi 2001).

$$f_i(x + e_i, t + \Delta t) = f_i(x, t) + \Omega_i(f(x, t)) \tag{2}$$

In Eq. (2), e is the unity vector and Δt represents the time step.

Basically, the calculations are of two steps, the streaming and the collision step. After initializing the solution, a set of particles is moving on the lattice, see Fig. 1, whilst the streaming step having specific speeds according to the lattice direction weights, see Table 1.

The streaming step is followed by a collision step, where particle–particle interactions are taken into account (Succi 2001).

$$\Omega_i(f(x, t)) = -\frac{f_i(x, t) - f_i^{eq}(x, t)}{\tau} \tag{3}$$

In the LBM, the original collision operator from the Boltzmann equation is replaced by an approximation and can be given by the Bathnagar–Gross–Krook (BGK) Model shown in Eq. (3). The particle distribution function is relaxed towards a local equilibrium f^{eq} , given in Maxwellian form, Eq. (4) (Succi 2001).

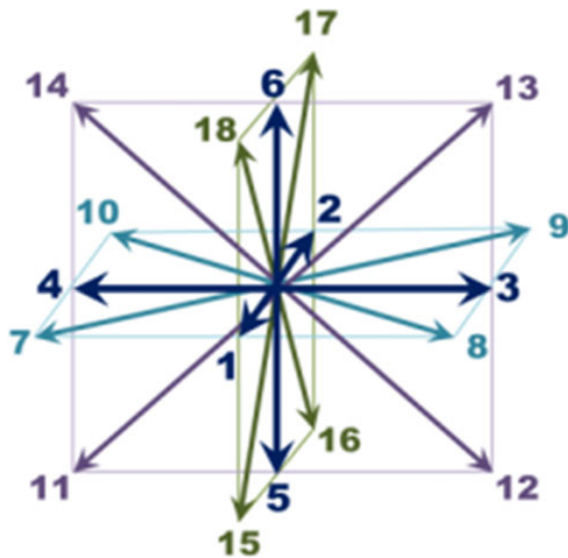


Fig. 1 Lattice with a D3Q19 scheme, representing a three-dimensional space with 19 velocity vectors

Table 1 Lattice weights for a D3Q19 Model

Direction \hat{e}_i	w_i
0	1/3
1, 2, 3, 4, 5, 6	1/18
7, 8, ..., 18	1/36

$$f_i^{eq} = w_i \rho(x) \left[1 + 3 \frac{\hat{e}_i v}{c^2} + \frac{9 (\hat{e}_i v)^2}{2 c^4} - \frac{3 v^2}{2 c^2} \right] \tag{4}$$

In Eq. (4) w is the weighting factor, ρ is the density, e is the unit vector, c is the lattice speed of sound, and v is the macroscopic fluid velocity.

Aligning the micro particle interactions, considered in Lattice units during the calculations, to the macroscopic world is done by two steps (i) recovery of the macroscopic values and (ii) conversion from Lattice units to SI units. On the one hand macroscopic properties can be derived from the calculations as shown for the macroscopic local density in Eq. (5) (Succi 2001).

$$\rho = \sum_i f_i \tag{5}$$

On the other hand, SI units of the macro process are converted to Lattice units (LU) allowing micro-scale calculations in the LB-scheme, and vice versa (Moaty Sayed et al. 2009). The methodology starts by choosing a dimensionless number describing the macroscopic process. Due to similarity considerations, the dimensionless number is used to obtain conversion factors for any proposed

property and the Lattice units can be retrieved (Mack et al. 2011), shown in detail for the application example in the following section.

$$\text{Conversion factor} = \frac{\text{Value}_{SI}}{\text{Value}_{LU}} \tag{6}$$

The previous section gives a brief introduction to the standard Lattice Boltzmann method. In the following sections, the LBM for diffusion modeling, required for the current study, is explained in more detail.

2.2 Problem description and application with LBM

The Lattice Boltzmann method is used in this study to model simultaneous heat and mass diffusion in cereal-based foam. Generally, SHMT in porous media is of current interest in science and several researches are carried out concerning this topic. Worth to mention, that additional challenges arise in the proposed due to time and temperature related varying complexity of the material.

When the cereal-based foam is exposed to thermal energy, several temperature-dependent processes are occurring simultaneously and closely linked to each other (Purlis and Salvadori 2009). Assembling a rough description of the material, the cereal-based foam is consisting of two components, the solid dough and embedded gas bubbles filled with CO₂ and other fermentation by-products produced by yeast or other leavening agents (Zhang and Datta 2005).

The solid dough component can be described as an interconnected visco-elastic starch-gluten network, where water is associated to starch, bound to proteins and to a minor degree partially free as droplets. The foam structure, consisting of gas bubbles surrounded by solid dough is shown in Fig. 2.

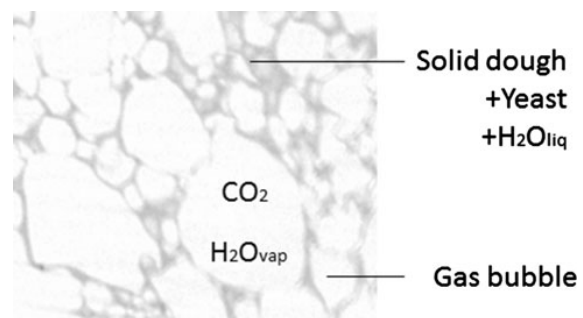


Fig. 2 Foam structure based on μ CT images (Anja Dietrich, Fraunhofer Development Center X-ray Technology EZRT, Fraunhofer Institute for Integrated Circuits IIS, F \ddot{u} rth, Germany); gas bubbles consist mainly of CO₂ and water vapor, liquid water is in the solid parts partly free but mainly bound of the dough to starch and gluten

Under the influence of heat, the gases expand due to the specific thermal expansion coefficient, and so does the water, it is evaporating towards the gas bubbles as well as towards the surrounding driven by a partial water vapor pressure difference. Therefore, volume and micro-structural changes occur by means of bubble dynamics, linked to phase transition phenomena. Further temperature-dependent processes are biochemical reactions, on the one hand, surface browning and flavor development, on the other hand starch gelatinization and protein denaturation (Zanoni et al. 1995b). Starch gelatinization is associated with absorption of water, whereas the protein denaturation process is accompanied with water release. Both processes are essential for solidification of the structure (Wagner et al. 2007).

Besides the temperature influence, the second main impact on the previously described processes is strongly related to the present water, constituting the focus of this study as heat and mass transfer processes inside the foam. Volume expansion and biochemical reactions are neglected.

The proposed LB-Model considers mass transfer occurring by means of water vapor diffusion, vapor is diffusing from the solid dough component acting as a water source to the surrounding and towards the gas bubbles, depending on concentration gradients as well as on the temperature-dependent mass diffusion coefficients, see Table 2. Heat is applied to the system by a heat source surrounding the foam and diffusion processes through the foam are solved by means of coupled thermal and mass diffusion.

In the absence of advection, equal to zero mean velocity flow, the governing LB equations for coupled heat and mass diffusion can be written as (Hussein and Becker 2010):

$$f_i = \begin{bmatrix} T_i \\ C_i \end{bmatrix}; \quad \Omega_i = \begin{bmatrix} -\frac{1}{\tau_T}(T_i - T_i^{eq}) \\ -\frac{1}{\tau_C}(C_i - C_i^{eq}) \end{bmatrix} \quad (7)$$

Due to the assumption of zero velocity, the equilibrium distribution function is given as

$$T_i^{eq} = w_i T; \quad C_i^{eq} = w_i C \quad (8)$$

The macroscopic temperature and water vapor content can be derived by:

Table 2 Thermal and mass diffusion coefficients at a temperature of 100 °C

Component	Mass diffusivity (m ² /s)	Thermal diffusivity (m ² /s)
Bubble	0.2 × 10 ⁻⁴ (100 °C)	0.192 × 10 ⁻¹ (100 °C)
Solid	0.3 × 10 ⁻⁸ (100 °C)	0.157 × 10 ⁻⁶ (100 °C)

$$T = \sum_i T_i; \quad C = \sum_i C_i \quad (9)$$

Coupling both heat and mass diffusion is important, since both processes are simultaneously dependent and influenced by each other (Hussein 2010). Thermal as well as mass diffusivity are implemented in the LB-code as temperature-dependent functions (Mack et al. 2011), Table 2 shows the resulting sample diffusivities at a temperature of 100 °C to emphasize the differences between them. The thermal diffusivity of the solid phase is calculated based on literature values for gas free dough (Mack et al. 2011).

The diffusivities are implemented in the LB-scheme via the relaxation time. According to (Wolf-Gladrow 2000) the relation between the diffusivity and the relaxation time is given by Eq. (10) for thermal diffusion α and mass diffusion D , respectively.

$$\tau_T = 3\alpha + \frac{1}{2}, \quad \tau_C = 3D + \frac{1}{2} \quad (10)$$

Under the assumed condition of non-advective flow, the single relaxation time (SRT) scheme is applied to ensure that energy unbalances are prevented due to independent Eigen values for each equation (Hussein 2010). To ensure numerical stability in the presence of no-advection, the relaxation time should be >0.5 (Wolf-Gladrow 2000).

Similarity is achieved by the introduction of the dimensionless Fourier number for thermal and mass diffusion, respectively.

$$Fo_T = \frac{\alpha \times t}{L^2} \quad Fo_C = \frac{D \times t}{L^2} \quad (11)$$

where α is the thermal diffusivity, D is the mass diffusivity, t is the characteristic time and L is the characteristic length. In transient conduction processes, the Fourier number gives the ratio of conducted heat to the amount of stored thermal energy. Similarly, the transient mass diffusion processes can be defined by a mass Fourier number. The first step in the non-dimensionalization requires the calculation of the non-dimensional Fourier number for the process in SI units. The next step is to choose a relaxation time satisfying stability conditions according to Eqs. (11) and (12).

Finally, the conversion factors, see Eq. (6), can now be calculated and based on this, all parameters can be converted to Lattice units required for the solution in the LBM and vice versa to get physical values as output. The Lattice Boltzmann code applied to carry out the calculations is a self-written code, further developed based on previous research (Hussein 2010; Hussein and Becker 2010; Mack et al. 2011). The Lattice Boltzmann code is validated by a benchmark problem for diffusion proposed by Noye and Tan (1989; Hussein and Becker 2010).

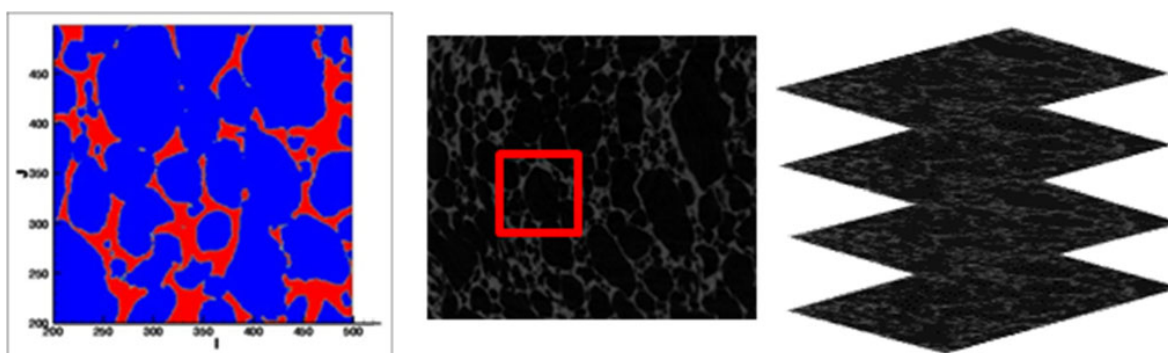


Fig. 3 Left binary image after processing; middle 2D μ CT image, square represents the cut-out zone; right stack of μ CT images

2.3 Constructing the modeling domain

To account for the characteristic micro-structural properties of the cereal-based foam, the modeling domain is constructed based on μ CT images of the foam provided by Anja Dietrich, Fraunhofer Development Center X-ray Technology EZRT, Fraunhofer Institute for Integrated Circuits IIS, Fürth, Germany.

Each of the two-dimensional μ CT images is processed with an edge detection algorithm, predicting the edges according to a specific threshold, see Fig. 3.

Thereafter, the stack of processed images is uploaded in the code and assembled together resulting in a three-dimensional obstacle file, see Fig. 4, where the solid component of the foam is displayed with the grid. The grid size was chosen to capture the meso-scale details of each component, satisfying numerical stability. The number of grid nodes was 10^6 and the size of each grid cell is 1 LU^3 .

The LB equations are then solved in the computational domain, distinguishing between both components by the related distribution functions for heat and mass diffusion and the specific relaxation times for each component.

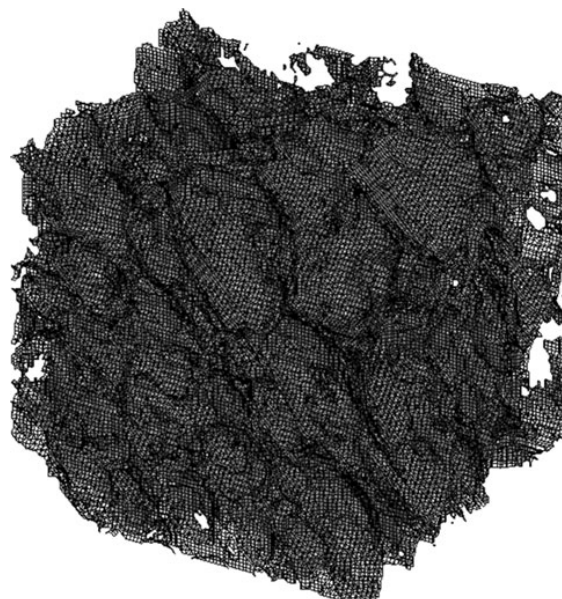


Fig. 4 Modeling domain with the grid displayed at the solid foam components

3 Results and discussion

3.1 Modeling humidity and temperature distribution

The simultaneous solved heat and mass transfer is illustrated in Figs. 5 and 6. Initial temperature values are $28 \text{ }^\circ\text{C}$ all over the domain. In the present study, water vapor diffusion is addressed non-dimensional, thus delivering insight in the vapor diffusion kinetics from a general point of view. Thus, the amount of water vapor is initialized at 1 in the solid components and 0 in the gaseous components. The contours of the temperature as well as the water vapor distribution in the middle of the modeling domain are

plotted for several time steps. Figure 5 shows the heat flux progressing from the surrounding heat source towards the center of the foam.

In Fig. 6 the water vapor is plotted for similar time and space. As can be seen in Fig. 6 the water is diffusing towards the gas pores due to the high water content in the solid component following a flux gradient. Diffusion towards the surrounding cannot be displayed visually, since this is implemented directly in the boundary conditions. Flux equilibrium boundary conditions are used in this study to account for heat and mass fluxes at the boundaries. To visualize the diffusion to the surrounding and to emphasize heat and mass flux through the foam, the flux vectors J of both properties are

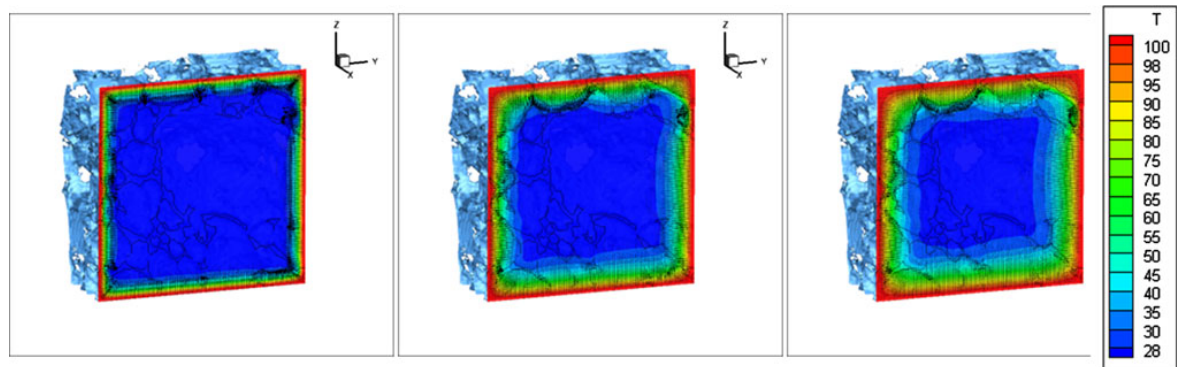


Fig. 5 Temperature distributions at several time steps (100, 950, and 1,800) representing proceeding heating of the cereal foam

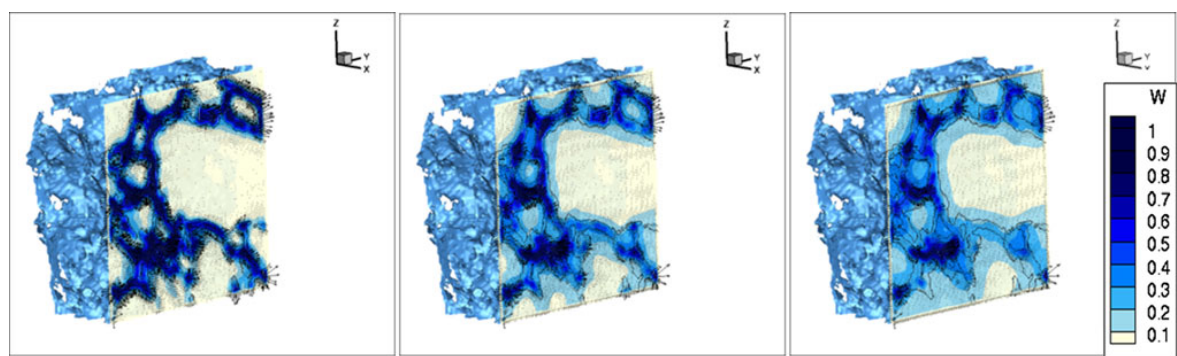
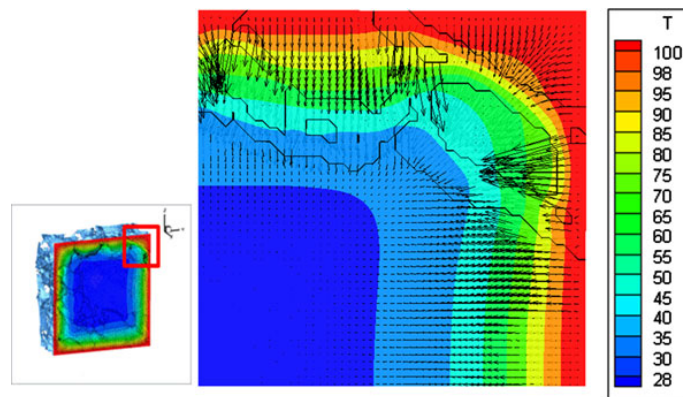


Fig. 6 Moisture distributions at several time steps (100, 950, and 1,800) showing the diffusion of vapor from solid towards the bubbles

Fig. 7 Flux vectors of temperature distribution; vector direction shows the flux, and vector length represents flux magnitude



calculated according to Eq. (12) and the results are shown in Fig. 7 for the heat flux, and Fig. 8 for mass flux, respectively.

$$J_{\Delta i}(f) = -\frac{(f_i - f_{i+1})}{\Delta i} \tag{12}$$

The flux vectors are represented as arrows showing the flux direction, where the vector length indicates the flux magnitude.

From the flux vectors, it can be seen that heat transfer inside the bubbles proceeds much quicker than in the solid phase, reasoned by the higher thermal diffusivity of the gas phase compared to the solid dough structure.

For mass diffusion, it can be seen that the vapor is diffusing towards the pores and towards the surrounding. The flux towards the surrounding proceeds much quicker due to the increased temperature gradient in the boundary,

Fig. 8 Flux vectors of moisture distribution; vector direction shows the flux, and vector length represents flux magnitude

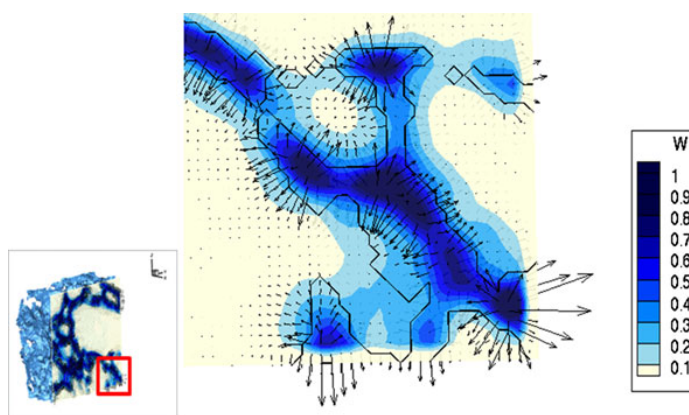
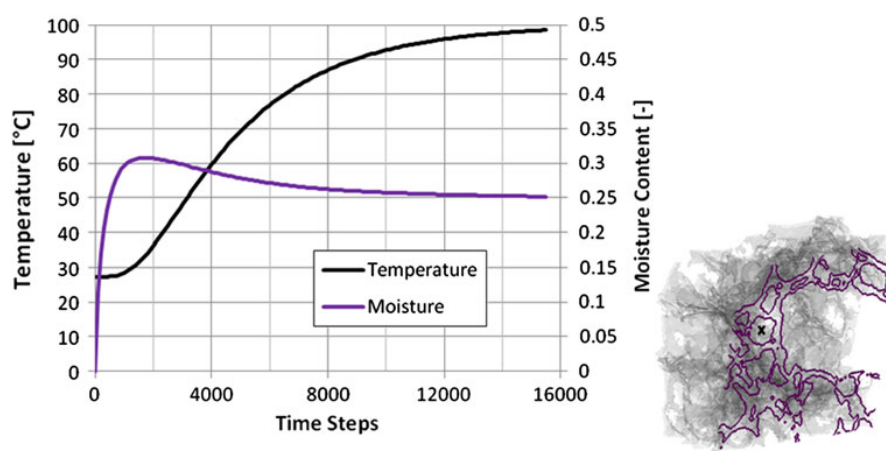


Fig. 9 Temperature and moisture distribution inside one bubble, location marked with a cross



yielding to the increased diffusion reasoned by the temperature-dependent mass diffusivity.

The temperature and moisture distribution were monitored during the simulation, and the outputs for one point are shown in Fig. 9. The solid parts of the foam are contoured. The location was chosen to show the progression of heat and mass diffusion inside a single bubble. The temperature curve follows sigmoid behavior until the end of heating. Such curve progression is reasoned by the decelerated heat flux inside the material requiring time for energy transfer in form of heat to reach the location to be examined. Simultaneously, the moisture content is increasing inside the bubble due to the diffusion from the solid to the gas component driven by concentration gradients. This process occurs instantaneously due to the close vicinity to the water source inside each bubble. After a maximum value is reached, the moisture content is decreasing slowly until the end of heating which can be explained by the counter directional flux towards the surrounding. The two counter-acting flux directions are the

flux towards the bubbles going along with moisture transfer through the gas phase and diffusion to the surrounding. The temperature gradient between surrounding and foam yields to high diffusion towards the surrounding going along with vapor loss, apparent in the slope change. Since diffusion is accelerated at higher temperatures and higher concentration gradients, the flux to the surrounding is predominant.

3.2 Varying the coefficients—impact of material properties

Optimizing the heat transfer through the proposed model foam is of interest due to the evident possibility to save energy during the heating process. For a single processing unit improved heat transfer may be insignificant, but considering the global bakery market in combination with the fact of growing industrial large-scale productions reducing the amount of required energy becomes crucial. Theoretically, heat transfer inside the cereal foam may be influenced by variations of the structure, e.g., porosity or

permeability, for further reading (Mack et al. 2011). Another approach may be variations of material properties such as the thermal, and the therewith-combined mass diffusion coefficients of the components.

The modeling results shown in the previous section are carried out based on literature values for the characteristic coefficients of heat and mass diffusion. Since the model considers the gas phase consisting exclusively of water vapor, the thermal and mass diffusivities of the gas phase are fixed. Nonetheless, the properties of the gas phase give theoretically the possibility to be influenced by the permeability of the solid structure to CO₂ or other fermentation by-products. In addition, the impact of the present CO₂ and the fermentation by-products is not clear and should be carried out in further studies. To get insight in the impact of material property variations, the thermal diffusion coefficient of the solid phase was changed and the virtual values in a realistic range are shown in Table 3. Experimentally determined thermal diffusivity coefficients for bread dough and other bakery products are given in the range of 0.1×10^{-6} – 0.24×10^{-6} m²/s (Zanoni et al. 1995a). Thus, the core of the variations is carried out in a realistic range, the extremity values at the start and end are included to provide a better understanding of the whole trend of the impact of the thermal diffusivity on the heating time. In practice, a change of such property may be achieved by variations in the recipe and the ingredients. Care has to be taken, since very big variations in the recipe may lead to a different product, which is not the objective. Further research should be done to examine the impact of specific ingredients on the diffusion coefficients, and especially the amount of water.

The results of the parameter variation study are shown in Fig. 10. The whole heating time is given by the number of time steps and is shown in Table 3. The end of heating is defined as the time step at which the temperature in the middle reached 98 °C, which is known to be the temperature where cereal foam is known to be ready (Rask 1989).

Table 3 Coefficient variations for thermal diffusion coefficients

Diffusion coefficient (m ² /s)	Required time steps
0.2×10^{-7}	19,400
0.6×10^{-7}	17,500
0.1×10^{-6}	16,400
0.2×10^{-6}	14,700
0.24×10^{-6}	14,300
0.28×10^{-6}	13,900
0.32×10^{-6}	13,500
0.36×10^{-6}	13,200
0.4×10^{-6}	13,000
1.0×10^{-6}	10,800

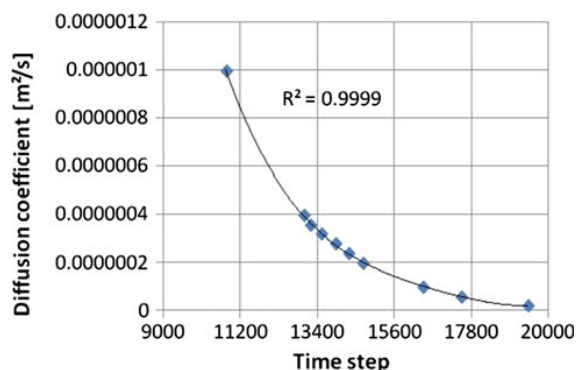


Fig. 10 Comparison of complete heating time for different thermal diffusivity coefficients in the solid phase

Following the conversion principles elaborated in previous sections, one time-step in the simulations is equal to 0.2025 s. Thus, the parameter variations result in a heating time range of 36–65 min. The results show that with increasing thermal diffusion coefficient the required heating time is decreased. Such results show that the impact of material properties is crucial and gives the potential to improve the heating process by optimized material properties. The curve shown in Fig. 10 follows a second-order fit proving to satisfy the mathematical obligation of parabolic differential equation such as the thermal diffusion equation.

The classical differential diffusion–advection equation is given by

$$\frac{dT}{dt} + v\nabla T = \alpha\nabla^2 T. \tag{13}$$

In the simple form, under the assumption of no-advection, the thermal diffusion takes the following form:

$$\frac{dT}{dt} = \alpha\nabla^2 T. \tag{14}$$

But taking the more conservative form where the thermal diffusivity is variable such as in this parametric investigation, the thermal diffusion equation would take the form:

$$\frac{dT}{dt} = \nabla^2(\alpha \times T) = \alpha\nabla^2 T + T\nabla^2\alpha. \tag{15}$$

Analyzing Eq. (15) in more detail gives a mathematical explanation of the curve progression. The temperature on the right-hand side remains constant according to a constant temperature gradient between the initial and final stages. This fact accounts to diminish the first term on the right-hand side. Therefore, the second term on the right-hand side prevails and entails the parabolic dependence of thermal diffusivity to heating time, since the changing parameters are time and thermal diffusivity.

4 Conclusion

Thermo-physical processes in cereal-based foam are highly complex, but sophisticated knowledge of such processes is required to optimize the heating process. Challenging thereby is the occurrence of such processes in the micro-scale. This work gives insight to the simultaneous heat and mass diffusion processes on a pore scale (in the order of 1 mm) by the use Lattice Boltzmann methods. This approach gave the possibility to visualize heat and mass diffusion processes at the pore scale. The application of a μ CT images based modeling domain allows the representation of the diffusion processes under realistic conditions. The proposed method represents a first step to enlighten micro-heat and mass diffusion processes and builds the groundwork to accomplish further work to model explicitly the evaporation–condensation mechanism which is of impact on the heat transfer. The parameter variation study showed the potential to optimize the heating process by variations of the material properties. Such modeling results support experimental work required to achieve improvement of the real process showing the direction of optimum structural and material properties. Further work should be carried out including a sensitivity study combining the whole bandwidth of influencing parameters to establish optimum conditions.

Acknowledgments This work was sponsored by the Deutsche Forschungsgesellschaft DFG grant number: BE 2245/8-1. The authors thank Anja Dietrich, Fraunhofer Development Center X-ray Technology EZRT, Fraunhofer Institute for Integrated Circuits IIS, Fürth, Germany for the μ CT images.

References

- Guo Z, Zhao TS (2002) Lattice Boltzmann model for incompressible flows through porous media. *Physical Review E* 66:036304
- Guo Z, Zhao TS (2005) A Lattice Boltzmann model for convection heat transfer in porous media. *Numer Heat Transf Part B* 47: 157–177
- Hussein MA (2010) On the theoretical and numerical development of Lattice Boltzmann models for biotechnology and its applications. Dissertation, TU München, Munich
- Hussein MA, Becker T (2010) An innovative micro-modelling of simultaneous heat and moisture transfer during bread baking using the Lattice Boltzmann method. *Food Biophysics* 5(3):161–176. doi:10.1007/s11483-010-9156-1
- Mack S, Hussein MA, Becker T (2011) Investigation of heat transfer in cereal based foam from a micro-scale perspective using the Lattice Boltzmann method. *J Non-Equilib Thermodyn*. doi: 10.1515/JNETDY.2011.019
- McNamara GR, Garcia AL, Alder BJ (1997) A hydrodynamically correct thermal Lattice Boltzmann model. *J Stat Phys* 87: 1111–1121
- Moaty Sayed A, Hussein MA, Becker T (2009) An innovative lattice Boltzmann model for simulating Michaelis–Menten-based diffusion–advection kinetics and its application within a cartilage cell bioreactor. *Biomech Model Mechanobiol* 9:141–151
- Noye BJ, Tan HH (1989) Finite difference methods for solving the two dimensional advection–diffusion equation. *Int J Num Methods Fluids* 26:1615–1629
- Purlis E, Salvadori VO (2009) Bread baking as a moving boundary problem. Part 1: Mathematical modelling. *J Food Eng* 91(3): 428–433
- Rask C (1989) Thermal properties of dough and bakery products: a review of published data. *J Food Eng* 9:167–193
- Succi S (2001) *The Lattice Boltzmann equation*. Oxford University Press, New York
- Wagner M, Lucas T, Le Ray D, Trystram G (2007) Water transport in bread during baking. *J Food Eng* 78:1167–1173
- Wolf-Gladrow D (2000) *Lattice-gas cellular automata and Lattice Boltzmann models*. Springer, Telos, Santa Clara
- Xuan YM, Zhao KZ, Li Q (2010) Investigation on mass diffusion process in porous media based on Lattice Boltzmann method. *Heat Mass Transf* 46:1039–1051
- Zanoni B, Peri C (1993) A study of the bread-baking process. I: A phenomenological model. *J Food Eng* 19(4):389–398
- Zanoni B, Peri C, Gianotti R (1995a) Determination of the thermal diffusivity of bread as a function of porosity. *J Food Eng* 26:497–510
- Zanoni B, Schiraldi A, Simonetta R (1995b) A naive model of starch gelatinization kinetics. *J Food Eng* 24(1):25–33
- Zhang J, Datta AK (2005) Transport processes and large deformation during baking of bread. *Bioeng Food Nat Prod* 51(9):2569–2580
- Zhang J, Datta AK (2006) Mathematical modeling of bread baking process. *J Food Eng* 75:78–89

2.2.4 Multicomponent phase transition kinetics in cereal foam – Part I: developing a lattice Boltzmann model

Microfluid Nanofluid

DOI 10.1007/s10404-014-1410-2

RESEARCH PAPER

Multicomponent phase transition kinetics in cereal foam—Part I: developing a lattice Boltzmann model

S. Mack · M. A. Hussein · T. Becker

Received: 25 November 2013 / Accepted: 25 April 2014
© Springer-Verlag Berlin Heidelberg 2014

Abstract Foam thermo-physics is a significant point of interest in current research in a broad range of applications reaching from material science, geology, chemical, biotechnology, ceramic processing to food science. The latter involves the challenge of continuous quality in combination with high-temperature processing. Thermal treatment strongly influences foam structure, stability and as well enforces chemical reactions or physical processes such as phase transitions. From a process engineering point of view, such reactions can be used for process optimization considerations. In cereal foam, heat transfer is suggested to depend, besides heat conduction in the lamella, on evaporation–condensation processes inside the foam bubbles. According to the meso-scale incidence of physical processes within complex foam micro-structures, the lattice Boltzmann method verifies its application to numerical investigations on the considered length scale. Thus, the objective of this study is the development of a lattice Boltzmann model covering heat and mass diffusion in combination with phase transition processes.

Keywords Numerical modeling · Lattice Boltzmann · Phase transitions · Cereal foam · Thermo-physics · Heat and mass transfer

1 Introduction

Concerning cereal foam and thermal-induced processes during production and heating, research in recent years

mainly addressed numerical investigations focusing on heat and mass transfer by continuum assumptions (Zanoni et al. 1995; Sablani et al. 1998; Thorvaldsson and Janestad 1999; Purlis and Salvadori 2009). Thus, foam is regarded as a continuous material, where physical processes occur depending on continuum descriptions yielding to an averaged treatment of the whole process. Nonetheless, neglecting the specific characteristics of the complex microstructure of cereal foam impedes a huge fraction of access to really understand the process from a micro-scale point of view. A sophisticated characterization of a process can only be reached if its micro-states are fully understood due to the fact that several different microscopic states can lead to the same macroscopic behavior (Wolf-Gladrow 2005). Thus, such knowledge is essential for process optimization purposes.

Particularly, under the influence of heat, processes occur which require the consideration of discrete particle interactions at micro-scale. Such temperature-dependent processes are (1) simultaneous heat and mass transfer; (2) biochemical reactions such as starch gelatinization or flavor and color development; (3) structural and material property changes; and (4) phase transition processes (Zanoni et al. 1995; Purlis and Salvadori 2009). The simultaneous heat and mass transfer processes are closely linked to phase transition processes. Following a straight physics point of view, the processes occurring inside an individual cereal foam bubble should be similar to a heat pipe (Sluimer and Krist-Spit 1987; de Vries et al. 1989; Wagner et al. 2007; Purlis and Salvadori 2009). Present dough water inside the foam lamella yields to evaporation to the surrounding, but as well toward the foam bubbles, according to temperature and partial pressure differences (Vanin et al. 2009). Depending on the local conditions, re-condensation occurs at locations of lower temperature or increased pressure, and

S. Mack (✉) · M. A. Hussein · T. Becker
Group of (Bio-) Process Analysis, Faculty of Life Science
Engineering, Technische Universität München,
Weihenstephaner Steig 20, 85354 Freising, Germany
e-mail: s.mack@wzw.tum.de

thus yields to a cyclic evaporation–condensation mechanism inside the foam bubbles (Wagner et al. 2007). This process is suggested to increase the heat transfer due to the absorption at the warmer side and release of latent heat at the colder side of the bubble (Purlis and Salvadori 2009). The previous described evaporation–condensation mechanism inside cereal foam is based on macro-scale observations together with basic physical principles, resulting in a reasonable theory, but lacking so far a proof, whether the thermo-physical conditions inside the microstructure really yield to evaporation–condensation.

Such complex processes embedded in a network of simultaneously occurring multiphase transport, multi-physics, structural and material property changing environment impede the implementation in a modeling tool (Datta 2007). The lattice Boltzmann method (LBM) is a powerful tool bridging the gap between continuum mechanics and molecular dynamics (MD) (Mohamad 2011). Discrete particle interactions are considered as particle distribution functions, thereby overcoming the drawbacks of noise and heavy computational effort of MD methods and yielding to a meso-scale description of flow properties (Raabe 2004). In addition, the LBM allows a re-covering of the macroscopic flow properties from the particle distribution interactions (Succi 2001). In spite of the growing usage of LBM and the promising application possibilities of complex processes at small length scales, it is still rarely used to implement phase transition kinetics. Several approaches were developed in the past to account for multiple phases and the interactions among them (oil water mixtures, Rayleigh–Taylor problems) by means of LBM (Sukop and Or 2004), but still suffer mainly from high density ratios, thermo-dynamical consistency, numerical stability and the isothermal limitations. In addition, the high computational effort of multiphase methods still limits the application to complex processes in particular under non-isothermal influences.

Thus, the objective of this study is the development of a physics-based multi-component lattice Boltzmann model comprising coupled heat and mass diffusion in combination with the thereby induced phase transition processes of water. According to the temperature-driven phase change inside the microstructure, the condensate is considered as additional developing component and interactions between vapor and the condensate is treated via sink/source terms. The carefully chosen modeling assumptions and the model development are given in detail allowing a meaningful interpretation of the simulation results. The model is validated by a validation test case and hereafter being applied to simulate the proposed processes in cereal foam under thermal treatment. The main goal hereby is to deliver insight in the thermo-physical processes occurring at micro-scale inside the foam bubbles and to use this knowledge for heat transfer optimizations during baking.

2 Materials and methods

2.1 Modeling assumptions and initial conditions

The possibility to achieve meaningful results by numerical methods is based on the modeling assumptions stated prior to simulations. Nonetheless, before such simplifications can be made, the process has to be known in detail to ensure consistency of objectives, assumptions, results and their reasonable interpretation. The interaction of temperature gradient-induced processes in cereal foam is shown in Fig. 1. Main impact on further processes is the application of heat yielding to a temperature gradient in the foam, linked to volume and pressure changes. Macroscopic volume increase is induced by yeast or other foaming agents due to CO₂ (and further fermentation by-products) production, saturation of the liquid phase and therewith partial pressure difference driven release toward air inclusions in dough (Pickett 2009). Such micro air inclusions are resulting from kneading and are necessary to induce CO₂–bubble formation, where the O₂ is metabolized by the yeast. Thus, the fermentation process which is necessary for the specific foam microstructure is resulting in a CO₂-saturated atmosphere where the initial amount of air can be neglected according to its minor amount in relation to CO₂. The presence of water, initially in the foam lamella, results due to the vapor pressure balance and resulting equilibrium addition to an increase of vapor inside the gas phase of the foam. The CO₂ is thereby replaced by the water vapor, where its high volatility is reasoned by the high vapor pressure of CO₂ (5.73 MPa at 20 °C) compared to water vapor pressure (2.34 kPa at 20 °C). This theoretical consideration can be confirmed by experimentation, measurements of humidity distribution in bread during the baking process showed that the relative humidity is increasing in the range of 92.2 at ~28 °C to 96.8 % at ~100 °C (Mack et al. 2013b). From these findings, the present specific humidity inside the gas phase can be elaborated which is defined as the ratio between the mass of water vapor and the mass of moist air (WMO-No. 8 2008). Thus, the specific humidity is a value in the range of 0–1, where dry air is given by 0 and air-free steam has a value of 1. For the measured conditions for bread dough, the specific humidity has a value of 0.96–0.99, where the value of 0.99 is reached after the first quarter of the baking process. Based upon the specific humidity close to 1, the assumption that the gas phase consists of water vapor and interactions with other gases can be neglected is acceptable. In addition, initial conditions, see Table 1, for the gas phase can be derived from the measurements, thus, initial temperature is 30 °C and the relative humidity is 92.2 %, which is equivalent to an initial amount of water molecules of 28.1 g/m³ (Mack et al. 2013b). Following the assumption of vapor-filled

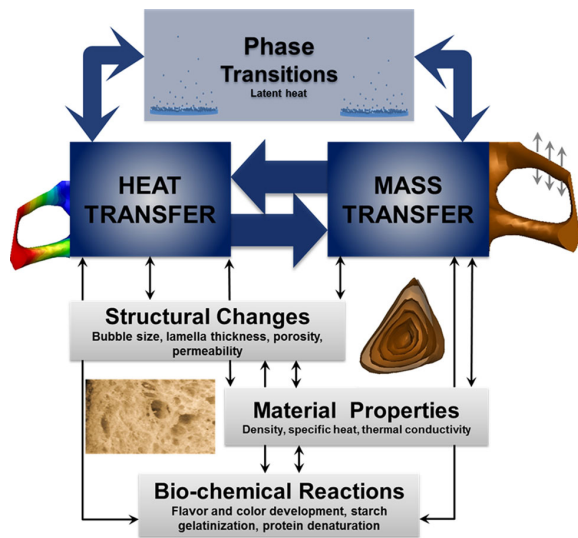


Fig. 1 Heat and mass transfer induced processes in cereal foam under thermal treatment, where the *arrows* represent the linkage and influence on each other

Table 1 Initial conditions and coefficients addressing the heat and mass transfer in cereal-based foam under thermal treatment

Property	Value	Units
Initial relative humidity (RH) bubbles	92.2 (30 °C)	%
Initial absolute humidity (AH) bubbles	28.1 (30 °C)	g/m ³
Bubble diameter	1	mm
Cell wall thickness	0.4	mm
Initial temperature	30	°C
Mass diffusivity $D_{lamella}$	0.3×10^{-8} (100 °C)	m ² /s
Mass diffusivity D_{vapor}	0.2×10^{-4} (100 °C)	m ² /s
Thermal diffusivity $\alpha_{lamella}$	0.157×10^{-6} (100 °C)	m ² /s
Thermal diffusivity α_{vapor}	0.192×10^{-4} (100 °C)	m ² /s

foam bubbles, the thermal diffusivity of the gas phase is depending on vapor properties. The thermal diffusivity can be given as a temperature-dependent function related to the thermal conductivity, the density and the specific heat, as given in Table 1. Likewise the temperature-dependent thermal as well as vapor diffusivity of the foam lamella can be elaborated, where the calculation is based on the material properties of gas-free dough.

Further attention has to be taken on the mass transport of water vapor inside the gas phase. Diffusion is generally depending on concentration differences, temperature and pressure (Hudson 2008). The proposed LB algorithm accounts depending on the specific temperature-dependent vapor diffusion coefficient for concentration and temperature-driven diffusion. Vapor pressure differences

are implemented in the model via the evaporation boundary conditions, but the question of the impact of pressure-driven diffusion remains. The pressure inside the gaseous phase is increasing due to the increasing temperature and the restriction of the elastic starch-gluten network, see Fig. 1. Besides the capability of wheat dough to hold the gas, the foam lamella is still permeable for gases yielding to release of CO₂ and to evaporation of vapor from the foam to the surrounding, thus equalizing major pressure differences. Nonetheless, measurements showed that during baking the pressure increases up to 0.4–1.0 kPa (Grenier et al. 2009). Pressure-driven diffusion is negligible when $\Delta p/p \ll 1$ (Hudson 2008). The estimated value of 0.0098 is much smaller than 1, therefore the effect of a pressure-driven diffusion coefficient can be neglected.

The processes included in the proposed lattice Boltzmann algorithm are focusing on heat and mass transfer and the linked phase transitions. Focusing on this objective requires a closer look on the mechanisms of phase transitions. The phase change of water is depending on the local conditions of temperature, amount of water molecules and pressure. The concentration of water vapor in the gas phase is limited and a maximum partial pressure of vapor exists which depends only on temperature (Sonntag et al. 2003). At high temperatures, the maximum absolute humidity, which is for the relative humidity RH = 100 % equal to the saturation humidity, is higher than at low temperatures. The absolute humidity AH can be given by Eq. 1,

$$AH = 216.7 \times \frac{RH}{100\%} \times A \times \exp\left(\frac{b \times T}{\gamma + T}\right) \quad (1)$$

with the saturation pressure P_{Sat} given in Eq. 2, the temperature T in °C and the relative humidity (RH), with the partial vapor pressure P_{vap} , given in Eq. 3. In a temperature range from 0 to 100.9 °C, the constants are $A = 6.10780$ hPa, $b = 17.08085$ and $\gamma = 234.175$ °C (Fortuin 2003).

$$P_{Sat} = A \times \exp\left(\frac{b \times T}{\gamma + T}\right) \quad (2)$$

$$RH = \frac{P_{vap}}{P_{Sat}} \times 100\% \quad (3)$$

The dewpoint temperature T_D , as given in Eq. 4, is the temperature where the actual partial pressure is equal to the saturation pressure, which is the temperature where water is condensing.

$$T_D = \gamma \times \frac{\ln \frac{P_{vap}}{A}}{b - \ln \frac{P_{vap}}{A}} = \gamma \times \frac{\ln(0.01 \times RH \times \frac{P_{Sat}}{A})}{b - \ln(0.01 \times RH \times \frac{P_{Sat}}{A})} \quad (4)$$

Thus, if the amount of water molecules is increasing beyond the temperature-dependent saturation limit, the “oversupplied” amount of vapor condenses. These basic

principles are implemented in the LB algorithm to account for local condensation inside the gas phase. Evaporation from the foam lamella as well as the re-evaporation from the condensed vapor is included via the boundary conditions, elaborated in detail in the subsequent sections. Linked to the evaporation–condensation mechanism, the absorbed and stored latent heat is released during condensation according to the amount of condensed vapor, and vice versa absorbed for evaporation. The latent heat is given in Eq. 5.

$$Q = m \times L \tag{5}$$

In Eq. 5, Q represents the amount of heat absorbed or released during the phase change, m the mass of substance and L the specific latent heat of vaporization. These processes are implemented via additional sink and source terms and account for a reasonable description of evaporation–condensation-based heat and mass transfer. Nonetheless, several simplifications are made to reduce the complexity:

- The development of the additional condensate is considered based on the assumption that the high density ratio between vapor and its liquid is not considered. Meaning, that the liquid water in the foam lamella is represented by vapor in saturation conditions, and thus, the condensate is represented by condensed vapor, yielding to the development of a wet steam region where vapor and its condensate co-exists, rather than a pure liquid.
- The condensate is regarded as an additional component and due to the fact that interactions between the components vapor and condensed vapor are driven by the temperature induced phase change.
- Surface tension effects between vapor and condensate are thus far neglected due to their minor impact on conducting the objective of the research.

2.2 Lattice Boltzmann modeling

The lattice Boltzmann Method (LBM) offers the possibility to bridge the gap between molecular and continuum behavior of any flow (Raabe 2004). The resulting meso-scale description considers that the flow is composed of an interacting particle distribution f , discretized in time t and space \mathbf{x} , as shown in Eq. 6.

$$f_i(\mathbf{x} + \mathbf{e}\delta t, t + \delta t) = f_i(\mathbf{x}, t) + \Omega_i(\mathbf{x}, t) + F_i \tag{6}$$

F_i is an external force term, δt is the time step, \mathbf{e} is the unit vector, and Ω_i is the collision term accounting for particle–particle interactions on a lattice site. The D3Q19 lattice is shown in Fig. 2, where the D3 represents the three-dimensional space and the Q19 the number of applied

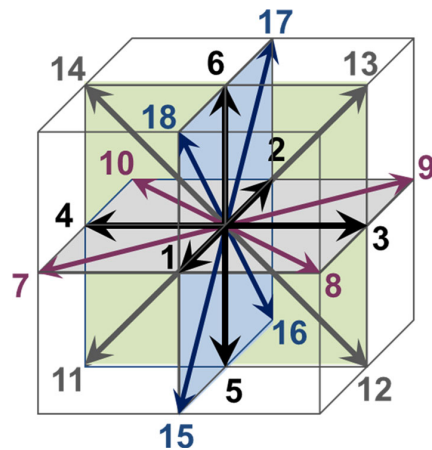


Fig. 2 D3Q19 Lattice configuration, thus a three-dimensional lattice space including 19 velocity vectors, including a zeroth velocity vector in the center

velocity directions, which is in this case 19 including a zeroth velocity vector in the center (Hussein and Becker 2010).

Thus, the particle distribution function is performing consecutively propagation steps to its neighbor lattice sites followed by a collision steps. Propagation occurs depending on the weight factors, which are specific for the lattice configuration. For the used D3Q19 lattice, the weight factors w depending on the direction are $w_0 = 1/3$, $w_{1-6} = 1/18$ and $w_{7-18} = 1/36$ (Succi 2001). The collision term, according to the Bhatnagar–Gross–Krook (BGK) approximation (Succi 2001), is given in Eq. 7,

$$\Omega_i(f(\mathbf{x}, t)) = -\frac{f_i(\mathbf{x}, t) - f_i^{eq}(\mathbf{x}, t)}{\tau} \tag{7}$$

Consequently, the particle distribution function is relaxed toward the local equilibrium f^{eq} taking relaxation time τ (Mohamad 2011). The local equilibrium function takes Maxwellian form as shown in Eq. 8.

$$f_i^{eq} = w_i \rho(\mathbf{x}) \left[1 + 3 \frac{\hat{e}_i v}{c^2} + \frac{9}{2} \frac{(\hat{e}_i v)^2}{c^4} - \frac{3}{2} \frac{v^2}{c^2} \right] \tag{8}$$

where $\rho(\mathbf{x})$ is the local density, \mathbf{e} is the direction vector, i is the direction, v is the macroscopic velocity, c is the basic lattice speed and w is the weight factor. The consideration of diffusion-based heat and mass transfer leads according to the absence of advection to zero velocity flow and thus diminishing the local equilibrium function to the relation given in Eq. 9.

$$f_i^{eq} = w_i \rho(\mathbf{x}) \tag{9}$$

The proposed LB algorithm is based on coupled heat and vapor diffusion, hence, the particle density ρ in Eq. 9 represents the heat and vapor distribution, as given in Eq. 10.

$$T_i^{eq} = w_i T; V_i^{eq} = w_i V \tag{10}$$

The simultaneously occurring heat T and vapor V diffusion is solved by two coupled lattice Boltzmann distribution functions, as shown in Eq. 11.

$$f_i = \begin{bmatrix} T_i \\ V_i \end{bmatrix}; \Omega_i = \begin{bmatrix} -\frac{1}{\tau_T}(T_i - T_i^{eq}) \\ -\frac{1}{\tau_V}(V_i - V_i^{eq}) \end{bmatrix} \tag{11}$$

Under the assumption of diffusion modeling, the relaxation time τ is related to the macroscopic diffusion coefficient, D for mass and α for heat, according to Eq. 12 (Wolf-Gladrow 2005; Sukop and Thorne 2007).

$$\tau_T = 3\alpha + \frac{1}{2}; \tau_V = 3D + \frac{1}{2} \tag{12}$$

Due to numerical stability considerations, the relaxation time has to be higher than 0.5 (Wolf-Gladrow 2005). Macroscopic quantities can be recovered from the lattice Boltzmann equation by the Chapman–Enskog relations (Succi 2001), given in Eq. 13.

$$T = \sum T_i; V = \sum V_i \tag{13}$$

The multicomponent characteristic of the proposed LB scheme is due to the fact that the cereal foam is composed of two components, the foam lamella and the foam bubbles, respectively. To account for the different material properties, the thermal diffusivity as well as the vapor diffusivity is implemented via their specific diffusion coefficients for each component, as given in Table 1.

In addition to the simultaneous heat and mass diffusion, the phase transitions including the latent energy transfer are implemented in the lattice Boltzmann equation via an additional sink and source term F . This term is composed of two parts, the phase change S and the additionally transferred energy H , as given in Eq. 14.

$$F_i = \begin{bmatrix} S_i \\ H_i \end{bmatrix} \tag{14}$$

In a temperature changing system, a change of phase from vapor V to its condensate C is depending on the local amount of water vapor in dependence of temperature and pressure. Hence, the local conditions are calculated each time step, and if the temperature-dependent saturation limit of the vapor phase is reached, phase transition occurs, the vapor condenses, and the additional component C develops locally. The framework of the saturation–condensation conditions are summarized in Eq. 15.

$$f_i = \begin{bmatrix} T_i \\ V_i \\ C_i \end{bmatrix} \begin{cases} -H_i & (dV > 0) \\ +H_i & (dC > 0) \\ -S_i & (V > V_{Sat}) \\ +S_i & (V < V_{Sat}) \end{cases} \tag{15}$$

The implementation of the sink and source term accounting for phase transitions in the lattice Boltzmann equation leads to an instantaneous phase change. Following a time scale estimation of the occurring processes, the characteristic time for the vapor diffusion is in the range of ms. In comparison, and related to the diffusion time, the phase change takes 7 μ s and therewith infinitesimal time to change (Fujikawa et al. 2011). The locally transitioned amount of vapor is calculated according to Eq. 1 in the lattice domain as given in Eq. 16. In addition, the latent heat Q is calculated according to Eq. 4 depending on the transitioned amount of vapor and implemented in the lattice domain via Eq. 17.

$$S_i = w_i \times \left[V - 216.7 \times \frac{A \times \exp(b \times T / (234.175 + T))}{(T + 273.15)} \right] \tag{16}$$

$$H_i = w_i \times \frac{AQ}{V \times c} \tag{17}$$

where w_i is the lattice weight, Q is the latent heat, V is the density of water vapor molecules, A (6.1078 hPa) and b (17.08085) are coefficients, T is the temperature in $^{\circ}$ C, and c is the specific heat (2,300 kJ/kg). In this context, the density of molecules is regarded here since the volume is one lattice unit (LU). The proposed algorithm is implemented in a self-written, and consecutively further developed, lattice Boltzmann code (Hussein and Becker 2010; Mack et al. 2013a, b).

2.3 Boundary conditions

In the present study, no-slip boundary conditions according to the concept of bounce-back are applied. Bounce-back boundary conditions are based on the reflection of particles at a wall node back to the lattice domain, but with rotated direction. The application of such boundary conditions is especially of interest in porous medium to model fluid flow through non-interacting porous material (Sukop and Thorne 2007). Comparative, all foam components are treated in the present model and interacting with each other; thus, bounce-back rules are applied only at the boundary of the computational domain. The interactions between the boundary foam lamella and foam bubble are treated by von Neumann-type flux boundary conditions. Hence, the evaporation of water vapor from the foam lamella and as well the re-evaporation from the condensed vapor is implemented in the solution by the mass flux according to Langmuir’s evaporation equation as given in Eq. 18.

$$\frac{dV}{dt} = (P_{\infty} - P_{Gas}) \sqrt{\frac{m}{2\pi kT}} \tag{18}$$

In Eq. 18, dV/dt is the mass flux, P_{∞} is the vapor pressure of lamella water and condensed vapor,

respectively, P_{Gas} is the partial vapor pressure of the vapor in the gas, T the temperature in °C k is the Boltzmann constant, and m the mass of vapor. In the case that P_{∞} exceeds P_{Gas} evaporation occurs. To account for heat flux, the boundary temperature is distributed to the neighbor particle distributions according to Eq. 19, where the equilibrium temperature value is assigned to the boundary particle distribution.

$$T_i^{eq} = w_i \times T_{Boundary} \tag{19}$$

$T_{Boundary}$ is the temperature at the boundary, T^{eq} is the equilibrium temperature, and w_i are the lattice weight factors.

2.4 Similarity considerations

Similarity analysis is required to ensure the link between the process in SI units and the computational domain. The numerical solution executed in the computational domain carried out in lattice units (LU), since real values cannot be directly addressed. A physical system can be described and therewith re-scaled by non-dimensional relations; thus, similarity considerations can be addressed by dimensionless numbers allowing up- or downscaling the process under the constraints of numerical stability (Sayed et al. 2009). In the present study, the non-dimensional Fourier number Fo is applied to non-dimensionalize the heat and mass diffusion processes, as given in Eq. 20.

$$Fo_T = \frac{\alpha \times t}{l^2}; Fo_V = \frac{D \times t}{l^2} \tag{20}$$

where Fo is the dimensionless Fourier number, α is the thermal diffusivity, D is the mass diffusion coefficient, t is the time and l is the characteristic length. The same Fourier number is applied in SI as well as in lattice units, satisfying similarity between both length scales and ensuring that both processes are dynamically equivalent. Based on the non-dimensional number describing the proposed process, the SI units can be converted to lattice units and vice versa, according to Eq. 21.

$$\text{Conversion factor} = \frac{\text{Value}_{SI}}{\text{Value}_{LU}} \tag{21}$$

In addition, to ensure a physically correct relation of the applied relaxation times to each other, the non-dimensional Lewis number is implemented in the similarity considerations. The Lewis number is given in Eq. 22 and relates the thermal diffusion coefficient to the mass diffusion coefficient.

$$Le = \frac{\alpha}{D} \tag{22}$$

3 Results and discussions

3.1 Validation

Validation can be addressed numerically or based on experiments, where the former verifies an accurate numerical solution, whereas the latter allows with its comparisons to experiments a physical validation. To verify the proposed model scheme, two validation test cases are carried out and the basic thermal diffusion LBM is validated numerically, whereas the phase transition is validated experimentally. The benchmark applied for the numerical validation of the thermal diffusion LBM is done according to the numerical description of an initial Gaussian pulse initiated inside a cuboid (Noye and Tan 1988). The simulated propagation of the pulse is compared with the exact solution and achieved an average error of 1.78×10^{-09} , and thus giving quite accurate results as shown in previous work (Hussein and Becker 2010).

The phase transition model is validated with two different experimental data sets of an evaporating droplet. The first test case is based on experimental data (Ranz and Marshall 1952) of an evaporating droplet in stagnant dry air. Worth to mention that, besides evaporation, the vapor condensation on the droplet surface effects heat and mass transfer (Elperin et al. 2007). The test case is based on a spherical droplet with initial diameter $d = 0.1$ cm and temperature $T_{Droplet} = 9.11$ °C, being present in stagnant dry air with temperature $T_{Air} = 24.9$ °C. The droplet squared diameter, resulting from the simulations with the present model is plotted versus the time and compared to the experimental data, as shown in Fig. 3.

The experimental determined droplet reduction follows linear curve progression, whereas the simulated curve

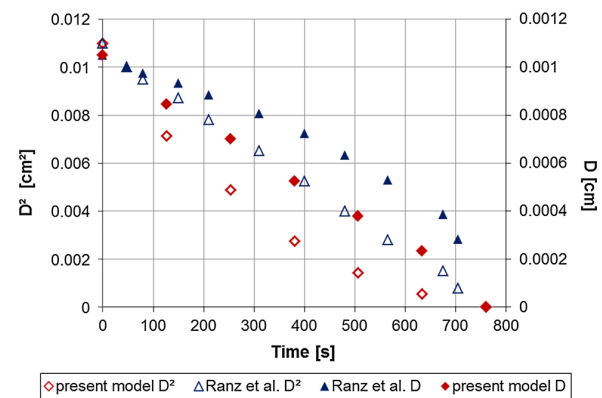


Fig. 3 Comparison of simulated and experimental data (Ranz and Marshall 1952) of an evaporating water droplet with initial diameter 0.1 cm, $T_{Droplet} = 9.11$ °C and $T_{Air} = 24.9$ °C. Filled dots represent the diameter given in d , whereas unfilled dots represent the diameter in d^2 (original work)

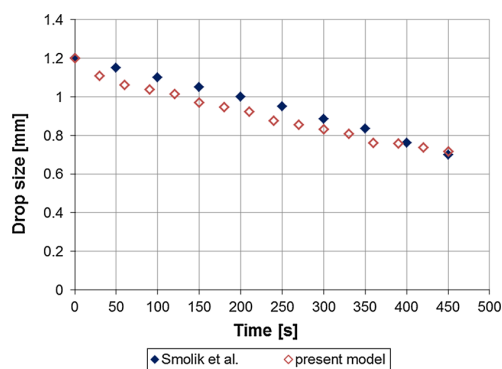


Fig. 4 Comparison of simulated and experimental data (Smolík et al. 2001) of an evaporating water droplet with initial diameter 1.2 mm, $T_{\text{Droplet}} = 24\text{ }^{\circ}\text{C}$ and $T_{\text{Air}} = 14\text{ }^{\circ}\text{C}$

follows a steeper decline. The evaporation of the simulated droplet proceeds initially quicker and is more flat in the final stages converging to zero. To confirm the applicability of the proposed model, an additional validation is carried out. The second test case is based on experimental data of an evaporating droplet of the size 1.2 mm (Smolík et al. 2001). The initial conditions are $T_{\text{Droplet}} = 24\text{ }^{\circ}\text{C}$ and $T_{\text{Air}} = 14\text{ }^{\circ}\text{C}$, hence inverse temperature starting conditions are given compared to the first test case. The results are plotted in Fig. 4 and show quite accurate simulation results in comparison with the experimental data.

Both validation cases show that the proposed model delivers realistic results for an evaporating droplet. Nonetheless, the results are comparable to greater or lesser extent depending on the specific application. The variations apparently among both validation cases may be reasoned by either experimental or numerical uncertainty. From a physical point of view, the main difference between both cases is due to the different initial conditions. In the first case, the water droplet has a lower initial temperature than the ambient, whereas in the latter case the water droplet has a higher initial temperature than its surrounding. In the prior case, the conditions yield to re-condensation at the bubble surface due to its lower temperature, may thus in a first step influence the heat transfer and therewith in a second-step limit the evaporation, which explains the belly shape response as shown in Fig. 3.

4 Conclusion

The numerical model is developed with the objective to model heat and mass transfer and the linked phase transition processes in cereal foam microstructures. Since the considered processes are occurring at micro-scale the lattice Boltzmann method is applied accounting for a physics-

based numerical description of the proposed processes. Insight in such processes inside cereal foam bubbles is of importance due to the fact that the heat transfer mechanisms are thus far investigated only by continuum descriptions, whereas a detailed micro-scale understanding of the processes supports the possibility to estimate relevant parameter variations on improved heat transfer. The proposed lattice Boltzmann model is based on a previously developed heat and mass diffusion model (Hussein and Becker 2010; Mack et al. 2013a), and in addition, the development as well as the coexistence of condensed vapor is considered in the model by means of phase transitions. The evaporation from the liquid boundaries, dough and condensed vapor, respectively, is following the evaporative mass flux balance as described by Langmuir's equation. Phase transitions inside the gas phase are treated according to the local saturation conditions, depending on temperature, humidity and vapor pressure, thus ensuring a realistic image of the vapor and its condensate. To disregard the high density ratio is acceptable for the present study, since that the focus to reach the objective of the study is the effect of phase transitions on the heat transfer, which is ensured by the fact that the change of phase is ruled by the saturation properties and the linked heat of vaporization is calculated depending on the amount of transitioned phase. The numerical model is validated with a test case describing the evaporation of a water droplet compared to literature values. The straight physics-based nature of the suggested model allows its usage in a broad range of applications in the presence of a temperature and vapor field, where evaporation–condensation may occur. Nonetheless, the next step is the application of the developed LBM to model heat and mass transfer processes in cereal foam.

Acknowledgments This work was sponsored by the Deutsche Forschungsgemeinschaft DFG Grant Number: BE 2245/8-1.

References

- Datta AK (2007) Porous media approaches to studying simultaneous heat and mass transfer in food processes. I: problem formulations. *J Food Eng* 80:80–95
- De Vries U, Sluimer P, Bloksma AH (1989) A quantitative model for heat transport in dough and crumb during baking. In *Cereal Science and Technology in Sweden, Proceedings of an International Symposium*, Sweden, Lund University, pp 174–188
- Elperin T, Fominykh A, Krasovtsov B (2007) Evaporation and condensation of large droplets in the presence of inert admixtures containing soluble gas. *J Atmos Sci* 64:983–995
- Fortuin G (2003) Anwendung mathematischer Modelle zur Beschreibung der technischen Konvektionstrocknung von Schnittholz. PhD Thesis. Universität Hamburg
- Fujikawa S, Yano T, Watanabe M (2011) Vapor–liquid interfaces, bubbles and droplets. Springer, Berlin

- Grenier D, Le Ray D, Lucas T (2009) Combining local pressure and temperature measurements during bread baking: insights into crust properties and alveolar structure of crumb. *J Cereal Sci* 52(1):1–8
- Hudson TL (2008) Growth, diffusion, and loss of subsurface ice on Mars: experiments and models. PhD Thesis, California Institute of Technology
- Hussein MA, Becker T (2010) An innovative micro-modelling of simultaneous heat and moisture transfer during bread baking using the Lattice Boltzmann Method. *Food Biophys* 5(3):161–176
- Mack S, Hussein MA, Becker T (2013a) Examination of thermo-physical and material property interactions in cereal foams by means of Boltzmann modeling techniques. *Microfluid Nanofluid* 15:387–395
- Mack S, Hussein MA, Becker T (2013b) Tracking the thermal induced vapor transport across foam microstructure by means of micro-sensing technology. *J Food Eng* 116(2):344–351
- Mohamad AA (2011) Lattice Boltzmann method. Fundamentals and engineering applications with computer codes. Springer, Berlin
- Noye BJ, Tan HH (1988) Finite difference methods for solving the two dimensional advection diffusion equation. *Int J Num Methods Fluids* 26:1615–1629
- Pickett MM (2009) Study of gas cell stability during bread making using x-ray microtomography and dough rheology. PhD Thesis. Kansas State University
- Purlis E, Salvadori VO (2009) Bread baking as a moving boundary problem. Part 1: mathematical modelling. *J Food Eng* 91:428–433
- Raabe D (2004) Overview of the lattice Boltzmann method for nano- and microscale fluid dynamics in materials science and engineering. *Model Simul Mater Sci Eng* 12:R13–R46
- Ranz WE, Marshall WR (1952) Evaporation from drops. *Chem Eng Prog* 48:173–180
- Sablani SS, Marcotte M, Baik OD, Castaigne F (1998) Modeling of simultaneous heat and water transport in the baking process. *Lebensm-Wiss u-Technol* 31:201–209
- Sayed AM, Hussein MA, Becker T (2009) An innovative lattice Boltzmann model for simulating Michaelis–Menten-based diffusion–advection kinetics and its application within a cartilage cell bioreactor. *Biomech Model Mechanobiol* 9(2):141–151
- Sluimer P, Krist-Spit CE (1987) Heat transport in dough during the baking of bread. In: Morton ID (ed) *Cereals in a European context*. Ellis Horwood, Chichester, pp 355–363
- Smolík J, Džumbová L, Schwarz J, Kulmala M (2001) Evaporation of ventilated water droplet: connection between heat and mass transfer. *J Aerosol Sci* 32:738–748
- Sonntag RE, Borgnakke C, Van Wylen GJ (2003) *Fundamentals of thermodynamics*. Wiley, New York
- Succi S (2001) *The Lattice Boltzmann equation for fluid dynamics and beyond*. Oxford University Press, Oxford
- Sukop MC, Or D (2004) Lattice Boltzmann method for modeling liquid–vapor interface configurations in porous media. *Water Resour Res* 40:1–11
- Sukop MC, Thorne DT Jr (2007) *Lattice Boltzmann modeling. An introduction for geoscientists and engineers*. Springer, Berlin
- Thorvaldsson K, Janestad H (1999) A model for simultaneous heat, water and vapour diffusion. *J Food Eng* 40:167–172
- Vanin FM, Lucas T, Trystram G (2009) Crust formation and its role during bread baking. *Trends Food Sci Technol* 20:333–343
- Wagner MJ, Lucas T, Le Ray D, Trystram G (2007) Water transport in bread during baking. *J Food Eng* 78:1167–1173
- WMO-No. 8 (2008) *Guide to meteorological instruments and methods of observation*
- Wolf-Gladrow DA (2005) *Lattice-gas cellular automata and Lattice Boltzmann Models—an introduction*. Springer, Berlin
- Zanoni B, Schiraldi A, Simonetta R (1995) A naive model of starch gelatinization kinetics. *J Food Eng* 24:25–33

2.2.5 Multicomponent phase transition kinetics in cereal foam – part II: Impact of microstructural properties

Microfluid Nanofluid

DOI 10.1007/s10404-014-1420-0

RESEARCH PAPER

Multicomponent phase transition kinetics in cereal foam—part II: impact of microstructural properties

S. Mack · M. A. Hussein · T. Becker

Received: 25 November 2013 / Accepted: 25 April 2014

© Springer-Verlag Berlin Heidelberg 2014

Abstract In the bakery industry, a considerably high amount of energy is used for the baking process. A possibility to decrease the baking time by means of optimized heat transfer through the bread microstructure would lead to less required baking time and cost reduction. Thermal treatment of cereal foam implicates thermo-physical processes such as simultaneous heat and mass transfer associated with evaporation–condensation-based heat transfer through the bubbles. Numerical investigations are carried out to deliver sophisticated insight into the heat transfer processes at microscale, supporting process understanding and visualization of phenomena inside the foam bubbles. In a further step, the elaborated knowledge is employed to determine the main influencing parameter on the heat transfer through the foam microstructure by means of lattice Boltzmann modeling techniques. For optimization purposes, the microstructure as well as individual foam lamella configurations are considered in the parameter variation studies.

Keywords Numerical modeling · Lattice Boltzmann · Phase transitions · Cereal foam · Thermo-physics · Heat and mass transfer

1 Introduction

In cereal foam microstructures, heat transfer is suggested to depend to a high degree on evaporation–condensation

processes inside the foam bubbles (Sablani et al. 1998; Thorvaldsson and Janestad 1999; Purlis and Salvadori 2009). This cyclic process is depending on heat and vapor transfer, as well as the associated transfer of latent heat. Heat is transferred through the foam lamella; considering an individual foam bubble surrounded by the lamella, water evaporates at the warmer side of the bubble, thereby absorbs latent heat of vaporization, diffuses through the bubble, and condenses again depending on the local conditions with release of the latent heat (de Vries et al. 1989; Wagner et al. 2007). This hypothesis is based on experimental investigations as well as on basic physical principles, where conclusions can be drawn based on the following considerations:

- (i) Heat transfer proceeds quicker in fermented than in unfermented dough during the baking process (de Vries et al. 1989).
- (ii) Cereal foam structure can be considered analogous to a heat pipe, where present water evaporation and condensation overtakes the major role of heat transfer (Sluimer and Krist-Spit 1987)
- (iii) Temperature inside bread during baking reaches a plateau of 100 °C (Thorvaldsson and Skjöldebrand 1998)
- (iv) Moisture transport toward the coldest spot of the loaf can be recorded (Thorvaldsson and Janestad 1999; Wagner et al. 2007)

Several researches are carried out to measure temperature and humidity distributions during baking (Zanoni and Peri 1993; Thorvaldsson and Janestad 1999; Wählby and Skjöldebrand 2001; Wagner et al. 2007; Purlis and Salvadori 2009). Temperature distributions during baking are well known, but vapor diffusion in combination with phase transitions kinetics is currently poorly reported. In particular, the high-temperature conditions impede the

S. Mack (✉) · M. A. Hussein · T. Becker
Group of (Bio-) Process Analysis, Faculty of Life Science
Engineering, Technische Universität München,
Weihenstephaner Steig 20, 85354 Freising, Germany
e-mail: s.mack@wzw.tum.de

measurement conditions. In addition, the complex microstructural characteristics of cereal foam and the occurrence of the phenomena of interest in the microscale yield to unfeasible measurement conditions. Therefore, it is not surprising that mismatching findings are the current state of research. On the one hand, moisture transfer toward the coldest spot is reported (Thorvaldsson and Janestad 1999; Wagner et al. 2007), and on the other hand, no moisture change inside the crumb was found (Zanoni and Peri 1993). Besides such drawbacks, the main challenge still remains: the small length scale and to get insight into processes inside the bubbles.

Promising options are numerical modeling techniques, offering the possibility to deliver insight without destroying or influencing the process. In recent researches, focus was set to simultaneous heat and mass transfer based on macroscopic descriptions of the processes. Thus, microstructural and material properties, as well as physical phenomena such as evaporation–condensation, are regarded as continuum quantities (Zanoni and Peri 1993; Purlis and Salvadori 2009). To gain insight into the processes at the mesoscale, the lattice Boltzmann method (LBM) proved to be a powerful tool, bridging micro- and macroscales (Zhang 2011). A simplified foam structure was used to model simultaneous heat and mass transfer through cereal foam under thermal treatment by the use of LBM, where heat transfer and mass transfer were regarded to depend only on heat and mass diffusion (Hussein and Becker 2010). The influence of material properties was subject of a further study, where thermal diffusivity of the foam lamella was varied in a realistic foam geometry based on μ CT-images, showing that higher thermal diffusivity increases the heat transfer rate (Mack et al. 2013a). These previous researches miss the implementation of evaporation–condensation processes, but build the basis for the current study. The objective of this work is the application of a recently developed lattice Boltzmann algorithm, considering the specific saturation conditions of water vapor, including phase transitions of water vapor to condensed vapor beyond saturation and vice versa. Furthermore, the associated uptake and release of latent heat depending on the amount of transitioned species are considered. Following the length scale of the foam, as given in Fig. 1, the simulations are carried out in the order of mm length scale. In a further step, the algorithm is used for an intensive parameter variation study elaborating the impact of microstructural properties on the heat transfer. The parametric investigations cover (1) porosity variations of the crumb, (2) variations of foam lamella, and (3) cross-correlations of varied thermal diffusivity of the foam lamella in dependence of the varied microstructural characteristics. These parametric investigations allow an estimation of the main influencing parameter on enhanced heat transfer. The

results can then be used to support experimental research to transfer the virtual elaborated main influencing parameter to the real baking process.

2 Materials and methods

2.1 Lattice Boltzmann diffusion modeling in combination with phase transitions

The applied lattice Boltzmann equation is given in Eq. 1 (Succi 2001; Sukop and Thorne 2007), where f represents the particle distribution function, \mathbf{x} is the space in x direction, e is the unit vector, t is the time, δt is the time step, \mathbf{e} is the unit vector, Ω_i is the collision operator, and F_i an external sink or source term.

$$f_i(\mathbf{x} + \mathbf{e}\delta t, t + \delta t) = f_i(\mathbf{x}, t) + \Omega_i(\mathbf{x}, t) + F_i \tag{1}$$

The proposed lattice Boltzmann algorithm is based on coupled heat and vapor diffusion. Therefore, two separate equations for each property are solved simultaneously, the temperature distribution T and the vapor distribution V , respectively, see Eq. 2.

$$f_i = \begin{bmatrix} T_i \\ V_i \end{bmatrix}; \Omega_i = \begin{bmatrix} -\frac{1}{\tau_T}(T_i - T_i^{eq}) \\ -\frac{1}{\tau_V}(V_i - V_i^{eq}) \end{bmatrix} \tag{2}$$

The collision operator Ω accounts for particle to particle interactions, where the particle distribution function relaxes toward a local equilibrium f^{eq} , according to the specific relaxation time τ (Succi 2001) as given in Eq. 3.

$$\Omega_i(f(\mathbf{x}, t)) = -\frac{f_i(\mathbf{x}, t) - f_i^{eq}(\mathbf{x}, t)}{\tau} \tag{3}$$

The equilibrium distribution function is shown in Eq. 4 for diffusion, where under the assumption of zero velocity flow, the original Maxwellian velocity distribution diminishes (Hussein and Becker 2010).

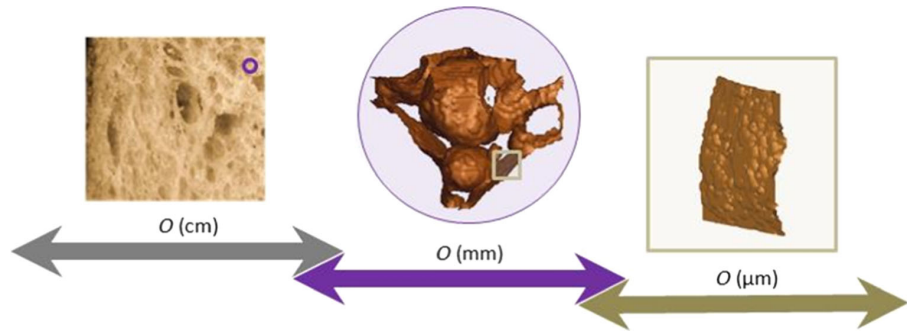
$$f_i^{eq} = w_i f \tag{4}$$

The relaxation time for each process is related to the thermal diffusivity according to Eq. 5 (Wolf-Gladrow 2005).

$$\tau_T = 3\alpha + \frac{1}{2}; \tau_V = 3D + \frac{1}{2} \tag{5}$$

where α represents the thermal diffusivity and D is the vapor diffusivity. Evaporation boundaries are implemented at the lamella–bubble interface and as well at the vapor–condensed vapor boundary. The evaporation rate is calculated based upon the partial vapor pressure dependent according to Langmuir’s equation, given in Eq. 6.

Fig. 1 Length scale of cereal foam, showing from left to right macro-, meso- and microstates of the foam with corresponding orders of length scales (O), thus showing the length scale of product (O cm), its composition of bubbles and lamella (O mm), as well as a single lamella (O μ m)



$$\frac{dV}{dt} = (P_{\infty} - P_{Gas}) \sqrt{\frac{m}{2\pi kT}} \tag{6}$$

dV/dt is the flux of vaporized water, P_{∞} is the vapor pressure of lamella water and condensed vapor, respectively, P_{Gas} is the partial vapor pressure of the vapor in the gas, m is the mass of water, k is the Boltzmann constant, and T the temperature in $^{\circ}C$. In addition, the current temperature, vapor density as well as saturation conditions are calculated locally, which constitute the framework of phase transition processes and the development of an additional mass source term C representing the condensed vapor, Eq. 7.

$$f_i = \begin{bmatrix} T_i \\ V_i \\ C_i \end{bmatrix} \begin{cases} -H_i & (dv > 0) \\ +H_i & (dC > 0) \\ -S_i & (V > V_{Sat}) \\ +S_i & (V > V_{Sat}) \end{cases} \tag{7}$$

The external sink and source term F extends the equation to take phase transition into account. F is composed of two individual parts, S is the source of transitioned species, whereas H represents the amount of absorbed or released heat, see Eq. 8.

$$F_i = \begin{bmatrix} H_i \\ S_i \end{bmatrix} \tag{8}$$

Macroscopic values are recovered according to the relation given in Eq. 9, where ρ is the macrodensity (Sukop and Thorne 2007).

$$\rho = \sum_i f_i \tag{9}$$

Linkage between the processes in SI units and the lattice domain is given by similarity considerations. Meaning that, the Fourier and the Lewis number are applied as non-dimensional parameters to ensure similarity conditions. Hence, SI units can be transferred according to Eq. 10 to lattice units (LU) and vice versa.

$$\text{Conversion factor} = \frac{\text{Value}_{SI}}{\text{Value}_{LU}} \tag{10}$$

2.2 Computational domain

The computational domain is generated based upon a stack of μ CT-images of bread to enable realistic insight into cereal foam microstructures. A detailed description of dough manufacture and μ CT-imaging is provided by Dietrich et al. (2012). The μ CT-images are uploaded in the Boltzmann code where an edge detection algorithm (Perez Alvarado et al. 2011) is applied to distinguish between foam lamella and foam bubble. Figure 2 shows the computational domain of a three-dimensional $2 \times 2 \times 2$ mm foam domain. Inner-bubble surfaces are displayed with the grid. Foam bubble diameter is in the range of 1 mm, whereas the cross-sectional thickness of foam lamella is ~ 200 μ m.

2.3 Modeling assumptions and initial conditions

The modeling domain is composed of two foam components, the lamella and the bubbles. The foam lamella consists of a water–starch–gluten network, where the specific material properties are calculated and applied in the simulations based on bread dough properties:

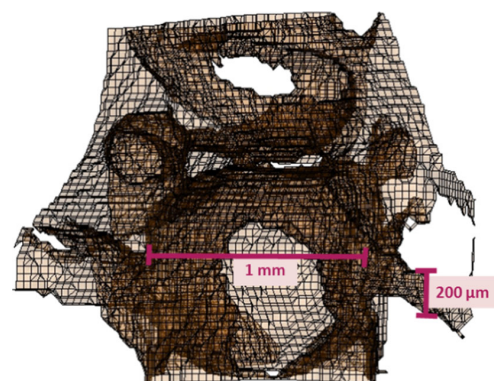


Fig. 2 Computational domain of the cereal foam, showing the mesh domain of a bubble which size is of approximately 1 mm, and foam lamella thickness of ~ 200 μ m

- (i) The thermal ($\alpha = 0.157 \times 10^{-6} \text{ m}^2/\text{s}$) and the mass diffusivity ($D = 3.0 \times 10^{-9} \text{ m}^2/\text{s}$), at a temperature of 100 °C, of the lamella are based on properties for unfermented dough.
- (ii) The thermal ($\alpha = 0.0192 \times 10^{-3} \text{ m}^2/\text{s}$) and mass diffusivity ($D = 0.02 \times 10^{-3} \text{ m}^2/\text{s}$), at a temperature of 100 °C, for the bubble component are based on water vapor properties.

The bubbles are regarded to be filled exclusively with water vapor, where additional gases are neglected due to their minor content. Initial relative humidity at 30 °C is 92.2 %. The initial values are taken from previously published experimental data (Mack et al. 2013b). The proposed LB algorithm so far considers the phase transition depending on the temperature-dependent saturation conditions of water vapor. This implies that the amount of vapor which is locally present and exceeds the temperature-dependent saturation limit undergoes a phase change and the condensed vapor phase develops, resulting in a wet steam region, composed of liquid droplets, rather than a continuous liquid phase. Depending on the amount of transitioned vapor, the corresponding amount of heat is added to the heat equation. Thus, the processes being of impact on the heat transfer are regarded in the current model.

2.4 Parameter variations

The upload of the μ CT-images and their linkage to the modeling domain is depending on a specific threshold used in the edge detection algorithm, to distinguish between gas phase and lamella. Lowering or increasing this threshold virtually offers the possibility to change the virtual crumb structure by means of pore size, lamella thickness, and increasing amount of voids in the lamella, whereas the general crumb structure remains similar. Due to this procedure, the microstructural changes are related to porosity variations, which are shown in Table 1.

The slightly differing microstructures are used to carry out parameter variation studies. Figure 3 shows the computational domain of each variation case. The inner iso-surfaces of cereal foam bubbles are illustrated in brown. A heat source is implemented on the right-hand side, shown by the red plane, see Fig. 3a, b. To emphasize the microstructural

Table 1 Crumb structure variations depending on the threshold

Threshold	Porosity (%)
8	66.7
9	69.4
10	72.1
11	74.8
12	77.5

changes, Fig. 3b shows slices through the middle of the modeling domain. Drawback of this method is that bubble size, lamella size, and the occurrence of microvoids are always directly linked to a different porosity, thus allowing conclusions on the heat transfer depending on porosity. If amount of lamella, bubble size, lamella thickness, or microvoids themselves are influencing the heat transfer rate and to which amount is not possible.

To overcome such drawbacks, a further parameter variation study is carried out focusing on the constitution of the lamella. The variation study considers an individual lamella, without and with increasing amount of similar sized voids and as well increasing size of a single void. The lamellas are generated artificial allowing a constant amount of mass, even though the constitution is varied. Furthermore, the amount of voids from 0 to 6 satisfies a similar increase of void space from 0 to 6 LU as the void size from 0 to 6. The parameter variation cases are focusing on microstructural properties, whereas additionally the thermal diffusivity of the foam lamella is varied in a realistic range for cereal dough, as summarized in Table 2. The combined implementation of material as well as microstructural properties offers the possibility to estimate which property overtakes the leading role by means of heating times reduction.

3 Results and discussion

3.1 Simulation results

Contour plots of temperature and vapor distribution are shown in Fig. 4a and b for proceeding time steps at a porosity of 72 %. In addition, the development of condensing vapor as well as its re-evaporation is shown in Fig. 4c. The computational domain consists of initially two components, the foam lamella and the foam bubbles. On the right-hand side, a heat source is implemented in the domain, resembling the heat flux from neighbor crumb sections with constant temperature of 100 °C. Figure 4a shows the temperature distribution through the domain, it can be seen, that heat flux through the bubbles proceeds quicker than through the foam lamella. This is reasoned by the higher thermal diffusivity of the vapor phase compared to the foam lamella, but as well due to the additional energy transfer based on the evaporation–condensation mechanism. The half-moon shaped temperature increase after 250 time steps inside the foam bubble is resulting from condensation next to the foam lamella–bubble interface. Due to concentration and partial vapor pressure gradients, water evaporates from the lamella, exceeding the saturation limit of the current temperature resulting in a phase

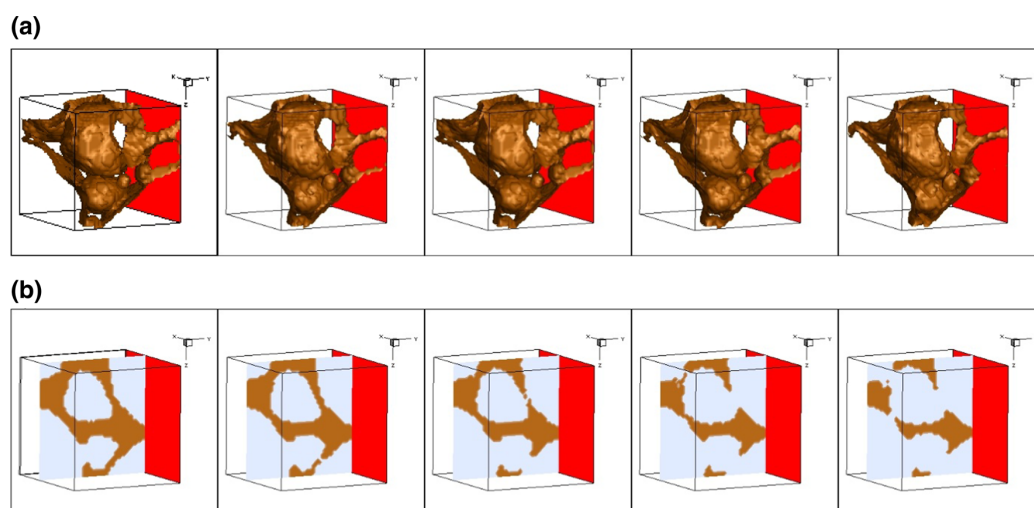


Fig. 3 Cereal foam microstructure variations, porosity increases from left to right from 66.7 to 77.5 %. **a** Three-dimensional illustration of a microstructure section, iso-surfaces of the foam bubbles are shown in *brown*, the heat source given in *red*. **b** Two-

dimensional illustration in the middle of the microstructural section, emphasizing the differing lamella constitutions with increasing porosity

Table 2 Parameters variation cases of foam lamella sections

Parameter variations	Lattice units	SI units
Amount of voids	0–6	0–240 μm
Void size	0–6 LU	0–240 μm
Thermal diffusivity	$1.1 \times 10^{-3} \text{ m}^2/\text{s}$ $- 2.3 \times 10^{-3} \text{ m}^2/\text{s}$	$0.117 \times 10^{-6} \text{ m}^2/\text{s}$ $- 0.197 \times 10^{-6} \text{ m}^2/\text{s}$

Variation parameters are amount of voids, void size, and thermal diffusivity of the lamella

change and the thereby released energy of the previous vapor phase. At advanced time steps, both heat transfer mechanisms are hard to distinguish, reasoned by the simultaneous occurrence of thermal diffusion and evaporation–condensation-based heat transfer. After 20,250 time steps, the temperature reached a level of 98 °C, which is the end point of the simulation due to the fact that cereal foam structure solidifies at this temperature level and the baking process ends (Rask 1989; Zaroni and Peri 1993). The related time in SI units to reach end of baking can be derived from the value conversion as given in Eq. 10. The computational domain represents a $2 \times 2 \times 2$ mm-sized section of cereal foam; thus, the required time to heat the domain in SI units is 38 s. Extrapolating this to a customary product height of 10 cm would yield to a required baking time of 32 min. Since the simulations are straightly carried out in the crumb domain without considering crust and oven conditions which indeed influence baking time, this time only gives an estimation

of the real heating time. Thus, the required heating time is given in time steps in the following.

The simultaneously solved vapor diffusion through the foam is shown in Fig. 4b. Vapor is diffusing through the bubbles as well as through the lamella, depending on the specific mass diffusion coefficients. At initial stages of the simulation, the amount of vapor is equally distributed among the foam bubbles, due to the initial conditions of a relative humidity of 92.2 % at a temperature of 30 °C. At time step 250, there is an increase of vapor visible at the right corner next to the foam lamella. This local increase of vapor in the gas phase is reasoned by the increasing temperature and thereby induced evaporation from the lamella toward the bubble. This effect can be tracked over the following time steps, resulting in an increase of vapor in the bubble phase. Thus, the vapor is evaporating depending on local temperature and therewith vapor pressure differences and diffusing through the bubbles.

The consequence of this temperature- and pressure-dependent vapor flux is shown in Fig. 4c. Depending on local amount of vapor, temperature and thus the local temperature-dependent saturation level, condensation occurs. The condensed vapor is illustrated in dark blue, and it can be seen that with proceeding time steps, the amount of condensed vapor increases according to the increasing amount of vapor in the bubbles. In addition, at the time steps 15,250 and 20,250, the re-evaporation can be seen by the decrease of condensed vapor. This re-evaporation occurs concisely at the final time steps due to the longer exposure of high temperature at this location associated with vapor displacement toward neighbor

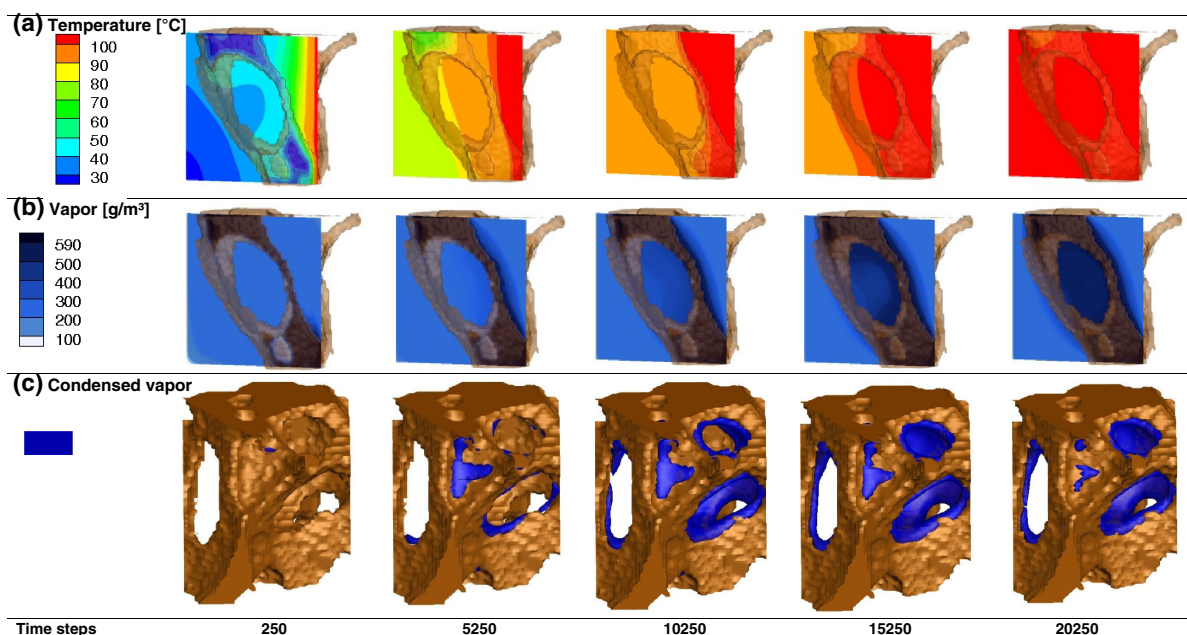


Fig. 4 Temperature, vapor, and condensed vapor distribution at proceeding simulation time steps in a foamed dough model structure

sections. Figure 5 shows the simulation results combined for heat flux, vapor diffusion, and evaporation–condensation. The temperature distribution is plotted at the crumb structure surface. The increasing evaporation front from the lamella toward the bubble phase is illustrated by a light gray-blue iso-surface, and the condensed vapor phase is shown by the dark blue layer.

The plots show the temperature flux through the domain, yielding to increased temperature-dependent evaporation from the lamella. An evaporation front is developing at the high-temperature regions at the right-hand side. Subsequently, an evaporation front is developing on the left-hand side as temperature increases. Reasoned by the increased amount of vapor in the bubbles, the amount of vapor which is locally beyond saturation condenses. According to local temperature and vapor pressure conditions, the previously condensed vapor re-evaporates again, visible at time step 20,250 on the right-hand side.

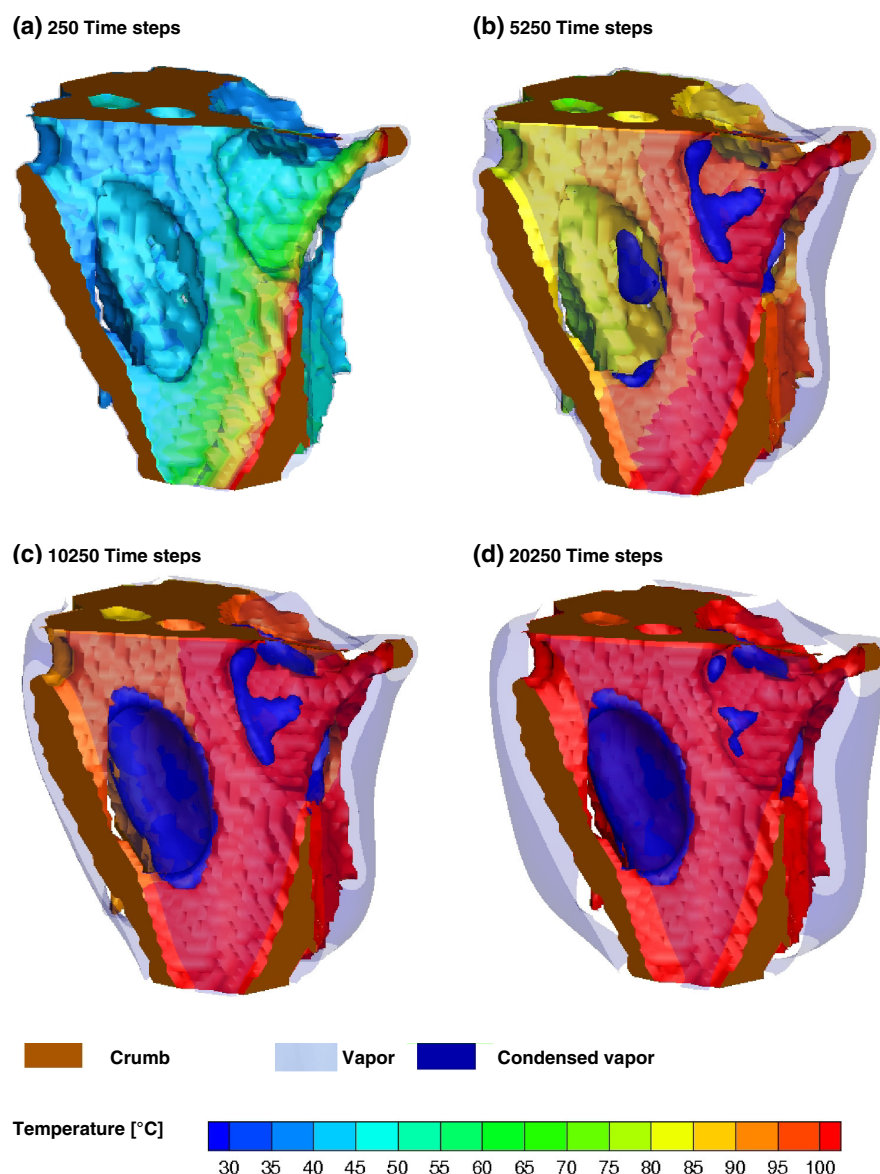
The evaporation–condensation mechanism includes evaporation from the lamella boundary, condensation inside the bubbles at the lamella–bubble interface, and re-evaporation from the condensed vapor. This cyclic evaporation–condensation occurs locally during the whole heating process as shown in Fig. 6. The plot shows the temperature (solid black line) dependent development of condensed vapor (solid pink line). Figure 6a–c shows the local amount of condensed vapor at the time steps 8,000, 8,500, and 9,000 at the lamella–bubble interface. At time step 8,000, the local amount of condensed vapor reached a local minimum due to re-evaporation of the condensed

vapor. The proceeding evaporation from the lamella due to increasing temperature and therewith increasing vapor pressure gradients yields to local increase of vapor in the bubble and thus if the amount is beyond saturation, the vapor condenses, see Fig. 6b. At time step 9,000, again a local minimum is reached due to re-evaporation of the condensed vapor. This cyclic evaporation–condensation process continues until the local conditions change due to less available water present in the lamella as it can be seen in the final stages of the heating process after 20,000 time steps where the condensed vapor curve flattens.

3.2 The role of evaporation–condensation heat transfer

The simulation results show that besides thermal conduction, heat is transferred according to the evaporation–condensation mechanism. Reconsidering that evaporation–condensation yields to release of additional heat during condensation, but as well absorbs energy during vaporization yielding to isothermal phase change at macroscale, which is the basic feature of latent heat transfer. In theory, if heat transfer by evaporation–condensation is of minor impact and heat transfer is mainly depending on thermal diffusivity through each phase, then variations of the influencing parameters, such as thermal conductivity, specific heat, and density of the foam lamella, are the point of interest to reach higher heat transfer. On the opposite, if a high amount of heat is transferred by the evaporation–condensation mechanism, then different or additional parameter variations should be taken into account. If

Fig. 5 Temperature distribution displayed at crumb surface in combination with the evaporation front in *gray-blue* and the development of condensed vapor shown in *dark blue* with proceeding time steps



evaporation–condensation heat transfer is dominant, then the amount of vapor and the possibility of its diffusion through the microstructure would influence the heat transfer. This is linked to the permeability of the foam lamella, the vapor diffusivity through the foam, and the free surface to bubble ratio leading to an increased evaporation rate. To estimate the ratio of thermal diffusion-driven heat transfer and combined evaporation–condensation heat transfer, the simulations are repeated under the same conditions but with neglecting the evaporation–condensation process. The results for both simulations, without evaporation–condensation and including evaporation–condensation, respectively, at a porosity of 72 % are plotted in Fig. 7.

The results show that indeed heat transfer proceeds quicker if evaporation–condensation is considered. Furthermore, the curve progression follows a steeper increase, meaning that for baking purposes, the conditions in the foam microstructure should be inside the range that evaporation–condensation takes place; thus, enough vaporizable water is present in the lamellas.

3.3 Parameter variation study

The next step covers the application of the proposed LB algorithm to determine the effect of microstructural variations on the heat transfer. The simulations are repeated for

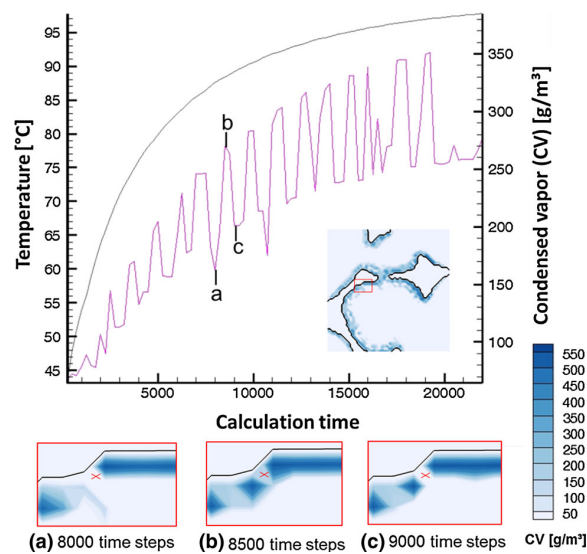


Fig. 6 Temperature and condensed vapor (CV) plotted versus calculation time. The pink curve shows the cyclic nature of the evaporation–condensation mechanism

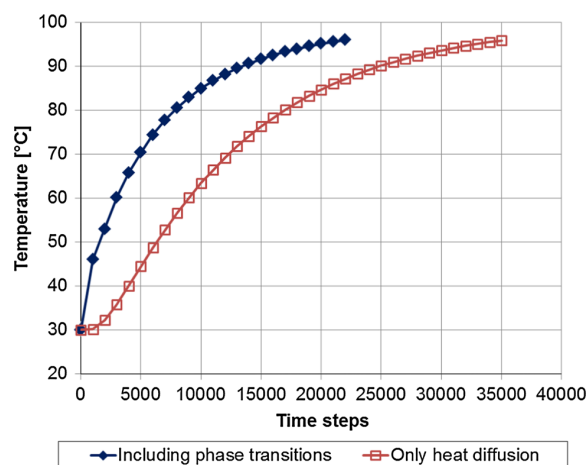


Fig. 7 Comparison of temperature progression dependent on solution time for simulations carried out including evaporation–condensation heat transfer and without considering such processes

different crumb microstructures, where the same μ CT-images are uploaded in the Boltzmann code with increasing thresholds yielding in a different lamella to bubble ratio and therewith varied porosity (66.7–77.5 %). The simulation results are shown in Fig. 8, where the required time steps to reach a temperature of 98 °C, are plotted versus the crumb porosity.

The results show a linear decrease of required heating time with increasing porosity. Increasing porosity is linked to lamella thinning and increase of voids inside the

lamellas. In conclusion, it can be suggested that such microstructural properties are responsible for the reduced heating time. Nonetheless, the applied edge detection algorithm used for the obstacle upload implies that these microstructural changes are related to a decrease in porosity and therewith a decrease of foam lamella mass in the computational domain. Thus, the heating time reduction may also be reasoned by this mass loss since the thermal diffusivity of the lamella is lower than through the bubble phase. To clarify the impact of the lamella configurations independent of lamella mass changes, artificial foam lamellas are generated having diverse amount of voids and increasing void size in combination with similar lamella mass in each variation case. Additionally, the thermal diffusivity of the foam lamella is varied to relate the possible heating time reduction of microstructural properties to

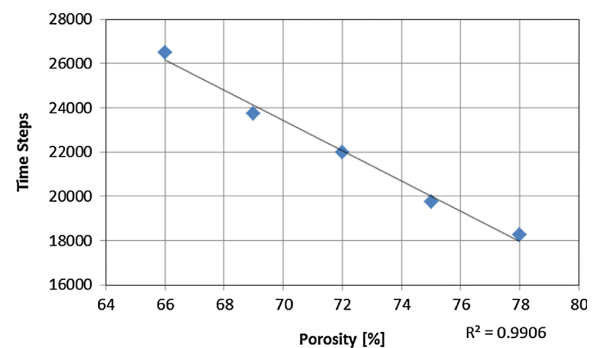


Fig. 8 Parameter variations of crumb porosity (thermal diffusivity remaining $0.157 \times 10^{-6} \text{ m}^2/\text{s}$), showing that heating time increases with decreasing porosity

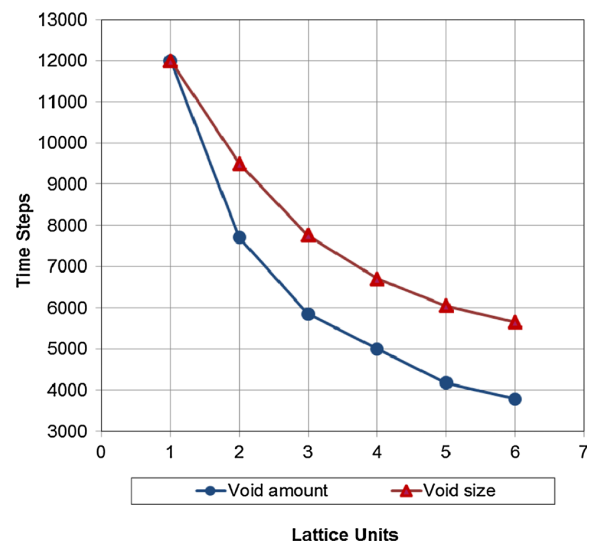
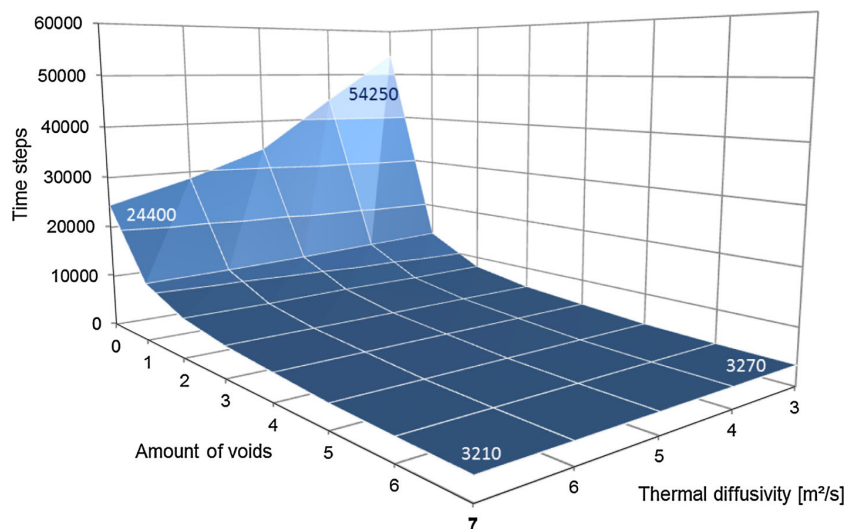


Fig. 9 Parameter variations of void amount and void size plotted in dependence of required time steps

Fig. 10 Parameter variations of void number and thermal diffusivity of foam lamella in dependence of required heating time



material properties and to allow an estimation of the main influencing parameter. The simulation results for these individual foam lamellas are shown in Fig. 9.

The variations of amount and void size are carried out at a thermal diffusivity of the foam lamella of $0.157 \times 10^{-6} \text{ m}^2/\text{s}$, the results show that with increasing void amount, and as well with increasing void size the required heating time decreases. This is reasoned by the increasing permeability of the foam lamella, allowing the vapor to diffuse with less resistance through the microstructure and thus yielding to a quicker heat spread. A further result of these variations is that the amount of voids has higher impact on the heat transfer than the size of a single void, where the amount of void space is kept similar in both cases. This effect is even rising with increasing void space. The reason for this progression may be the fact that increasing the amount of voids is linked to an increasing amount of free surface of the foam lamella thus enabling more vaporization from the lamella and therefore yielding to increased heat transfer by increased evaporation–condensation. The amount of free surface as well increases if the void size is increased but to a minor degree than in the case of increased amount of voids. The final part of the parameter variation study addresses the correlation of void number and thermal diffusivity of the foam lamella.

The results are shown in Fig. 10, where the amount of voids and the varied thermal diffusivity of each amount of voids are plotted versus the required time steps to finish the simulation. The results show that more time is required for a complete dense lamella and the lowest thermal diffusivity. Increasing the thermal diffusivity through such a dense lamella decreases the required heating time, but is still much higher than in the presence of voids. Generally speaking, increasing the amount of voids and increasing the

thermal diffusivity yields to the quickest heat transfer. Worth to mention is that the impact of the thermal diffusivity of the lamella on the heating rate has a higher influence if fewer voids are present.

4 Conclusion

The LBM is used to enlighten the thermo-physical processes inside the microstructure of cereal foam. The results give insight into the coupled heat and mass diffusion as well as the linked phase transition processes of water inside the bubbles. It is shown that heat transfer in such microstructures is depending on evaporation–condensation heat transfer, besides thermal diffusion. In addition, the algorithm is used to deliver insight into the impact of microstructural properties on the heat transfer, and it could be shown that the main effect on heat transfer optimization is given by an increased amount of voids inside the foam lamellas. The presented results deliver the possibility how to optimize the heat transfer, but the conversion of these findings to an experimental continuation remains challenging. In this context, increasing the amount of free water in the dough seems to be straightforward from the simulation results but from a technological point of view simply increasing the amount of water would lead to production problems due to the specific water uptake of flours starch and thus different process conditions in worst case leading to a different final product. In conclusion, care has to be taken by the interpretation of the results by means of simply transferring the findings without considering the linked processes. But in spite of the challenge to convert the simulation results to a practical basis, the numerical investigations can be used to support the experimental heat

transfer optimizations in cereal foam showing the directions experimental research should focus on. Besides the conversion to an experimental basis, further work should be done to include the agglomeration of the condensed vapor phase to liquid water and the implementation of flow considerations of this liquid phase.

Acknowledgments This work was sponsored by the Deutsche Forschungsgemeinschaft DFG Grant Number: BE 2245/8-1. The authors thank Anja Dietrich, Fraunhofer Development Center X-ray Technology EZRT, Fraunhofer Institute for Integrated Circuits IIS, Fürth, Germany for the μ CT-images.

References

- De Vries U, Sluimer P, Bloksma AH (1989) A quantitative model for heat transport in dough and crumb during baking. In: *Cereal Science and Technology in Sweden, Proceedings of an International Symposium*. Sweden, Lund University, pp 174–188
- Dietrich A, Nachtrab F, Salamon M, Khabta M, Uhlmann N, Hanke R (2012) Characterization of food foams using fast laboratory micro CT. In: *Cellular materials—CELLMAT 2012*, Dresden, Germany, 7–9 Nov 2012
- Hussein MA, Becker T (2010) An innovative micro-modelling of simultaneous heat and moisture transfer during bread baking using the lattice Boltzmann method. *Food Biophys* 5(3):161–176
- Mack S, Hussein MA, Becker T (2013a) Examination of thermo-physical and material property interactions in cereal foams by means of Boltzmann modeling techniques. *Microfluid Nanofluid* 15:387–395
- Mack S, Hussein MA, Becker T (2013b) Tracking the thermal induced vapor transport across foam microstructure by means of micro-sensing technology. *J Food Eng* 116(2):344–351
- Perez Alvarado F, Hussein MA, Becker T (2011) Image processing in life science. In: *Applications from cells to food*. 10. Dresdner sensor-symposium, Dresden, Germany
- Purlis E, Salvadori VO (2009) Bread baking as a moving boundary problem. Part 1: mathematical modelling. *J Food Eng* 91:428–433
- Rask C (1989) Thermal properties of dough and bakery products: a review of published data. *J Food Eng* 9:167–193
- Sablani SS, Marcotte M, Baik OD, Castaigne F (1998) Modeling of simultaneous heat and water transport in the baking process. *Lebensm-Wiss u-Technol* 31:201–209
- Sluimer P, Krist-Spit CE (1987) Heat transport in dough during the baking of bread. In: Morton ID (ed) *Cereals in a European context*. Ellis Horwood, Chichester, UK, pp 355–363
- Succi S (2001) *The lattice Boltzmann equation for fluid dynamics and beyond*. Oxford University Press, Oxford
- Sukop MC, Thorne DT Jr (2007) *Lattice Boltzmann modeling. An introduction for geoscientists and engineers*. Springer, Berlin
- Thorvaldsson K, Janestad H (1999) A model for simultaneous heat, water and vapour diffusion. *J Food Eng* 40:167–172
- Thorvaldsson K, Skjöldebrand C (1998) Water diffusion in bread during baking. *Lebensm-Wiss U-Technol* 31:658–663
- Wagner MJ, Lucas T, Le Ray D, Trystram G (2007) Water transport in bread during baking. *J Food Eng* 78:1167–1173
- Wählby U, Skjöldebrand C (2001) NIR measurements of moisture changes in foods. *J Food Eng* 47:303–312
- Wolf-Gladrow DA (2005) *Lattice-gas cellular automata and lattice Boltzmann models—an introduction*. Springer, Berlin
- Zanoni B, Peri C (1993) A study of the bread-baking process. I: a phenomenological model. *J Food Eng* 19:389–398
- Zhang J (2011) Lattice Boltzmann method for microfluidics: models and applications. *Microfluid Nanofluid* 10:1–28

3. Discussion

The relevance of a micro-scale description of thermo-physical and material property interactions in cereal foam is given by the necessity to investigate heat transfer optimizations. Recent researches mainly omitted micro-scale effects and regarded thermal treatment of cereal foam from a straight continuum perspective. Nonetheless, the spatio-temporal, as well as non-equilibrium, incidence of driving heat transfer associated processes requires consideration from a micro- or meso-scale perspective.

The present work combines theoretical investigations of heat and mass transfer processes in cereal foam microstructures with measurement and multi-scale modeling techniques. The relevant time- and length scales of the thermo-physical processes are identified theoretically, emphasizing the multi-scale and multi-physics character of the whole process. Detailed knowledge of the time and length-scales is required to identify the main driving processes and restrictions arising from diffusion limitations. Furthermore, the identification of the spatio-temporal range of the driving processes is essential to analyze temperature and humidity measurements as well as to set up an appropriate modeling environment. Syllogism, the application of the meso-scale lattice Boltzmann method allows addressing multi-physical processes based on particle interactions, but certainly deducing continuum properties from micro-scale characteristics.

Prior to numerical investigations, the heat and mass transfer is measured whilst thermal treatment, giving insight in macroscopic temperature and humidity distribution. The results showed that temperature approaches towards a temperature plateau of around 100 °C, thus it can be concluded that continuous evaporation and condensation occurs inside the crumb microstructure. Contrariwise, the temperature inside the crust region exceeds this level, tending towards oven temperature, implying that water evaporation proceed that fast that energy transfer is resulting in a temperature change, rather than being required for the evaporation of water. The results are in agreement with published data (Patel et al., 2005; Purlis et al., 2009a). In addition it could be shown, that humidity increases inside the crumb at the coldest spot, implying that evaporation-condensation yields to an internal humidity flux. The

results contribute to enlighten the moisture distribution inside cereal foam microstructures confirming previously published research studies (Thorvaldsson et al., 1998; Purlis et al., 2009a). The additionally presented contradictive results in literature (Zanoni et al., 1993; Wagner et al. 2007) may be reasoned by the applied measurement techniques or solely by the fact, that difference in raw material, processing and baking conditions yields to a significant shift of humidity fluxes. This might be reasoned by too less vaporizable water present in the lamella, due to the amount or the degree of bounding to starch or protein. Additionally, too quick evaporation to the surrounding based on high temperature conditions, or the point in time of crust development might, as well as specific microstructural characteristics of the crumb may yield to differences in the humidity flux. Further work is required to identify the impact of raw material and process conditions on the humidity flux. Despite the fact, that miniature commercially available temperature and humidity sensor was used in this study the results give only insight in macroscopic properties, thus allow only indirect conclusions on heat and humidity flux through the microstructure. Current sensing techniques is limited to a range of 2-3 mm (Crawford et al., 2008), thus unfeasible to directly measure processes inside a single foam bubble or a foam lamella during the heating process. Certainly, forecasting further research, it may be conceivable due to increasing research activity in nanotechnology (Crawford et al., 2008). Thus, allowing measurement-wise the determination of material properties of the micro-scale components with respect to heat transfer. Figure 3.1 illustrates the size relation of the applied sensing tool to the cereal foam microstructure.

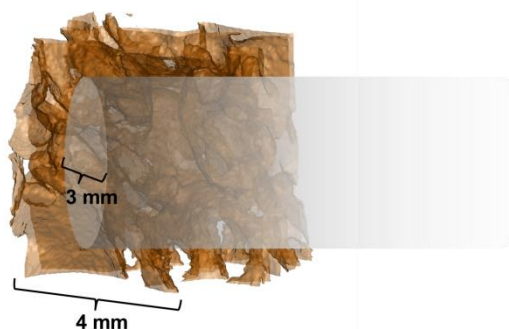


Figure 3.1 Projection of the applied temperature and humidity sensor probe (diameter 3 mm) inside a section of cereal foam microstructure. Indicating the limitations of commercial available sensing tools (Crawford et al., 2008), to determine thermo-physical processes inside a single foam bubble, or lamella respectively.

It can be seen that the sensing tool covers a comparative large area in relation to foam microstructure. Therefore, the presented measurement results enforce the

necessity of more detailed research to investigate heat and mass transfer at smaller length scales. Due to the multi- component, -scale, and -physics character of the processes, as well as the related sensing limitations, emphasis is taken on numerical investigations in the present study. The developed numerical models combine the theoretical investigations of micro-processes and the results from measurements of macro-properties. The multi-component character of the cereal foam microstructure covering different length scales of both structural- as well as thermodynamic processes led to the required application of a meso-scale modeling technique, the lattice Boltzmann method, bridging micro-and macro-scales. Thus, the underlying thermo-physical processes are theoretically investigated, combined in a numerical algorithm by means of a lattice Boltzmann modeling, and implemented in a self-written lattice Boltzmann code.

The cereal foam microstructures are implemented by the usage of μ CT-images, building the basis of the computational domain, thereby allowing a realistic picture of the microstructure from a bubble scale of length. In a first step heat and mass transfer through the foam microstructure are addressed by means of diffusion, giving insight in the heat and vapor fluxes inside, as well as to vapor flux towards the surrounding. Diffusion is generally depending on concentration differences, temperature and pressure (Hudson et al., 2008). In the proposed model diffusion is calculated depending on concentration gradients, which is directly related to the partial vapor pressure, additionally the diffusion coefficients are implemented temperature dependent. Diffusion implies per definition zero mean velocity flow, thus flow velocity dependent terms vanish in the following equilibrium function.

$$f_i^{eq} = w_i \rho(x) \left[1 + 3 \frac{u v_i}{c^2} + \frac{9 (u v_i)^2}{2 c^4} - \frac{3 u^2}{2 c^2} \right] \quad (3-1)$$

Where $\rho(x)$ is the local density, v is the particle velocity, i is the direction, u is the flow velocity, $c = \Delta x / \Delta t = 1$ is the basic lattice speed and w is the weight factor.

Remaining the relevant question, if certainly heat and mass transfer can be addressed solely by diffusion, and if advection inside the bubbles can be neglected under the constraints of the present temperature and partial vapor pressure

differences. Discussing this point requires the inclusion of the next step addressed in this study, the phase transition processes of water occurring inside the microstructure. The developed model is based on multi-component heat and mass diffusion, evaporation from the lamella, condensation of water vapor according to local temperature, humidity and partial pressure conditions, as well as re-evaporation from the condensed phase. To estimate the impact of advection inside the bubbles, the flow velocity is additionally computed, and is shown in figure 3.2. In the case of diffusion, the flow velocity is equal to zero, thus advection can be neglected if the mean flow velocity is much smaller than the lattice speed.

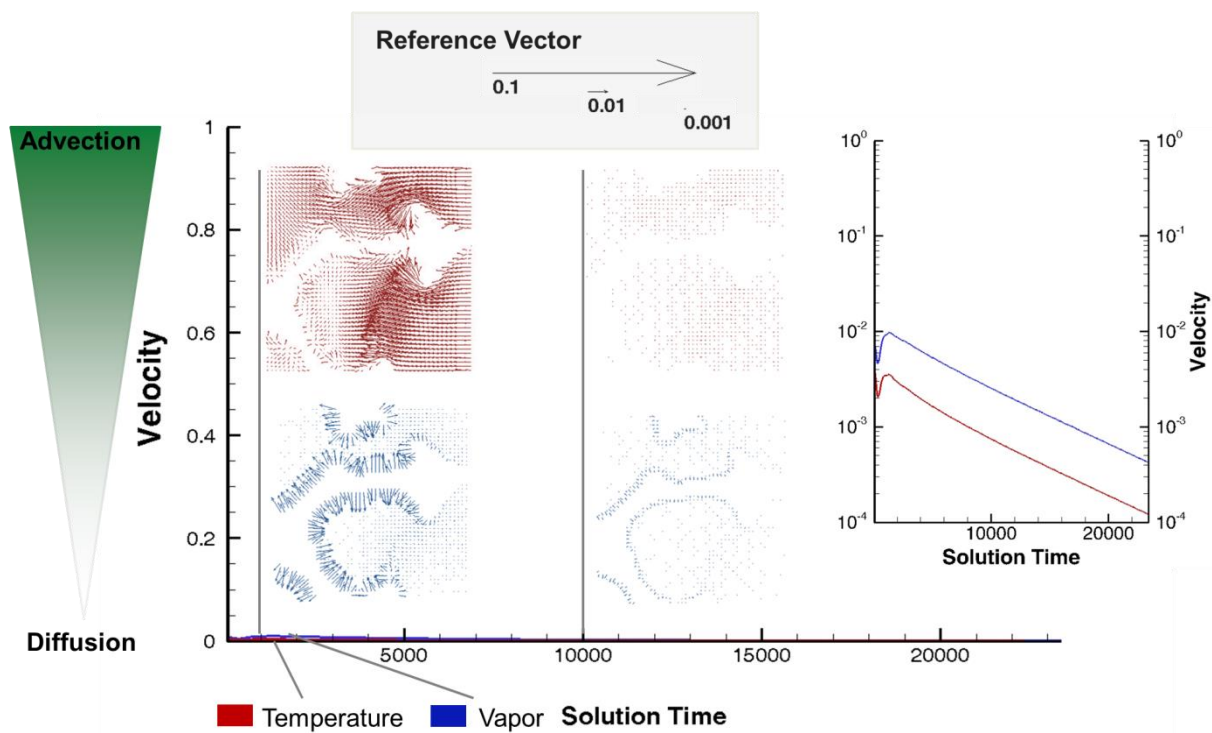


Figure 3.2 The flow velocity based on the temperature (red) and vapor (blue) transport (in lattice units) inside a foam bubble is plotted versus the solution time. Transport processes occur based on diffusion if the flow velocity is zero. The simulation results show that the flow velocity is much smaller than the lattice speed ($c=1$ Lattice Units) and additionally converging to zero, therefore transport processes are dominant in the diffusion regime and advection can be neglected. Velocity vectors are plotted at a single slice of the computational domain at time step 1000 and time step 10000, indicating the flux directions, being dominant in the evaporation boundary. Nonetheless, comparison to the reference vectors show, the minor impact of velocity which is at least two orders of magnitude lower and further decreasing with proceeding time steps.

In figure 3.2, the flow velocity inside a bubble is plotted versus the solution time, in lattice units. It can be seen that the velocity of both, temperature (red line) and vapor (blue line), is much smaller than the basic lattice speed ($c=1$) and with proceeding time steps converging towards zero. Therefore, advection inside the bubbles is of minor impact and can be neglected.

In addition, the velocity is plotted on a logarithmic scale, emphasizing the velocity progress. Having a closer look on the velocity vector profile shows that advection plays a role solely in the evaporation boundary region at initial time steps. The velocity vectors are shown for temperature (red) and vapor (blue) at time steps 1000 and 10000, and can be compared to the reference vectors, plotted for velocities of 0.1, 0.01 and 0.001. Since advection is a local phenomenon, and additionally the velocity is converging to zero throughout the foam bubbles, it could be shown that diffusion is dominant and is therefore the driving processes to be considered in the model.

The complexity of the whole process, including several unknowns, requires simplification and thus impedes a perfectly realistic model. Nonetheless, a model covering the essential physics of the proposed process is suitable to interpret the process (Attig et al., 2004). Numerical modeling comprises thereby the challenge to include all relevant aspects and make simplifications where possible, with respect to the computational effort. In the present study several processes occurring in cereal foam under thermal treatment are neglected, summarized in the following:

- Structural changes (bubble expansion/coalescence, lamella thinning/rupture)
- Bio-chemical reactions as starch gelatinization, protein denaturation, flavor- or browning kinetics
- Density ratio of water vapor/liquid
- Presence of additional gases in the void fraction
- Advection in the void fraction
- Presence of condensation nuclei

Being aware of the main objective of the study, the driving processes and main relevant physical processes are included in the study to estimate the impact of evaporation-condensation heat transfer inside the microstructure. Nonetheless, the

developed algorithms build the basis for further research focusing to implement the so far neglected processes. In this context, significant for a correct interpretation of the simulation results is the awareness of the modeling assumptions as well as simplifications. The straight physics based model shows, that the hypothetical evaporation-condensation indeed takes place in cereal foam microstructures due to the present thermo-physical conditions. Evaporation- condensation based heat transfer yields to cyclic evaporation- and condensation processes, being accompanied by additional energy absorption and release depending on the kind of phase change. The simulation results show that the evaporation-condensation process is of cyclic nature in the void fraction of the cereal foam microstructure, as shown in figure 3.3.

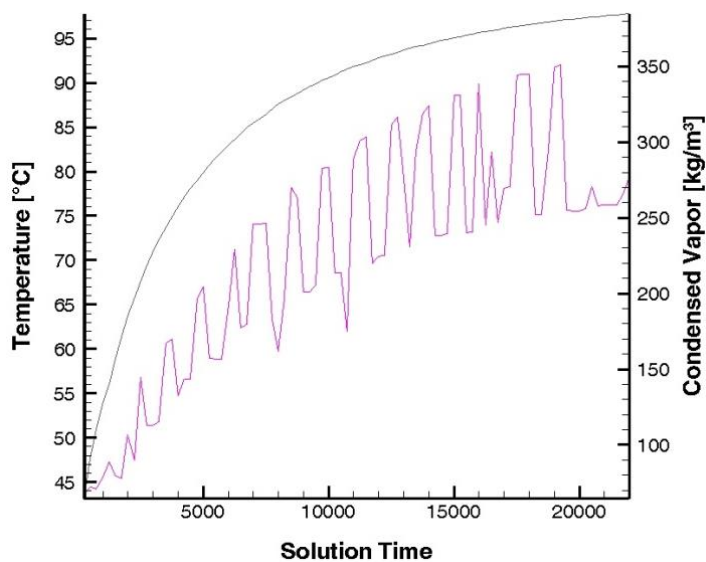


Figure 3.3 Temperature (black line) progression during thermal treatment and cyclic evaporation-condensation, shown by the amount of condensed vapor (pink line) at the bubble interface. According to the increasing amount of vapor inside the bubble, due to vaporization from the lamella, condensation is increasing, dependent on local conditions.

Furthermore, it could be shown that the incidence of this process increases the overall heat transfer through the product. Based on the elaborated heat and mass transfer processes, the developed code is used for parameter variation studies to identify the main relevant micro-structural as well as material property constitutions of the foam for improved heat transfer. The parameter variations cover foam porosity, thermal diffusivity of the lamella, amount and size of micro-voids in the lamella. It could be shown that the amount of micro-voids inside the lamella, connecting the bubbles and yielding to increased permeability, has the main effect on enhanced heat transfer. This is linked to the increased free surface area of the lamella allowing

amplified vaporization. The increased humidity present in the void fraction in turn accelerates the evaporation-condensation process, thus heat transfer proceeds quicker.

An additional objective of the study is the visualization of thermo-physical processes occur inside a single foam bubble. Likewise, the micro-structural effect on the heat transfer can be visualized, as shown by the temperature distribution in figure 3.4 at a time step of 2500. Slices are cut out from the modeling domain emphasizing different microstructural constitutions of the foam. The black lines thereby border the foam lamellas.

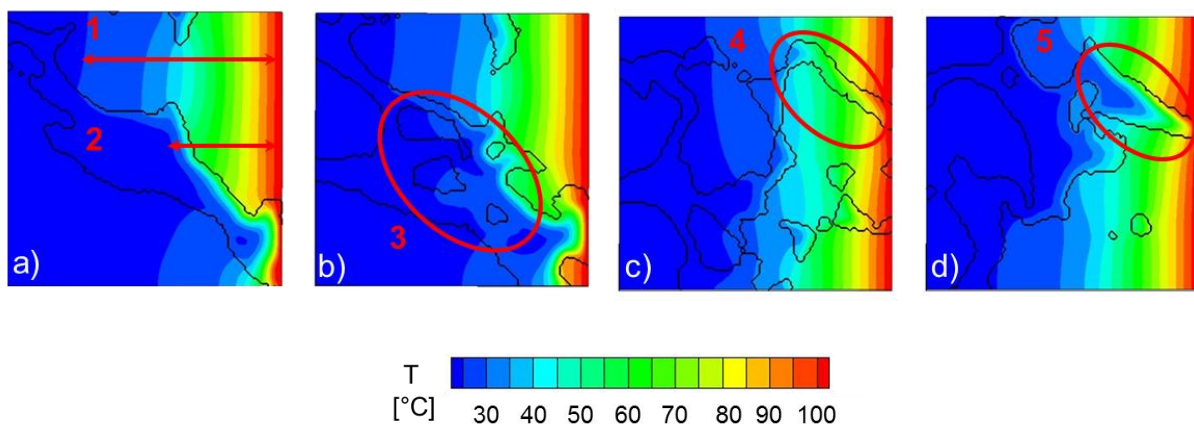


Figure 3.4 a) Heat diffusion proceeds quicker through the gas bubbles (1) in comparison to the lamellas (2); b) Micro-bubbles inside the lamella (3) Additionally increase the heat transfer; c)/d) Heat transfer proceeds quicker in thin lamellas (4) than in thicker (5) ones.

In figure 3.4a it can be seen that the heat spread through the foam bubbles (1) proceeds quicker in comparison to the lamella (2) which is reasoned by the higher thermal diffusivity of the gas phase. Comparing figure 3.4a and 3.4b shows that the presence of micro-bubbles (3) inside the lamella increases the heat transfer. Additionally, lamella thickness has an influence on the heat transfer, and it can be seen in figure 3.4 c&d that heat transfer proceeds quicker in thin lamellas (4) in comparison to thicker lamellas (5).

Drawing a first conclusion, the developed algorithms give innovative insight in the thermo-physical processes inside the microstructure and furthermore allow an estimation of the impact of material and structural aspects on the heat transfer.

Nonetheless, in addition to the theoretical and numerical investigations, a practical link to technological processing is required. It would be futile to establish theoretically meaningful possibilities to increase the heat transfer which are not transferable, and practicable in the real process. Caution has to be taken, aiming on increasing heat transfer by microstructural variations, without major effects on the characteristics of the final product. The numerical parameter variation studies can thereby predict the main influencing parameters, based on the physical models and dough microstructure configurations to support the technologists in which direction experimental research should focus on.

Further work should be done on experimental work to convert and apply the results of the parametric investigations. For instance, it is well known, that differences in processing have an influence on the microstructure (Patel et al., 2005). Thereby mixing and kneading are the most critical steps during bread preparation and deliver the basis for the final product microstructure (Chinachoti et al., 2001). In this step, ingredients are brought together, starch gets hydrated, and micro air bubbles are embedded in the developing starch-gluten matrix, acting as the fundament of final bubble size distribution in the final product (Bellido et al., 2006). Characteristic cereal foam microstructure development is depending on these initial air micro-bubbles in combination to the visco-elastic starch-gluten matrix. The lamellas consist of a visco-elastic starch-gluten matrix, where gluten plays the major role to develop a foamy structure, delivering the required visco-elasticity to expand but also to hold the fermentation induced gases inside the matrix (Chinachoti et al., 2001). The flour composition additionally affects the possibility to encapsulate gas inside the network according to the impact of gluten (Chinachoti et al., 2001). If the lamellas are too stiff, no expansion can take place, and fermentation gases as CO₂ are released to the surrounding, due to the increasing internal pressure (Chinachoti et al., 2001). A further consequence is that the viscoelasticity of dough directly influences the bubble size distribution, distance between bubbles, as well as the number of bubbles, as shown by μ CT-image analysis (Bellido et al., 2006). Another study carried out by the use of μ CT imaging examined the impact of steaming on loaf volume during thermal treatment. Steaming affects heat transfer during oven rise, permeability of crust

which was higher and crust was thinner for lower steaming (Le-Bail et al., 2011). Permeability of crust region, and as well its thickness, which is important due to water vapor diffusivity through it and therewith water release to the surrounding, where low steaming yields to non-gelatinized starch in crust (Le-Bail et al., 2006). These findings can be related to the numerical investigations of the present study. Increasing connectivity additionally allows the vapor to diffuse freely through the micro-structure, which is of importance for the heat transfer. Since the main impact on heat transfer is achieved by increasing the free surface area of the lamella, which can be due to an increasingly amount of micro-voids inside the lamella, connecting the bubbles.

During fermentation, bubbles expand according to CO₂ and other fermentation by-products, produced by yeast. The air nuclei, embedded during mixing, play the major role building the source of foam bubbles. During fermentation, new bubbles cannot be formed according to the required pressure (Chinachoti et al., 2001). CO₂, which is continuously produced during the fermentation step saturates in the liquid dough phase, CO₂ produced over the saturation limit yields to gas cell expansion due to diffusion. Thereby, the gluten network acts as a barrier, CO₂ remains in the dough and is partly released to the surrounding (Vanin et al., 2009). Additionally, expanding smaller gas bubbles requires a higher pressure than expanding bigger bubbles. Thus, the smallest air bubbles will remain in their size, being still present in the final product (Chinachoti et al., 2001). The presence of these micro air bubbles is of importance due to the fact that they on the one hand the presence of the micro air bubbles influences the heat transfer as shown in figure 3.4, and on the other hand they may support the development of connecting micro-gaps in the lamella, thus increasing the permeability through the void fraction. This is of impact on enhanced heat transfer, as shown numerically in the presented study.

In addition, it could be shown that the thermal diffusivity of the lamella has an influence on the heat transfer. Bearing in mind, that thermal diffusivity is a function of thermal conductivity, density and specific heat. Thermal conductivity and specific heat are related to the water content, in correlation to the findings that more vapor in the void fraction accelerates the evaporation-condensation process, the conclusion

can be drawn that increasing amount of water has a positive effect on the heat transfer, by shifting the thermo-physical conditions inside the void fraction to increased condensation. Nonetheless, the specific uptake of water by starch during processing, in relation to optimum kneaded dough, limits the amount of additional water to a specific range (Puhr et al., 1992).

It is well known that besides the thermo-physical conditions, the amount of nuclei is of high impact on the condensation process, distant from surfaces condensation can only occur if condensation nuclei are present to induce droplet growth from the excess water vapor (Roach, 1994). The presence of these nuclei is neglected in this work, and condensation is addressed from a straight saturation level based point of view. This simplification is feasible due to the fact that in normal atmosphere condensation nuclei are omnipresent and super-saturation in a negligible range of 0.01-0.03 % (Roach, 1994). Nonetheless, one should be aware that increasing amount of such nuclei leads progressively to condensation. In food materials as cereal foam, the amount of such nuclei is assumed to be fairly high, but thus far not quantitatively determinable. Further work is required to elaborate the presence and the effect of such condensation nuclei, since their presence might as well contribute to increased heat transfer by accelerated condensation.

Besides further work addressing cereal foam thermo-physical, microstructural and material property interactions, further research should be conducted by means of lattice Boltzmann modeling. The presented model accounts for the phase transition process and quantitatively to the transitioned amount of vapor related transferred energy. Nonetheless, the condensed phase is represented by a wet steam region, rather than a pure liquid phase. Such simplification is acceptable, under the background of the objective, to elaborate heat transfer mechanism, and the amount of energy transferred, which is addressed physically correct. Further investigations should be carried out to implement high density ratios, to allow insight in the flow characteristics of the liquid phase. In the current model, such processes are in the sub-grid range, and implementing the additional liquid flow would require the application of multi-grid methods facing additional interesting numerical challenges. Additional processes are the interactions of water molecules, specifically during the

phase transition processes. Of minor importance for cereal technology, since meso-scale considerations are sufficient, but from a physical point of view further research to link these physical processes would offer the possibility for a broad range of multi-scale applications. For instance by means of coupling molecular dynamics to the main lattice Boltzmann model delivering hybrid methods.

The physics-based developed lattice Boltzmann code allows the application of the developed algorithms to other porous media in the presence of vaporizing fluids and temperature gradients. Essentially, adjust μ CT-images of the material, as well as the initial conditions and the specific material properties. For instance, the developed code was successfully used to model heat and mass transfer through a cappuccino section, where additionally the release of flavor compounds was implemented. Figure 3.5 shows extracted slices of the modeled cappuccino foam showing the different simultaneously proceeding coupled processes through the structure, induced by the coffee-boundary condition acting as heat source.

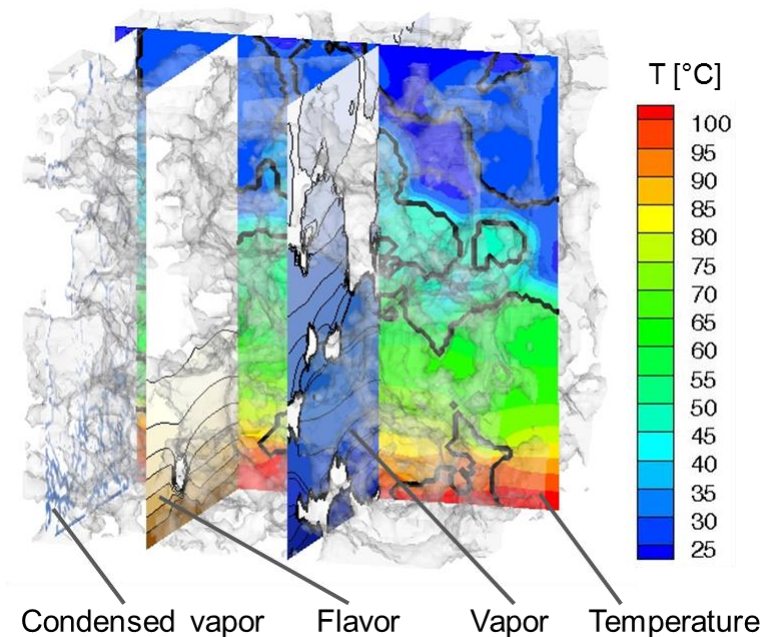


Figure 3.5 Simulation results of heat and mass transfer, including evaporation-condensation, through a cappuccino foam section. Mass transfer is addressed by means of vapor as well as diffusion of a flavor compound. The temperature induced processes are induced by a heat source in the bottom of the domain, implemented via the boundary conditions, representing coffee.

Further possible applications are in a broad range, reaching from food science to geology, building physics, ceramics, material science, chemical- or biotechnological engineering, amongst others.

The conclusion can be drawn that the theoretical investigations, covering the whole length scale, the measurements, covering macro-scale, and the modeling, combining due to the meso-scale character micro- and macro scales, deliver a multi-scale insight in the process. Length-scales covered by the applied sensing and modeling techniques provide a combination of both procedures delivering the required insights in a unite nature. The key benefits of both, sensing and modeling techniques, respectively are used, and furthermore straightening the drawbacks by their combined application. Under the conditions where sensing is limited, numerical investigations can deliver further insight and support the correct interpretation of the measurements. The innovative meso-scale considerations visualize the heat and mass transfer processes in the microstructure, as well as the presence of evaporation-condensation. Based on the elaborated heat transfer mechanisms a parameter variation study is carried out to deliver insight in the impact of the microstructure on the heat transfer. In addition, the simulations carried out by means of lattice Boltzmann modeling allow the visualization of, and give novel insight in, the formerly hidden thermo-physical processes inside the void fraction of cereal foam.

4. References

- Anderson, C. (2008). Thermal Heat Transport Characterization for Macroscale, Microscale, and Nanoscale Heat Conduction. PhD Thesis. University of Minnesota.
- Antonietti, M., Ozin, G. A. (2004). Promises and Problems of Mesoscale Materials Chemistry or Why Meso? *Chemistry - A European Journal* 10: 28-41.
- Aristov, V.V. (2001). Direct Methods for Solving the Boltzmann Equation and Study of Nonequilibrium Flows. Kluwer Academic Publishers.
- Attig, N., Binder, K., Grubmüller, H., Kremer, K. (2004). Computational Soft Matter: From Synthetic Polymers to Proteins. John von Neumann Institute for Computing.
- Bagchi, B., Chakravarty, C. (2010). Interplay between multiple length and time scales in complex chemical systems. *J. Chem. Sci.* 122(4): 459-470.
- Beisbart, C., Hartmann, S. (2011). Probabilities in physics. Oxford University Press.
- Bejan, A., Kraus A. D. (2003). Heat Transfer Handbook. John Wiley & Sons.
- Bellido, G. G., Scanlon M. G., Page, J. H., Hallgrimsson, B. (2006). The bubble size distribution in wheat flour dough. *Food Research International* 39: 1058-1066.
- Bellomo, N., Bellouquid, A., Herrero, M. A. (2007). From microscopic to macroscopic description of multicellular systems and biological growing tissues. *Computers and Mathematics with Applications* 53: 647-663.
- BeMiller, J., Whistler, R. (2009). Starch: Chemistry and Technology. Food Science and Technology, International Series.
- Bernaschi, M., Melchionna, S., Succi, S., Fyta, M., Kaxiras, E., Sircar, J. K. (2009). MUPHY: A parallel Multi PHYSics/scale code for high performance bio-fluidic simulations. *Computer Physics Communications* 180: 1495-1502.
- Berthier, J., Silberzan, P. (2010). Microfluidics for Biotechnology. Artech house Norwood.
- Brennen, C. E. (2005). Fundamentals of Multiphase Flows. Cambridge University Press.
- Buleon, A., Colonna, P., Planchot, V., Bali, S. (1998). Starch granules: structure and biosynthesis. *International Journal of Biological Macromolecules* 23 (2): 85-112.
- Cauvain, S. P. (2000). Bread making – Improving quality. Woodhead Publishing in Food Science and Technology.
- Cauvain, S. P., Young, L. S. (2006). Baked Products: Science, Technology and Practice. Blackwell Publishing Ltd.
- Cengel, Y. A. (2007). Heat and Mass Transfer: A Practical Approach. McGraw-Hill.

- Chen, S., Doolen, G. D., Eggert, K. G. (1994). Lattice- Boltzmann Fluid Dynamics a versatile tool for multiphase and other complicated flows. *Los Alamos Science* 22: 99-111.
- Chinachoti, P., Vodovotz, Y. (2001). *Bread Staling*. CRC Press LLC.
- Chung, T. J. (2007). *General Continuum Mechanics*. Cambridge University Press.
- Cosgrove, T. (2010). *Colloid Science – Principles, Methods and Applications*. John Wiley & Sons Ltd.
- Crawford, B., Esposito, D., Jain, V., Pelletier, D. (2008). Flexible Carbon Nanotube Based Temperature Sensor for Ultra-Small-Site Applications. Capstone Design Program: Mechanical Engineering. Paper 55. Northeastern University.
- Datta, A. K., Zhang, J., Mukherjee, S. (2005). Transport Processes and Large Deformation During Baking of Bread. *AIChE Journal* 51(9): 2569-2580.
- De Vries, U., Sluimer, P., Bloksma, A. H. (1989). A quantitative model for heat transport in dough and crumb during baking. *Cereal Science and Technology in Sweden, Proceedings of an International Symposium, Sweden, Lund university*, 174-188.
- Dietrich, A., Nachtrab, F., Salamon, F., Khabta, M., Uhlmann, N., Hanke, R. (2012). Characterization of food foams using fast laboratory micro CT. *Cellular Materials - CELLMAT 2012, 7.-9.*, Dresden, Germany.
- Gan, Z., Ellis, P.R., Schofield J.D., (1990). The Microstructure and Gas Retention of Bread Dough. *Journal of Cereal Science* 12: 15-24.
- Ge, J., Bedeaux, D., Simon, J. M., Kjelstrup, S. (2007). Integral relations, s simplified method to find interfacial resistivities for heat and mass transfer. *Physica A* 385: 421-432.
- Gilbert, J. K., Treagust, D. (2009). *Models and Modeling in Science Education. Multiple Representations in Chemical Education*. Springer.
- Gray, W. (2002). On the definition and derivatives of macroscale energy for the description of multiphase systems. *Advances in Water Resources* 25: 1091-1104.
- He, H., Hosney, R. C. (1992). Factors Controlling Gas Retention in Nonheated Doughs. *Cereal Chem.* 69(1): 1-6.
- Hemminger, J. (2012). *From Quanta to the Continuum: Opportunities for Mesoscale Science*. University of California, Irvine.
- Hoffmann, K. A., Chiang, S. T. (2000). *Computational Fluid Dynamics Volume 1-3. Engineering Education System*.
- Hudson, T. L., (2008). Growth, diffusion, and loss of subsurface ice on Mars: experiments and models. Dissertation (Ph.D.), California Institute of Technology.

- Hussein, M. A., Becker, T. (2010). An innovative Micro-modelling of Simultaneous Heat and Moisture Transfer during Bread Baking using the Lattice Boltzmann Method. *Food Biophysics*. 161-176.
- Jekle, M., Becker, T. (2011). Dough microstructure: Novel analysis by quantification using confocal laser scanning microscopy. *Food Research International* 44: 984-991.
- Jiji, L.M., Dames, C. (2009). *Heat Conduction*. Springer Berlin Heidelberg.
- Kotoki, D., Deka, S. C. (2010). Baking loss of bread with special emphasis on increasing water holding capacity. *J food Sci Technol* 47(1): 128-131.
- Kukudzhanov, V. N. (2013). *Numerical Continuum Mechanics*. Walter de Gruyter GmbH, Berlin/Boston.
- Kulp, K., Ponte, J. G. (2000). *Handbook of Cereal Science and Technology*. Marcel Dekker, Inc.
- Kokawa, M., Fujita, K., Sugiyama, J., Tsuta, M., Shibata, M., Araki, T., Nabetani, H. (2012). Quantification of the distributions of gluten, starch and air bubbles in dough at different mixing stages by fluorescence fingerprint imaging. *Journal of Cereal Science* 55: 15-21.
- Landry, E. S., Mikkilineni, S., Paharia, M., McGaughey, A. J. H. (2007). Droplet evaporation: A molecular dynamics investigation. *Journal of applied Physics* 102: 1-7.
- Le-Bail, A., Fortoul, R. D. C. A., Dessev, T., Rosell, C., Leray, D., Lucas, T., Chevallier, S., Jury, V. (2011). Impact of steaming conditions on the structure and on the properties of bread crust; in the case of a crispy roll. *iCEF11 Congress Proceedings Volume I*. 199-200.
- Leuzzi, L. Nieuwenhuizen, T. M. (2008). *Thermodynamics of the glassy state Series in condensed matter physics*. Taylor & Francis.
- Liu, Z., Scanlon, M. G. (2003). Predicting mechanical properties of bread crumb. *Trans IChemE* 81(C): 224-238.
- Manneville, P. (2010). *Instabilities, Chaos and Turbulence*. ICP Fluid Mechanics – Vol. 1. Imperial College Press.
- Markowski, P., Richardson, Y. (2010). *Mesoscale Meteorology in Midlatitudes*. Wiley-Blackwell.
- Meller, J. (2001). *Molecular Dynamics*. Encyclopedia of Life Science, Nature Publishing Group.
- Miguel, A. S. M., Martins-Meyer, T. S., da Costa Figueiredo, E. V., Lobo, B. W. P., Dellamora-Ortiz, G. M. (2013). *Enzymes in Bakery: Current and Future Trends*, Food Industry, Dr. Innocenzo Muzzalupo (Ed.), ISBN: 978-953-51-0911-2, InTech, DOI: 10.5772/53168.

- Mohamad, A. A. (2011). Lattice Boltzmann Method. Fundamentals and Engineering Applications with Computer Codes. Springer.
- Monaco, E., Luo, K. H., Qin, R. S. (2007). New Trends In Fluid Mechanics Research. Proceeding of the Fifth International Conference on Fluid Mechanics Shanghai, China. Tsinghua University Press & Springer.
- Nguyen, N. T., Wereley, S. T. (2002). Fundamentals and Applications of microfluidics. Artech House, Inc.
- Nield, A. N., Bejan, A. (2006). Convection in Porous Media. Springer Science+Business Media. Inc.
- Pan, A. (2012). China Market Report. China Renmin University Press.
- Patel, B.K., Waniska, R.D., Seetharaman, K. (2005). Impact of different baking processes on bread firmness and starch properties in breadcrumb. Journal of Cereal Science 42: 173-184.
- Puhr, D. P., D'Appolonia, B. L. (1992). Effect of Baking Absorption on Bread Yield, Crumb Moisture, and Crumb Water Activity. Cereal Chem. 69(5): 582-586.
- Purlis, E., Salvadori, V. O. (2009a). Bread baking as a moving boundary problem. Part 1: Mathematical modeling. Journal of Food Engineering 91: 428-433.
- Purlis, E., Salvadori, V. O. (2009b). Bread baking as a moving boundary problem. Part 2: Model validation and numerical simulation. Journal of Food Engineering 91: 434-442.
- Rae, A. I. M. (2002). Quantum Mechanics. IOP Publishing Ltd.
- Rask, C. (1989). Thermal properties of dough and bakery products: a review of published data. Journal of Food Engineering, 167-93.
- Reddy, J. N. (2008). An Introduction to Continuum Mechanics. Cambridge University Press.
- Reif, F. (1965). Fundamentals of Statistical and Thermal Physics. McGraw-Hill.
- Roach, W. T. (1994). Back to basics: Fog: Part 1 - Definitions and basic physics. Weather 49, 411-415.
- Robinson, S. (2004). Simulation: The Practice of Model Development and Use. John Wiley & Sons, Ltd.
- Roco, M. C., Mirkin, C. A., Hersam, M. C. (2010). Nanotechnology Research Directions for Societal Needs in 2020 Retrospective and Outlook. WTEC, Springer.
- Rohsenow, W. M. Hartnett, J. P., Cho, Y .I. (1998). Handbook of heat transfer. MacGraw-Hill Companies, Inc.

- Sablani, S. S., Marcotte, M., Baik, O. D., Castaigne, F. (1998). Modeling of Simultaneous Heat and Water Transport in the Baking Process. *Lebensm.-Wiss. u.-Technol.*, 201-209.
- Saha, S. K., Celata, G. P. (2011). Advances in modeling of biomimetic fluid flow at different scales. *Nanoscale Research Letters* 6: 1-11.
- Sluimer, P., Krist-Spit, C. E. (1987). Heat Transport in Dough during Baking. Ellis Horwood, Chichester, UK, 355–368.
- Sonntag, R. E., Borgnakke, C. (2009). *Fundamentals of Thermodynamics*. John Wiley & Sons, Inc.
- Sroan, B. S., Bean, S. R., and MacRitchie, F. (2009). Mechanism of gas cell stabilization in bread making. I. The primary gluten-starch matrix. *Journal of Cereal Science*. 49: 32-40.
- Succi, S. (2001). *The Lattice Boltzmann Equation for Fluid Dynamics and Beyond*. Oxford University Press.
- Succi, S., Karlin, I. V., Chen, H. (2002). Role of the H theorem in lattice Boltzmann hydrodynamic simulations. *Rev. Mod. Phys.* 74: 1203-1220.
- Sukop, M. C., Thorne, D. T. (2006). *Lattice Boltzmann Modeling. An Introduction for Geoscientists and Engineers*. Springer.
- Sungtaek Ju, Y., Goodson, K. E. (1999). *Microscale heat conduction in integrated circuits and their constituent films*. Kluwer Academic Publisher.
- Therdthai, N., Zhou, W., Adamczak, T. (2002). Optimization of the temperature profile in bread baking. *Journal of Food Engineering* 55: 41-48.
- Thorvaldsson, K., Skjöldebrand, C. (1998). Water Diffusion in Bread During Baking. *Lebensm.-Wiss. U. Technol.* 31: 658-663.
- Thorvaldsson K., Janestad, H. (1999). A model for simultaneous heat, water and vapour diffusion. *Journal of Food Engineering* 40: 167-172.
- Tielemann, P. (2006). Computer simulations of transport through membranes: passive diffusion, pores, channels and transporters. *Proceedings of the Australian Physiological Society* 37: 15-27.
- Vanin, F. M., Lucas, T., Trystram, G. (2009). Crust formation and its role during bread baking. *Trends in Food Science & Technology* 20: 333-343.
- Wagner, M., J., Lucas, T., Le Ray, D., Trystram, G. (2007). Water transport in bread during baking. *Journal of Food Engineering* 78: 1167-1173.
- Wahlund, K. G., Gustavsson, M., MacRitchie, F., Nylander, T., and Wannerberger, L. (1996). Size Characterisation of Wheat Proteins, Particularly Glutenin, by Asymmetrical Flow Field-Flow Fractionation. *Journal of Cereal Science* 23: 113-119.

- Wang, M. (2012). Structure Effects on Electro-Osmosis in Microporous Media. *Journal of Heat Transfer* 134: 1-6.
- Wilson, K. G. (1979). Problems in Physics with Many Scales of Length. Scientific American, Inc. 158-159.
- Wolf-Gladrow, D. A. (2005). Lattice-Gas Cellular Automata and Lattice Boltzmann Models – An Introduction. Springer.
- Yazdchi, K., Srivastava, S., Luding, S. (2011). Microstructural effects on the permeability of periodic fibrous porous media. *International Journal of Multiphase Flow* 37: 956-966.
- Yip, S. (2005). Handbook of Materials Modeling. Springer.
- Zanoni, B., Peri, C. (1993). A Study of the Bread-Baking Process. I: A Phenomenological Model. *Journal of Food Engineering* 19: 389-398
- Zanoni, B., Peri, C., Gianotti, R. (1995a). Determination of the Thermal Diffusivity of Bread as a Function of Porosity. *Journal of Food Engineering* 26: 497-510
- Zanoni, B., Peri, C., Bruno, D. (1995b). Modelling of browning kinetics of bread crust during baking. *Lebensm.-Wiss. Technol.* 28: 604-609.
- Zanoni, B., Schiraldi, A., Simonetta, R. (1995c). A Naïve Model of Starch Gelatinization Kinetics. *Journal of Food Engineering* 24: 25-33.
- Zhang, J. (2010). Lattice Boltzmann method for microfluidics: models and applications. *Microfluid Nanofluid.* DOI 10.1007/s10404-010-0624-1.
- Zwanzig, R. (2001). Nonequilibrium Statistical Mechanics. Oxford University Press.